UC San Diego

UC San Diego Electronic Theses and Dissertations

Title

The impact of cell architecture on activation and output of the p53 stress response pathway

Permalink

https://escholarship.org/uc/item/0kt0s647

Author

Wong, Ee Tsin

Publication Date

2006

Peer reviewed|Thesis/dissertation

UNIVERSITY OF CALIFORNIA, SAN DIEGO

The impact of cell architecture on activation and output of the p53 stress response

pathway

A dissertation submitted in partial satisfaction of the requirements for the

degree Doctor of Philosophy

in

Biology

by

Ee Tsin Wong

Committee in charge:

      Professor Geoffrey M. Wahl, Chair
      Professor Webster K. Cavenee
      Assist. Professor Frank Furnari
      Professor Tony Hunter
      Professor Randall S. Johnson
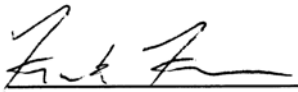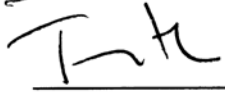   Professor Jean Y. J. Wang

2006
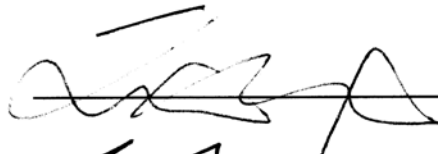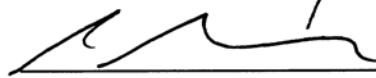
The dissertation of Ee Tsin Wong is approved, and it is acceptable in quality and form for publication on microfilm:

FRANK FURNARI

WEBSTER CAVENEE

Jean YJ WANG

Randall Johnson

GEOFF WAHL

Chair

University of California, San Diego

2006

TABLE OF CONTENTS

LIST OF FIGURES

Chapter IV

LIST OF TABLES

ACKNOWLEDGEMENTS

The text of Chapter II, in full, is a reprint of the material as it appears in *Nucleic Acids Research, 33:e147(2005).* The dissertation author is the primary researcher and author, and J Kolman, YC Li, L Mesner, W Hillen and C Berens are secondary authors in this publication. Geoffrey M. Wahl directed and supervised the research that forms the basis for this chapter.

VITA

Oct 13, 1975	Born, Singapore
1995	Diploma in Biotechnology with merit
1995-1997	Research Technician, Department of Biochemistry, National University of Singapore
2000	B.S. National University of Singapore, 1st class honors
2000	Research Assistant, John Hopkin Singapore
2001-3	Teaching Assistant, Department of Biology, University of California, San Diego
2000-2006	Research Assistant, University of California, San Diego and The Salk Institute For Biological Studies, La Jolla, California
2006	Ph.D., University of California, San Diego

PUBLICATIONS

Ee Tsin Wong, Geoffrey M. Wahl. Cellular architecture can affect the biologic outcome of the p53 stress response pathway through Hdmx regulation. *In preparation*.

Mark Wade, **Ee Tsin Wong,** Mengjia Tang, Lyubomir T. Vassilev, Geoffrey M. Wahl. Hdmx modulates the outcome of p53 activation in human tumor cells. *In press*.

Wong ET, Kolman JL, Li YC, Hillen W, Wahl G. High level tetracycline-inducible transgene expression at a single genomic locus introduced by Cre-recombinase cassette exchange. Nucleic Acids Res 33:e147 (2005)

Lee AT, Ren J, **Wong ET**, Ban KH, Lee LA, Lee CG. The hepatitis B virus X protein sensitizes HEPG2 cells to UV-induced DNA damage. JBC 280: 33525-35 (2005)

Wong ET, Ngoi SM, Lee CG. Improved co-expression of multiple genes in vectors containing internal ribosome entry sites (IRESes) from human genes. Gene Ther, 9(5):337-44 (2002).

Tang BL, Ong YS, Huang B, Wei S, **Wong ET**, Qi R, Horstmann H, Hong W. A membrane protein enriched in endoplasmic reticulum exit sites interacts with COPII. JBC 276:4008-17 (2001).

Tang BL, Zhang T, Low DYH, **Wong ET**, Horstmann H, Hong W. Mammalian homologues of yeast Sec31p: an ubiquitously expressed form is localized to ER exit sites and is essential for ER-Golgi transport. JBC 275:13597-13604 (2000)

Natesavelalar C, **Wong ET**, Chang CF. Differential oligomerization of membrane-bound CD38/ADP-ribosyl cyclase in porcine heart microsomes. Biochem. Mol. Bio. Int, 44(6) 1225-1233 (1998).

ABSTRACT OF THE DISSERTATION

The impact of cell architecture on activation and output of the p53 stress response

pathway

by

Ee Tsin Wong

Doctor of Philosophy in Biology

University of California, San Diego, 2006

Professor Geoffrey M. Wahl, Chair

Most studies of cell signaling *in vitro* use cells grown as monolayers on rigid and

non-physiological substrata. However, epithelial cells *in vivo* are attached on

malleable extracellular matrix (ECM) and are organized into three dimensional (3D)

structures with the aid of cell-cell and cell-ECM interactions. The rigidity of the ECM

and the 3D cellular architecture have a profound influence on cell growth, survival and

differentiation mediated through changes in cell signaling and gene transcription. P53

is a transcription factor capable of responding to a variety of stresses and signals. Furthermore, the level of P53 negative regulator Hdm2 is influenced by mitogenic signalings from the environment. Since the activity of P53 is influenced by the levels of its upstream regulators, changes in cell architecture may influence Hdm2 level and P53 activity. To study the modulation of P53 activity by different transgenes, an improved Cre-loxP recombination system was characterized. The new LoxP site (designated L3), which when used with the original LoxP site (designated L2), allows highly efficient and directional replacement of chromosomal DNA at a defined locus with incoming DNA. When used in combination with a stringent inducible system, the level of transgene expression can be controlled at physiologically relevant levels in an *in vitro* setting. The study of the influence of cell architecture and the impact of neighboring stromal cells on P53 activity and levels of its upstream regulators were described in subsequent chapters. We found that cells grown in 3D were more resistant to apoptosis induced by a combination of doxorubicin and Nutlin. The sensitivity to apoptosis correlated with the efficiency of Hdmx downregulation. Lowering Hdmx level by shRNA in 3D cells sensitizes these cells to apoptosis induced by doxorubicin and Nutlin. Hence, the cell architecture is one factor to consider in determining the efficacy of chemotherapeutic agents as it can impact on Hdmx level to reduce P53-dependent apoptosis.

I

Introduction

Introduction

P53 and its regulation

P53 is a critical tumor suppressor that maintains genetic stability and inhibits tumorigenesis. Loss of function through mutations of the *p53* gene are found in about 50% of sporadic human cancers (Hollstein et al., 1991; Levine et al., 1991). Although P53 may induce apoptosis by non-transcriptional mechanisms (Caelles et al., 1994; Chipuk et al., 2004; Marchenko et al., 2000), the main function of P53 as a transcriptional regulator is critical for effective tumor suppression (reviewed in (Wahl et al., 2005)). P53 protein consists of an N-terminal transactivation domain (TAD), a central DNA binding domain (DBD) and a C-terminal tetramerization domain. The active DNA binding form of P53 is a tetramer, which recognizes and binds the P53 DNA consensus recognition element (RE) (Friedman et al., 1993; McLure and Lee, 1998). The RE consists of two half-sites separated by 0-13 nucleotides and each half-site consists of inverted repeats ($\rightarrow\leftarrow$) of pentameric sequence (AGPuCATGPyCC, where Pu:Purine and Py:pyrimidine) (revised in (Wei et al., 2006)).

P53 function in tumors that retain the wild-type *p53* allele may be compromised due to overexpression of its negative regulators (Hdm2 and Hdmx, which designate the human form of mouse proteins, Mdm2 and Mdmx). Upon exposure to stress, such as DNA damage and oncogene activation, P53 protein is stabilized and can activate or repress target genes. This can lead to either cell cycle arrest, apoptosis, senescence or DNA repair, thereby preventing aberrant cells from proliferating. See figure 1.1 for a summary of P53 regulation in unstressed and stressed cells.

Regulation of P53 stability by Hdm2

Due to the detrimental effect of activated P53 on cell cycle progression and cell survival, P53 activity must be carefully regulated. Hdm2 is a major negative regulator of P53. *Mdm2*-null is embryonic lethal and lethality is rescued by concomitant *p53* deficiency (Jones et al., 1995; Montes de Oca Luna et al., 1995). The N-terminal of Hdm2 binds P53 and inhibits its transactivation function (Momand et al., 1992). Additionally, Hdm2 has a C-terminal RING-finger domain that is required for promoting P53 ubiquitination and subsequent degradation by the proteasome (Haupt et al., 1997; Honda et al., 1997; Kubbutat et al., 1997). Beside Mdm2, other E3 ubiquitin ligases have also been reported to regulate P53 ubiquitination and stability (see Table 1.1).

The pathways that moderate the level and activity of Hdm2 in a cell can dramatically affect P53 activation. Hdm2 is overexpressed or amplified in many human cancers (Momand et al., 1998; Reifenberger et al., 1993) and overexpression antagonizes P53 function and promotes tumorigenesis (Bond et al., 2004; Jones et al., 1998; Oliner et al., 1992). Moreover, the presence of single nucleotide polymorphism in the *hdm2* promoter region can increase Hdm2 expression in an estrogen receptor dependent manner and predisposes some premenopausal women in the population to a higher risk of breast cancer development (Bond et al., 2004). Conversely, lowering Mdm2 level potentiates P53 activation and induction of apoptosis and cell cycle arrest (Mendrysa et al., 2003).

In unstressed cells, the level of Hdm2 is regulated at both the transcriptional level and at the level of protein stability. Mitogenic signaling via MAPK (Erk)

promotes *hdm2* gene transcription (Ries et al., 2000), while Akt directly phosphorylates Hdm2 to enhance the protein stability (Ashcroft et al., 2002; Gottlieb et al., 2002). Hdm2 protein stability is also a balance of self-ubquitination (Stommel and Wahl, 2004) and deubiquitination by HAUSP (*H*erpes *v*irus *a*ssociated *u*biquitin *s*pecific *p*rotease) (Cummins et al., 2004; Li et al., 2004; Li et al., 2002b). For P53 activation after DNA damage, phosphorylation of Hdm2 mediated by ATM and other kinases leads to HAUSP dissociation from Hdm2 which leads to further ubiquitination and destabilization of Hdm2 (Meulmeester et al., 2005; Stommel and Wahl, 2004). The highly unstable Hdm2 can no longer effectively antagonize P53, leading to P53 accumulation and activation (Stommel and Wahl, 2004). Activated P53 also leads to increased transcription of downstream genes including Hdm2. The accumulation of Hdm2 after stress functions in a negative feedback loop to switch off P53 after the noxious stress is removed.

Induction of apoptosis after DNA damage plays a role in tumor regression in response to conventional chemotherapy. About 50% of human cancers retain the wildtype *p53* gene, giving rise to the opportunity for activating P53 function in these cells as a therapeutic approach to selectively kill cancer cells. However, DNA damaging agents have undesirable side effects, including damage to nonmalignant cells, and mutagenic effects which create the potential for development of secondary malignancies. This has fueled the search for less toxic alternatives. Recently, the development of small molecules that disrupt P53-Hdm2 interactions has created new opportunities for cancer therapies. The cis-imadazoline compound (Nutlin) binds Hdm2 and blocks Hdm2 interaction with P53 and can activate P53 in cancers that

over-express Hdm2 (Vassilev et al., 2004). When used alone (Vassilev et al., 2004) or in combination with genotoxic agents (Coll-Mulet et al., 2006; Secchiero et al., 2006; Stuhmer et al., 2005), Nutlin reduces tumor cell survival and blocks tumor progression. However, not all tumors with wildtype *p53* undergo apoptosis in response to Nutlin, suggesting that pathways downstream of P53 may be defective or that pro-survival signals dominate in certain contexts. Elucidation of the factors that determine sensitivity to this novel class of p53 activating drugs may thus provide novel targets for future chemotherapies.

Regulation of P53 by Hdmx

Mdmx is also a critical negative regulator of P53 as gene ablation is associated with P53-dependent embryonic lethality in mice (Finch et al., 2002; Migliorini et al., 2002b; Parant et al., 2001). Human tumors and cancer cell lines with wild-type *p53* often overexpress Hdmx (Danovi et al., 2004; Ramos et al., 2001; Riemenschneider et al., 1999), suggesting that Hdmx overexpression may attenuate P53 activation during tumorigenesis. Therefore, understanding the mechanisms behind Hdmx function and regulation is important for the design of therapeutics to reactivate P53 in tumors that overexpress Hdmx.

Mdmx has a high degree of homology with Mdm2 especially in the P53 binding domain (Shvarts et al., 1996). Mdmx binds P53 at the N-terminal transactivation domain and inhibits its transactivation function. Embryonic lethality seen in either Mdm2 or Mdmx ablation suggests the critical function of both proteins in the negative regulation of P53 and that Mdm2 and Mdmx have non-overlapping

functions such that neither can substitute for the loss of the other. Furthermore, tissue specific knockouts in the brain emphasize the non-redundant role of Mdm2 and Mdmx in the same cell types in the negative regulation of P53 (Francoz et al., 2006; Xiong et al., 2006). Loss of *mdmx* by gene knockout results in increased transactivation of target genes and enhanced cell cycle arrest or apoptosis in some cell types (Finch et al., 2002; Francoz et al., 2006; Migliorini et al., 2002b; Parant et al., 2001; Xiong et al., 2006). In contrast to Mdm2, Mdmx expression is not induced by P53 (Shvarts et al., 1996) and it lacks ubiquitin E3 ligase activity and therefore does not directly control P53 stability (Stad et al., 2001). Instead, Hdmx is a critical inhibitor of P53 transcription. In the absence of Mdmx, Mdm2 alone is insufficient to inhibit P53 because it is not an effective inhibitor of P53 transactivation and there may not be sufficient Mdm2 around as it is an unstable protein. On the other hand, conditional Mdm2 knockout mouse models indicate a more important role of Mdm2 in the negative regulation of P53 stability (Francoz et al., 2006; Toledo et al., 2006; Xiong et al., 2006). In the absence of Mdm2, P53 is stabilized and accumulates to high level, more than the endogenous level of Mdmx can handle.

The stability of Hdmx is regulated by the balance between Hdm2 (E3 ubiquitin enzyme) and HAUSP (de-ubiquitinating enzyme) activity. The downregulation of Hdmx is required for P53 activation following DNA damage, as overexpression of Hdmx attenuates induction of Hdm2 and P21CIP (Kawai et al., 2003) while knockdown by shRNA potentiates P53 activation (Chen et al., 2005). Mdmx can interact with Mdm2 through their respective RING finger domains (Stad et al., 2001). The destabilization of Mdmx after DNA damage is promoted by Mdm2-dependent

ubiquitination and requires the RING finger domain of Mdm2 (de Graaf et al., 2003; Kawai et al., 2003; Pan and Chen, 2003). In unstressed cells, HAUSP also interacts with and deubiquitinates Hdmx, leading to Hdmx stabilization (Meulmeester et al., 2005). Upon stress, Hdmx is phosphorylated at positions serine 342, serine 367, and serine 403 by damage-activated ATM and Chk2 kinases (Chen et al., 2005; Pereg et al., 2005). Phosphorylation promotes HAUSP dissociation from Hdmx (Meulmeester et al., 2005), leading to ubiquitination and degradation of Hdmx by the proteasome. Hdmx phosphorylated at serine 367 promotes 14-3-3 binding and this is associated with Hdmx degradation, although the mechanism remains unclear (LeBron et al., 2006; Okamoto et al., 2005).

The efficiency of Hdmx degradation may be affected by its subcellular localization. Transfection and overexpression studies indicate that Hdmx is mainly cytoplasmic in unstressed cells (Gu et al., 2002; Li et al., 2002a; Migliorini et al., 2002a). Endogenous Hdmx also appears to be predominantly cytosolic in some cell types (Rallapalli et al., 1999). DNA damage promotes entry of Hdmx into the nucleus and this is dependent on Hdm2 and requires the RING domain of Hdm2 (Li et al., 2002a; Pan and Chen, 2003). Hdmx protein with a serine-to-alanine mutation at residue 367 is relatively stable and does not accumulate in the nucleus after DNA damage as compared to the wildtype protein (LeBron et al., 2006). Consistent with this, the phosphorylated form of Hdmx is preferentially localized in the nucleus after DNA damage (LeBron et al., 2006). These data suggest that Hdmx is phosphorylated by damage-induced kinases, interacts with Hdm2 and possibly with other proteins and is retained in the nucleus where it is rapidly degraded. However, it is presently unclear

how Hdmx shuttles between the nucleus and the cytoplasm and how phosphorylation affects shuttling or nuclear retention. More puzzling is why Hdmx is preferentially brought into the nucleus after DNA damage where P53 is to be activated? Studies using Hdmx phosphorylation mutants or RING domain mutants that can potentially interfere with Hdm2 interaction, nuclear entry or its degradation will provide further insights into the mechanism of Hdmx regulation.

Both genetic and biochemical studies emphasize the critical role of Mdmx in negative regulation of P53. A recent large-scale analysis of human tumor samples indicated overexpression of Hdmx mRNA in a significant percentage of tumor types (Danovi et al., 2004). Additionally, in tumors with wildtype *p53*, *hdmx* and *hdm2* gene amplification are mutually exclusive. Overexpression of Mdmx in mouse embryonic fibroblasts (MEF) causes cell immortalization and transformation in combination with H-Ras^{V12} (Danovi et al., 2004). The ability of cells to respond to genotoxic and non-genotoxic activators of P53 can also be affected by Hdmx level. Lowering Hdmx level by shRNA enhances P53 activation and cell cycle arrest after IR (Chen et al., 2005). The efficiency of the Mdm2 antagonist, Nutlin, to inhibit tumor cell growth is also affected by the level of Hdmx expression since Nutlin does not dissociate Hdmx from P53 (Patton et al., 2006). These data suggests that downregulation of Hdmx should be considered as a new chemotherapeutic strategy.

Normal tissue architecture and homeostasis

Most human cancers originate from epithelial cells, and the survival of epithelial cells and their responses to cancer therapies can be profoundly influenced by

tissue architecture, cell-cell and cell-extracellular matrix (ECM) attachment (Zahir and Weaver, 2004). Yet, it is unknown if the activation and output of the P53 pathway is affected by the three-dimensional (3D) structural organization of the tissue.

Epithelial cells make up the linings of our body surfaces and internal organs. Epithelial type organs are composed of cells organized to form 3D structures such as cysts and tubules (reviewed in O'Brien *el al* (O'Brien et al., 2002)). Cysts (found in the mammary gland, lung and thyroid) are spherical monolayers of cells that enclose a central lumen, while tubules are cylindrical tubes with central hollow lumens. The fundamental property of the epithelial cell architecture is their polarized nature; cells have lumen facing apical surfaces, lateral surfaces that adhere to neighboring cells and basal surfaces that adhere to the ECM. With the aid of cell-cell and cell-ECM adhesion molecules, the intracellular cytoskeleton networks are connected between cells and with the ECM to form a unifying structural and functional unit. The ECM is a fibrous network of proteins embedded in a visco-elastic gel consisting of proteoglycans, glycosaminoglycans and glycoproteins. Collagens and fibronectins that form part of the fibrous network serve as mechanical platforms for cell attachment and movement. The cytoskeleton is a network of fibrous proteins (actin, intermediate filaments and microtubules) found in the cytosol of all mammalian cells. It provides the mechanical framework and tensile strength for the cell, coordinates cell movements, facilitates intracellular transport and allows separation of chromosomes during mitosis. Adhesion molecules are transmembrane proteins, which consist of a ligand-binding extra-cellular domain and a cytoskeleton-binding intracellular domain.

Cadherins and integrins are the 2 major families of adhesion molecules. Cadherins are proteins that mediate cell-cell adhesion while integrins mediate cell-ECM adhesion.

Importance of form and function- tensegrity

The basic concept of the tensegrity model states that the interactions between various cytoskeleton components influences the behavior of the connected cells (Discher et al., 2005; Huang and Ingber, 1999; Ingber, 2003) (Figure 1.2). Tensional forces and mechanical distortions from the environment are sensed via cell surface receptors, which induce alterations in the cytoskeletal structures and trigger biochemical responses. Ultimately, this leads to changes in signal transduction and gene expression and may dictate cell fate (Huang et al., 1998; Lelievre et al., 1998; Maniotis et al., 1997; Wang et al., 1998). The tensegrity model may in part explain why a particular stress can have context-dependent effects. An attached cell is in a state of "isometric tension" when tensional forces from the cytoskeleton balance the tensional forces from the ECM. Hence, the cellular response to the same degree of stress may differ depending on the initial isometric tension in the cell. Integration of tensional signals with biochemical signals from growth factors and ECM will then determine cell fate. A classical example that illustrates the tensegrity model is that endothelial cells divide when spread on solid surfaces (high tension force from substratum), will die when given limited adhesion (low tension force) or can differentiate into hollow capillary tubes when subjected to an intermediate degree of spreading or tension (Chen et al., 1997; Dike et al., 1999; Folkman and Moscona, 1978; Huang et al., 1998; Ingber, 2003).

Altered tissue architecture and malignant phenotype

The balance of structural and tensional cues between the cells and their environment is disrupted in solid tumors. Compared to the soft malleable tissue with organized and polarized architecture found in the normal organ, a tumor is a stiff mass (Bercoff et al., 2003; McKnight et al., 2002) composed of cells with disrupted architecture that exhibit loss of polarity. The rigidity or stiffness of the tumor mass is attributed to an increased solid pressure from tumor expansion (Padera et al., 2004), increased interstitial fluid pressure from altered tumor vasculature (Padera et al., 2004), altered elasticity of cells due to altered cytoskeleton architecture (Beil et al., 2003), and increased matrix rigidity due to fibrosis (or enhanced ECM deposition) (Paszek et al., 2005). The solid tumor mass and fibrotic lesions constitute the electron dense (or high density) areas of mammogram, and high density mammograms are often associated with increased risk for breast cancer development (Vacek and Geller, 2004). However, the molecular mechanisms linking tumor rigidity or fibrosis with tumor behavior is less clear. The stiffness of the ECM is likely to influence the behavior of the attached cells via ECM receptors called integrins.

Tumor/ECM rigidity has a direct impact on growth factor receptors and integrin signaling to influence the proliferation and morphogenesis of epithelial cells. A malleable ECM reduces mitogenic signaling and promotes growth arrest and morphogenesis of the attached cells (Paszek et al., 2005; Wang et al., 1998), which is consistent with normal differentiation and function of the tissue. Conversely, a rigid matrix promotes assembly of focal adhesion complexes and triggers mitogenic signaling and cell proliferation, but prevents morphogenesis of mammary epithelial

cells (Paszek et al., 2005), consistent with a phenotype associated with malignant growth. Tumor/ECM rigidity may also influence the efficacy of anti-cancer treatment (Desoize and Jardillier, 2000). The penetration of therapeutic drugs into the interior of the tumor mass can be reduced due to increased collagen deposits around the tumor or compression of intratumoral blood and lymphatic vessels (Netti et al., 2000; Padera et al., 2004). Cells within spheroids (spherical aggregates of cells) are more resistant to apoptosis, perhaps due to increased pro-survival or decreased anti-apoptotic signals (Frankel et al., 1997; Weaver et al., 2002). In addition, cells within spheroids are more resistant to drugs that perturb DNA replication or transcription due to lower rates of proliferation and transcription in these structures (Desoize and Jardillier, 2000).

Due to the ease of genetic and biochemical manipulations, *in vitro* 3D cell culture has provided many insights into the influence of matrix rigidity on signal transduction and cell fate. Cells in 3D growth are more representative of the topology of cells found *in vivo* than cells grown in monolayers. Hence, evaluation of chemotherapeutics in 3D cell culture systems may be more representative of the response *in vivo*.

Mammary acinus as a tool to study the influence of cell architecture on cellular functions

The normal human breast is a modified sweat gland consisting of epithelial cells arranged as a branched ductal network that is surrounded by a "stroma" consisting of adipose cells, fibroblasts, blood vessels, ECM and proteoglycan. With the onset of puberty, the ducts extend and branch into the stromal space, and small

grapelike structures called alveoli (or lobuloalveoli, acini or terminal ductal lobular units) are formed at the ends of the branching ducts. Each acinus is composed of an inner monolayer of luminal epithelial cells surrounding a central hollow lumen, interspersed with myoepithelial cells on the outer layer and rested upon a complex ECM called basement membrane.

Normal mammary epithelial cells differentiate into functional 3D units resembling mammary acini when they are cultured *in vitro* in the presence of basement membrane-type ECM. The ECM extracted from EHS (Engelbreth-Holm-Swarm) tumors or the commercially available matrigel, is a complex mixtures of different ECM including the key ECM component, laminin (Gudjonsson et al., 2002), which supports the formation of polarized spheres with central lumens (Petersen et al., 1992). Several experiments confirm that this 3D culture system more closely recapitulates the situation *in vivo* compared to studies using cells grown in 2D *in vitro*. For example, in the presence of lactogenic hormones, HMECs (Human mammary epithelial cells) form polarized acini capable of producing and secreting β-casein (the protein found in milk) when cultured in 3D while non-polarized cells in 2D do not (Roskelley et al., 1994). Cells in 3D also undergo apoptosis and autophagy during lumen formation, processes that are also observed during organismal development and tissue remodeling (Jin and El-Deiry, 2005). Cells in 2D and 3D also differ with respect to mitogenic and cell survival signaling. Even though PI3-K, AKT and ERK pathways are key signaling events regulating cell survival in 2D, cells in 3D downregulate the expression and activity of β1-integrin, EGFR (Delcommenne and Streuli, 1995; Wang et al., 1998), Erk (Wang et al., 1998), AKT and FAK (Paszek et al., 2005). Hence

inhibiting AKT signaling only modestly compromises HMEC survival in 3D (Zahir et al., 2003). Instead, other prosurvival signaling such as NFκB signaling plays important role in protecting 3D cells from apoptosis in response to noxious stresses (Weaver et al., 2002). Clearly, the 3D culture system has the potential of revealing differences in signaling and cellular responses that are not observed in the conventional 2D culture system.

However, we should also be aware that the HMEC 3D culture system is only a simplified model of the mammary acini. As it lacks myoepithelial cells and the surrounding stromal cells, more complex co-culture systems are available to enable ones to probe paracrine and cell-cell signalings in mammary development and cancer progression (Gudjonsson et al., 2003; Gudjonsson et al., 2002; Parrinello et al., 2005).

Scope of thesis

Work done in fulfillment of the PhD degree is divided into 3 parts. The first involves the characterization of an improved loxP sequence for the reproducible and high efficiency integration of a transgene into a defined genomic locus. The second, which constitutes the main part of the thesis involves the investigation of the impact of epithelial cell architecture on P53 activation by genotoxic and non-genotoxic agents. The final part aims to investigate the influence of stromal fibroblasts in co-culture on epithelial cell morphogenesis and P53 stress response.

Mouse models and *in vitro* transfection studies show that small changes in the concentration of factors implicated in P53 regulation can significantly influence its stability and functional output (Gu et al., 2002; Mendrysa et al., 2003). More

importantly, the regulation of the activity and abundance of Hdm2 and Hdmx are crucial for the appropriate and timely regulation of P53 under stressful conditions. The approach in Chapter 2 describes the characterization of an improved LoxP recombination system which, when used in combination with the tetracycline-inducible system allows for the reproducible, uniform and inducible expression of a transgene in stable clones that were derived at high frequencies through Cre-mediated integration of transgene at a single chromatin site. Using this system, the mechanisms whereby Hdm2 and Hdmx regulate P53 can be studied through the expression of various Hdm2/x mutants at physiologically relevant expression levels.

Epithelial cells in our body are organized into 3D structures. Studies have shown that the rigidity of the ECM and the 3D structures of the cells can impact on cell survival signaling. To closely mirror the tissue structure *in vivo* and drugs commonly used in breast cancer therapy, we compared immortalized mammary epithelial cells cultured in 2D and 3D and evaluated the influence of cell architecture on P53 regulation in response to genotoxic and non-genotoxic activators of P53 in chapter 3 of the thesis. Cells in 3D exhibited lower Hdmx and higher P53 protein levels than 2D cells. However, the data show that the DNA damage response and P53 transactivation of p21CIP, Hdm2 and PUMA are similar in cells cultured in 2D and 3D. The ability of cells to undergo cell cycle arrest after IR or apoptosis in response to doxorubicin are also similar when cultured in 2D and 3D. Nutlin, a Hdm2 antagonist, also activated most of the P53 downstream genes examined equally well when cultured in 2D and 3D. However, when doxorubicin is combined with Nutlin, 2D cells were more sensitive to apoptosis. This raised the important question of which factor(s)

compromise P53 activation in 3D cells. Further analysis showed that Hdmx is downregulated more effectively in 2D cells. ECM attachment alone does not confer resistance to doxorubicin and Nutlin. Lowering Hdmx level by shRNA in 3D cells sensitizes these cells to apoptosis induced by doxorubicin and Nutlin. Hence, Hdmx serves as a buffer to prevent P53-dependent apoptosis and signals from the cell architecture or cell-cell adhesion may impact on the pathways that regulate Hdmx stability. This study demonstrates the importance of Hdmx level in dictating the epithelial cells response to P53 activating agents. As approximately 50% of tumors retain wild-type *p53* gene and that most cancers arise in epithelial tissues, such studies may have significant impact on our understanding of how cancer cells respond to chemotherapy and how drug resistance may arise.

Epithelial cancers arise and progress as a result of the cooperation between the cancerous epithelial cells and their microenvironment. Other than the ECM, the stromal compartment which also includes the fibroblasts, endothelial cells and immune cells are also altered in the cancer state (Allinen et al., 2004; Hu et al., 2005). In chapter 4, the role of mammary fibroblasts on epithelial cells' ability to form acini and their responses to genotoxic stresses were evaluated in the *in vitro* coculture system. Thus far, the data indicates that coculture with mammary fibroblasts or their conditioned culture media alter the ability of immortalized mammary epithelial cells to form acini in matrigel but the epithelial cells' ability to arrest in response to IR is unaffected.

Figure 1.1: P53 regulation in unstressed and stressed state

In an unstressed state, P53 is low in abundance and inactive due to negative regulation by the two major inhibitors, Mdm2 and Mdmx. Mdm2's main function is an E3 ubiquitin ligase to promote ubiquitin-dependent proteasomal degradation of P53. Even though Mdm2 can bind the N-terminal transactivation domain of P53, it is a weak inhibitor of P53 transactivation. Instead, Mdmx which also binds the same region of P53 as Mdm2, is the major antagonist of P53 output. Mdm2 can self-ubiquitinate or ubiquitinate Mdmx, but both proteins are maintained relatively more stable than in the stressed state due to their binding to and de-ubiquitination by HAUSP. After DNA damage, P53, Mdm2 and Mdmx undergo a series of post-translational modifications. HAUSP dissociates from Mdm2 and Mdmx and the target specificity of Mdm2 is changed so that Mdm2 preferentially targets itself and Mdmx for degradation, enabling P53 to be stabilized and activated. Activated P53 turns on a number of downstream target genes including Mdm2. Mdm2 accumulation serves two roles, first, it participates in a feed forward loop to enhance Hdmx degradation and hence P53 activation; second, Hdm2 participates in a feedback loop to degrade P53 and returns P53 to the basal level after the stress is removed. HAUSP reassociates with Mdm2 and Mdmx and the stability of Mdm2 and Mdmx reverts back to the unstressed state.
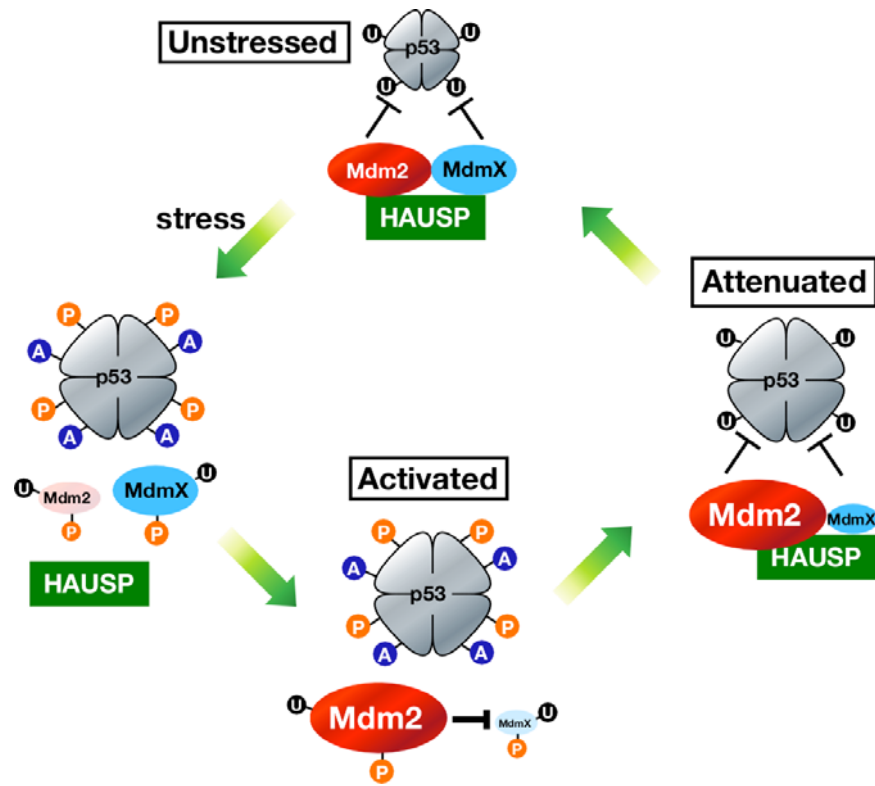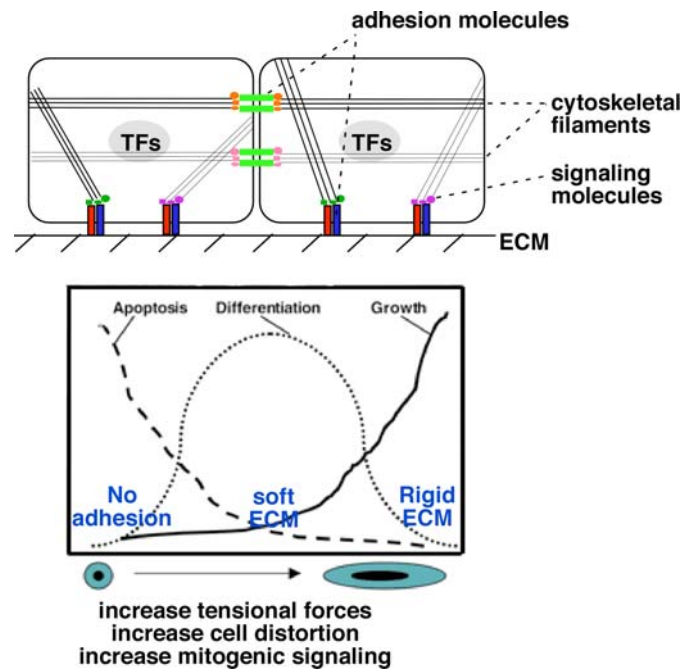
Figure 1.2: Tensegrity model and how it influences cell behavior

Cells form connections with neighboring cells and ECM through cell adhesion molecules. The cell adhesion molecules are also connecting points where the exterior of the cells are connected to the intracellular signaling molecules and cytoskeletal filaments. Through the cytoskeletal filaments, mechanical tension and forces are generated upon cell-cell and cell-ECM adhesion. The ECM can transmit forces to the cell interior via the cell adhesion molecules and cytoskeletal filaments (outside-in signaling) and vice versa (inside-out signaling). Increasing the rigidity of the ECM will generate higher tensional forces and greater mechanical distortion within the attached cells. This in turn can influence intracellular signaling and gene transcription events to influence the cell fate. TFs: transcription factors.

Table 1.1: E3 ubiquitin ligases of P53

NA: Not availbale

E3 Ubiquitin ligase	Type	Expression	Feedback Loop	Mode of inactivation during stress	Loss of function phenotype	Overexpression	References
Mdm2	RING	Ubiquitious	Yes	Destabilization, dissociation from P53	embryonic lethal, rescued by p53-null	7% amplification in all cancers	Jones, 1995; Momand, 1992; Haupt, 1997; Stommel, 2004
Pirh2	RING	low in brain, spleen, muscle	Yes	NA	RNAi slightly stabilizes p53	84% lung cancers	Leng, 2003; Duan 2004
COP1	RING	Ubiquitious	Yes	Destabilization, dissociation from P53	embryonic lethal; not rescued by p53-null	81% Breast cancer; 44% ovarian cancers	Dornan, 2004,2006
ARF-BP1	HECT	Ubiquitious	No	ARF inhibits ubiquitin ligase activity	RNAi enhances death in U2OS	80% breast cancer cell lines	Chen, 2005

References

Allinen, M., Beroukhim, R., Cai, L., Brennan, C., Lahti-Domenici, J., Huang, H., Porter, D., Hu, M., Chin, L., Richardson, A.*, et al.* (2004). Molecular characterization of the tumor microenvironment in breast cancer. Cancer Cell *6*, 17-32.

Ashcroft, M., Ludwig, R. L., Woods, D. B., Copeland, T. D., Weber, H. O., MacRae, E. J., and Vousden, K. H. (2002). Phosphorylation of HDM2 by Akt. Oncogene *21*, 1955-1962.

Beil, M., Micoulet, A., von Wichert, G., Paschke, S., Walther, P., Omary, M. B., Van Veldhoven, P. P., Gern, U., Wolff-Hieber, E., Eggermann, J.*, et al.* (2003). Sphingosylphosphorylcholine regulates keratin network architecture and visco-elastic properties of human cancer cells. Nat Cell Biol *5*, 803-811.

Bercoff, J., Chaffai, S., Tanter, M., Sandrin, L., Catheline, S., Fink, M., Gennisson, J. L., and Meunier, M. (2003). In vivo breast tumor detection using transient elastography. Ultrasound Med Biol *29*, 1387-1396.

Bond, G. L., Hu, W., Bond, E. E., Robins, H., Lutzker, S. G., Arva, N. C., Bargonetti, J., Bartel, F., Taubert, H., Wuerl, P.*, et al.* (2004). A single nucleotide polymorphism in the MDM2 promoter attenuates the p53 tumor suppressor pathway and accelerates tumor formation in humans. Cell *119*, 591-602.

Caelles, C., Helmberg, A., and Karin, M. (1994). p53-dependent apoptosis in the absence of transcriptional activation of p53-target genes. Nature *370*, 220-223.

Chen, C. S., Mrksich, M., Huang, S., Whitesides, G. M., and Ingber, D. E. (1997). Geometric control of cell life and death. Science *276*, 1425-1428.

Chen, L., Gilkes, D. M., Pan, Y., Lane, W. S., and Chen, J. (2005). ATM and Chk2-dependent phosphorylation of MDMX contribute to p53 activation after DNA damage. Embo J *24*, 3411-3422.

Chipuk, J. E., Kuwana, T., Bouchier-Hayes, L., Droin, N. M., Newmeyer, D. D., Schuler, M., and Green, D. R. (2004). Direct activation of Bax by p53 mediates mitochondrial membrane permeabilization and apoptosis. Science *303*, 1010-1014.

Coll-Mulet, L., Iglesias-Serret, D., Santidrian, A. F., Cosialls, A. M., de Frias, M., Castano, E., Campas, C., Barragan, M., de Sevilla, A. F., Domingo, A.*, et al.* (2006). MDM2 antagonists activate p53 and synergize with genotoxic drugs in B-cell chronic lymphocytic leukemia cells. Blood *107*, 4109-4114.

Cummins, J. M., Rago, C., Kohli, M., Kinzler, K. W., Lengauer, C., and Vogelstein, B. (2004). Tumour suppression: disruption of HAUSP gene stabilizes p53. Nature *428*, 1 p following 486.

Danovi, D., Meulmeester, E., Pasini, D., Migliorini, D., Capra, M., Frenk, R., de Graaf, P., Francoz, S., Gasparini, P., Gobbi, A.*, et al.* (2004). Amplification of Mdmx (or Mdm4) directly contributes to tumor formation by inhibiting p53 tumor suppressor activity. Mol Cell Biol *24*, 5835-5843.

de Graaf, P., Little, N. A., Ramos, Y. F., Meulmeester, E., Letteboer, S. J., and Jochemsen, A. G. (2003). Hdmx protein stability is regulated by the ubiquitin ligase activity of Mdm2. J Biol Chem *278*, 38315-38324.

Delcommenne, M., and Streuli, C. H. (1995). Control of integrin expression by extracellular matrix. J Biol Chem *270*, 26794-26801.

Desoize, B., and Jardillier, J. (2000). Multicellular resistance: a paradigm for clinical resistance? Crit Rev Oncol Hematol *36*, 193-207.

Dike, L. E., Chen, C. S., Mrksich, M., Tien, J., Whitesides, G. M., and Ingber, D. E. (1999). Geometric control of switching between growth, apoptosis, and differentiation during angiogenesis using micropatterned substrates. In Vitro Cell Dev Biol Anim *35*, 441-448.

Discher, D. E., Janmey, P., and Wang, Y. L. (2005). Tissue cells feel and respond to the stiffness of their substrate. Science *310*, 1139-1143.

Finch, R. A., Donoviel, D. B., Potter, D., Shi, M., Fan, A., Freed, D. D., Wang, C. Y., Zambrowicz, B. P., Ramirez-Solis, R., Sands, A. T., and Zhang, N. (2002). mdmx is a negative regulator of p53 activity in vivo. Cancer Res *62*, 3221-3225.

Folkman, J., and Moscona, A. (1978). Role of cell shape in growth control. Nature *273*, 345-349.

Francoz, S., Froment, P., Bogaerts, S., De Clercq, S., Maetens, M., Doumont, G., Bellefroid, E., and Marine, J. C. (2006). Mdm4 and Mdm2 cooperate to inhibit p53 activity in proliferating and quiescent cells in vivo. Proc Natl Acad Sci U S A *103*, 3232-3237.

Frankel, A., Buckman, R., and Kerbel, R. S. (1997). Abrogation of taxol-induced G2-M arrest and apoptosis in human ovarian cancer cells grown as multicellular tumor spheroids. Cancer Res *57*, 2388-2393.

Friedman, P. N., Chen, X., Bargonetti, J., and Prives, C. (1993). The p53 protein is an unusually shaped tetramer that binds directly to DNA. Proc Natl Acad Sci U S A *90*, 3319-3323.

Gottlieb, T. M., Leal, J. F., Seger, R., Taya, Y., and Oren, M. (2002). Cross-talk between Akt, p53 and Mdm2: possible implications for the regulation of apoptosis. Oncogene *21*, 1299-1303.

Gu, J., Kawai, H., Nie, L., Kitao, H., Wiederschain, D., Jochemsen, A. G., Parant, J., Lozano, G., and Yuan, Z. M. (2002). Mutual dependence of MDM2 and MDMX in their functional inactivation of p53. J Biol Chem *277*, 19251-19254.

Gudjonsson, T., Ronnov-Jessen, L., Villadsen, R., Bissell, M. J., and Petersen, O. W. (2003). To create the correct microenvironment: three-dimensional heterotypic collagen assays for human breast epithelial morphogenesis and neoplasia. Methods *30*, 247-255.

Gudjonsson, T., Ronnov-Jessen, L., Villadsen, R., Rank, F., Bissell, M. J., and Petersen, O. W. (2002). Normal and tumor-derived myoepithelial cells differ in their ability to interact with luminal breast epithelial cells for polarity and basement membrane deposition. J Cell Sci *115*, 39-50.

Haupt, Y., Maya, R., Kazaz, A., and Oren, M. (1997). Mdm2 promotes the rapid degradation of p53. Nature *387*, 296-299.

Hollstein, M., Sidransky, D., Vogelstein, B., and Harris, C. C. (1991). p53 mutations in human cancers. Science *253*, 49-53.

Honda, R., Tanaka, H., and Yasuda, H. (1997). Oncoprotein MDM2 is a ubiquitin ligase E3 for tumor suppressor p53. FEBS Lett *420*, 25-27.

Hu, M., Yao, J., Cai, L., Bachman, K. E., van den Brule, F., Velculescu, V., and Polyak, K. (2005). Distinct epigenetic changes in the stromal cells of breast cancers. Nat Genet *37*, 899-905.

Huang, S., Chen, C. S., and Ingber, D. E. (1998). Control of cyclin D1, p27(Kip1), and cell cycle progression in human capillary endothelial cells by cell shape and cytoskeletal tension. Mol Biol Cell *9*, 3179-3193.

Huang, S., and Ingber, D. E. (1999). The structural and mechanical complexity of cell-growth control. Nat Cell Biol *1*, E131-138.

Ingber, D. E. (2003). Tensegrity II. How structural networks influence cellular information processing networks. J Cell Sci *116*, 1397-1408.

Jin, Z., and El-Deiry, W. S. (2005). Overview of cell death signaling pathways. Cancer Biol Ther *4*, 139-163.

Jones, S. N., Hancock, A. R., Vogel, H., Donehower, L. A., and Bradley, A. (1998). Overexpression of Mdm2 in mice reveals a p53-independent role for Mdm2 in tumorigenesis. Proc Natl Acad Sci U S A *95*, 15608-15612.

Jones, S. N., Roe, A. E., Donehower, L. A., and Bradley, A. (1995). Rescue of embryonic lethality in Mdm2-deficient mice by absence of p53. Nature *378*, 206-208.

Kawai, H., Wiederschain, D., Kitao, H., Stuart, J., Tsai, K. K., and Yuan, Z. M. (2003). DNA damage-induced MDMX degradation is mediated by MDM2. J Biol Chem *278*, 45946-45953.

Kubbutat, M. H., Jones, S. N., and Vousden, K. H. (1997). Regulation of p53 stability by Mdm2. Nature *387*, 299-303.

LeBron, C., Chen, L., Gilkes, D. M., and Chen, J. (2006). Regulation of MDMX nuclear import and degradation by Chk2 and 14-3-3. Embo J *25*, 1196-1206.

Lelievre, S. A., Weaver, V. M., Nickerson, J. A., Larabell, C. A., Bhaumik, A., Petersen, O. W., and Bissell, M. J. (1998). Tissue phenotype depends on reciprocal interactions between the extracellular matrix and the structural organization of the nucleus. Proc Natl Acad Sci U S A *95*, 14711-14716.

Levine, A. J., Momand, J., and Finlay, C. A. (1991). The p53 tumour suppressor gene. Nature *351*, 453-456.

Li, C., Chen, L., and Chen, J. (2002a). DNA damage induces MDMX nuclear translocation by p53-dependent and -independent mechanisms. Mol Cell Biol *22*, 7562-7571.

Li, M., Brooks, C. L., Kon, N., and Gu, W. (2004). A dynamic role of HAUSP in the p53-Mdm2 pathway. Mol Cell *13*, 879-886.

Li, M., Chen, D., Shiloh, A., Luo, J., Nikolaev, A. Y., Qin, J., and Gu, W. (2002b). Deubiquitination of p53 by HAUSP is an important pathway for p53 stabilization. Nature *416*, 648-653.

Maniotis, A. J., Chen, C. S., and Ingber, D. E. (1997). Demonstration of mechanical connections between integrins, cytoskeletal filaments, and nucleoplasm that stabilize nuclear structure. Proc Natl Acad Sci U S A *94*, 849-854.

Marchenko, N. D., Zaika, A., and Moll, U. M. (2000). Death signal-induced localization of p53 protein to mitochondria. A potential role in apoptotic signaling. J Biol Chem *275*, 16202-16212.

McKnight, A. L., Kugel, J. L., Rossman, P. J., Manduca, A., Hartmann, L. C., and Ehman, R. L. (2002). MR elastography of breast cancer: preliminary results. AJR Am J Roentgenol *178*, 1411-1417.

McLure, K. G., and Lee, P. W. (1998). How p53 binds DNA as a tetramer. Embo J *17*, 3342-3350.

Mendrysa, S. M., McElwee, M. K., Michalowski, J., O'Leary, K. A., Young, K. M., and Perry, M. E. (2003). mdm2 Is critical for inhibition of p53 during lymphopoiesis and the response to ionizing irradiation. Mol Cell Biol *23*, 462-472.

Meulmeester, E., Maurice, M. M., Boutell, C., Teunisse, A. F., Ovaa, H., Abraham, T. E., Dirks, R. W., and Jochemsen, A. G. (2005). Loss of HAUSP-mediated deubiquitination contributes to DNA damage-induced destabilization of Hdmx and Hdm2. Mol Cell *18*, 565-576.

Migliorini, D., Danovi, D., Colombo, E., Carbone, R., Pelicci, P. G., and Marine, J. C. (2002a). Hdmx recruitment into the nucleus by Hdm2 is essential for its ability to regulate p53 stability and transactivation. J Biol Chem *277*, 7318-7323.

Migliorini, D., Denchi, E. L., Danovi, D., Jochemsen, A., Capillo, M., Gobbi, A., Helin, K., Pelicci, P. G., and Marine, J. C. (2002b). Mdm4 (Mdmx) regulates p53-induced growth arrest and neuronal cell death during early embryonic mouse development. Mol Cell Biol *22*, 5527-5538.

Momand, J., Jung, D., Wilczynski, S., and Niland, J. (1998). The MDM2 gene amplification database. Nucleic Acids Res *26*, 3453-3459.

Momand, J., Zambetti, G. P., Olson, D. C., George, D., and Levine, A. J. (1992). The mdm-2 oncogene product forms a complex with the p53 protein and inhibits p53-mediated transactivation. Cell *69*, 1237-1245.

Montes de Oca Luna, R., Wagner, D. S., and Lozano, G. (1995). Rescue of early embryonic lethality in mdm2-deficient mice by deletion of p53. Nature *378*, 203-206.

Netti, P. A., Berk, D. A., Swartz, M. A., Grodzinsky, A. J., and Jain, R. K. (2000). Role of extracellular matrix assembly in interstitial transport in solid tumors. Cancer Res *60*, 2497-2503.

O'Brien, L. E., Zegers, M. M., and Mostov, K. E. (2002). Opinion: Building epithelial architecture: insights from three-dimensional culture models. Nat Rev Mol Cell Biol *3*, 531-537.

Okamoto, K., Kashima, K., Pereg, Y., Ishida, M., Yamazaki, S., Nota, A., Teunisse, A., Migliorini, D., Kitabayashi, I., Marine, J. C.*, et al.* (2005). DNA damage-induced phosphorylation of MdmX at serine 367 activates p53 by targeting MdmX for Mdm2-dependent degradation. Mol Cell Biol *25*, 9608-9620.

Oliner, J. D., Kinzler, K. W., Meltzer, P. S., George, D. L., and Vogelstein, B. (1992). Amplification of a gene encoding a p53-associated protein in human sarcomas. Nature *358*, 80-83.

Padera, T. P., Stoll, B. R., Tooredman, J. B., Capen, D., di Tomaso, E., and Jain, R. K. (2004). Pathology: cancer cells compress intratumour vessels. Nature *427*, 695.

Pan, Y., and Chen, J. (2003). MDM2 promotes ubiquitination and degradation of MDMX. Mol Cell Biol *23*, 5113-5121.

Parant, J., Chavez-Reyes, A., Little, N. A., Yan, W., Reinke, V., Jochemsen, A. G., and Lozano, G. (2001). Rescue of embryonic lethality in Mdm4-null mice by loss of Trp53 suggests a nonoverlapping pathway with MDM2 to regulate p53. Nat Genet *29*, 92-95.

Parrinello, S., Coppe, J. P., Krtolica, A., and Campisi, J. (2005). Stromal-epithelial interactions in aging and cancer: senescent fibroblasts alter epithelial cell differentiation. J Cell Sci *118*, 485-496.

Paszek, M. J., Zahir, N., Johnson, K. R., Lakins, J. N., Rozenberg, G. I., Gefen, A., Reinhart-King, C. A., Margulies, S. S., Dembo, M., Boettiger, D.*, et al.* (2005). Tensional homeostasis and the malignant phenotype. Cancer Cell *8*, 241-254.

Patton, J. T., Mayo, L. D., Singhi, A. D., Gudkov, A. V., Stark, G. R., and Jackson, M. W. (2006). Levels of HdmX expression dictate the sensitivity of normal and transformed cells to Nutlin-3. Cancer Res *66*, 3169-3176.

Pereg, Y., Shkedy, D., de Graaf, P., Meulmeester, E., Edelson-Averbukh, M., Salek, M., Biton, S., Teunisse, A. F., Lehmann, W. D., Jochemsen, A. G., and Shiloh, Y. (2005). Phosphorylation of Hdmx mediates its Hdm2- and ATM-dependent degradation in response to DNA damage. Proc Natl Acad Sci U S A *102*, 5056-5061.

Petersen, O. W., Ronnov-Jessen, L., Howlett, A. R., and Bissell, M. J. (1992). Interaction with basement membrane serves to rapidly distinguish growth and differentiation pattern of normal and malignant human breast epithelial cells. Proc Natl Acad Sci U S A *89*, 9064-9068.

Rallapalli, R., Strachan, G., Cho, B., Mercer, W. E., and Hall, D. J. (1999). A novel MDMX transcript expressed in a variety of transformed cell lines encodes a truncated protein with potent p53 repressive activity. J Biol Chem *274*, 8299-8308.

Ramos, Y. F., Stad, R., Attema, J., Peltenburg, L. T., van der Eb, A. J., and Jochemsen, A. G. (2001). Aberrant expression of HDMX proteins in tumor cells correlates with wild-type p53. Cancer Res *61*, 1839-1842.

Reifenberger, G., Liu, L., Ichimura, K., Schmidt, E. E., and Collins, V. P. (1993). Amplification and overexpression of the MDM2 gene in a subset of human malignant gliomas without p53 mutations. Cancer Res *53*, 2736-2739.

Riemenschneider, M. J., Buschges, R., Wolter, M., Reifenberger, J., Bostrom, J., Kraus, J. A., Schlegel, U., and Reifenberger, G. (1999). Amplification and overexpression of the MDM4 (MDMX) gene from 1q32 in a subset of malignant gliomas without TP53 mutation or MDM2 amplification. Cancer Res *59*, 6091-6096.

Ries, S., Biederer, C., Woods, D., Shifman, O., Shirasawa, S., Sasazuki, T., McMahon, M., Oren, M., and McCormick, F. (2000). Opposing effects of Ras on p53: transcriptional activation of mdm2 and induction of p19ARF. Cell *103*, 321-330.

Roskelley, C. D., Desprez, P. Y., and Bissell, M. J. (1994). Extracellular matrix-dependent tissue-specific gene expression in mammary epithelial cells requires both physical and biochemical signal transduction. Proc Natl Acad Sci U S A *91*, 12378-12382.

Secchiero, P., Barbarotto, E., Tiribelli, M., Zerbinati, C., di Iasio, M. G., Gonelli, A., Cavazzini, F., Campioni, D., Fanin, R., Cuneo, A., and Zauli, G. (2006). Functional integrity of the p53-mediated apoptotic pathway induced by the nongenotoxic agent nutlin-3 in B-cell chronic lymphocytic leukemia (B-CLL). Blood *107*, 4122-4129.

Shvarts, A., Steegenga, W. T., Riteco, N., van Laar, T., Dekker, P., Bazuine, M., van Ham, R. C., van der Houven van Oordt, W., Hateboer, G., van der Eb, A. J., and Jochemsen, A. G. (1996). MDMX: a novel p53-binding protein with some functional properties of MDM2. Embo J *15*, 5349-5357.

Stad, R., Little, N. A., Xirodimas, D. P., Frenk, R., van der Eb, A. J., Lane, D. P., Saville, M. K., and Jochemsen, A. G. (2001). Mdmx stabilizes p53 and Mdm2 via two distinct mechanisms. EMBO Rep *2*, 1029-1034.

Stommel, J. M., and Wahl, G. M. (2004). Accelerated MDM2 auto-degradation induced by DNA-damage kinases is required for p53 activation. Embo J *23*, 1547-1556.

Stuhmer, T., Chatterjee, M., Hildebrandt, M., Herrmann, P., Gollasch, H., Gerecke, C., Theurich, S., Cigliano, L., Manz, R. A., Daniel, P. T., *et al*. (2005). Nongenotoxic activation of the p53 pathway as a therapeutic strategy for multiple myeloma. Blood *106*, 3609-3617.

Toledo, F., Krummel, K. A., Lee, C. J., Liu, C. W., Rodewald, L. W., Tang, M., and Wahl, G. M. (2006). A mouse p53 mutant lacking the proline-rich domain rescues Mdm4 deficiency and provides insight into the Mdm2-Mdm4-p53 regulatory network. Cancer Cell *9*, 273-285.

Vacek, P. M., and Geller, B. M. (2004). A prospective study of breast cancer risk using routine mammographic breast density measurements. Cancer Epidemiol Biomarkers Prev *13*, 715-722.

Vassilev, L. T., Vu, B. T., Graves, B., Carvajal, D., Podlaski, F., Filipovic, Z., Kong, N., Kammlott, U., Lukacs, C., Klein, C., *et al*. (2004). In vivo activation of the p53 pathway by small-molecule antagonists of MDM2. Science *303*, 844-848.

Wahl, G. M., Stommel, J. M., Krummel, K. A., and Wade, M. (2005). Gatekeepers of the guardian: p53 regulation by post-translational modification, mdm2 and mdmx. In 25 Years of p53 Research, *K. Wiman*, and *P. Hainaut*, eds. (*Netherlands*: Springer), pp. *73-113*.

Wang, F., Weaver, V. M., Petersen, O. W., Larabell, C. A., Dedhar, S., Briand, P., Lupu, R., and Bissell, M. J. (1998). Reciprocal interactions between beta1-integrin and epidermal growth factor receptor in three-dimensional basement membrane breast cultures: a different perspective in epithelial biology. Proc Natl Acad Sci U S A *95*, 14821-14826.

Weaver, V. M., Lelievre, S., Lakins, J. N., Chrenek, M. A., Jones, J. C., Giancotti, F., Werb, Z., and Bissell, M. J. (2002). beta4 integrin-dependent formation of polarized three-dimensional architecture confers resistance to apoptosis in normal and malignant mammary epithelium. Cancer Cell *2*, 205-216.

Wei, C. L., Wu, Q., Vega, V. B., Chiu, K. P., Ng, P., Zhang, T., Shahab, A., Yong, H. C., Fu, Y., Weng, Z., *et al*. (2006). A global map of p53 transcription-factor binding sites in the human genome. Cell *124*, 207-219.

Xiong, S., Van Pelt, C. S., Elizondo-Fraire, A. C., Liu, G., and Lozano, G. (2006). Synergistic roles of Mdm2 and Mdm4 for p53 inhibition in central nervous system development. Proc Natl Acad Sci U S A *103*, 3226-3231.

Zahir, N., Lakins, J. N., Russell, A., Ming, W., Chatterjee, C., Rozenberg, G. I., Marinkovich, M. P., and Weaver, V. M. (2003). Autocrine laminin-5 ligates

alpha6beta4 integrin and activates RAC and NFkappaB to mediate anchorage-independent survival of mammary tumors. J Cell Biol *163*, 1397-1407.

Zahir, N., and Weaver, V. M. (2004). Death in the third dimension: apoptosis regulation and tissue architecture. Curr Opin Genet Dev *14*, 71-80.

II

Reproducible doxycycline-inducible transgene expression at specific loci generated by

Cre-recombinase mediated cassette exchange

Abstract

Comparative analysis of mutants using transfection is complicated by clones exhibiting variable levels of gene expression due to copy number differences and genomic position effects. Recombinase-mediated cassette exchange (RMCE) can overcome these problems by introducing the target gene into predetermined chromosomal loci, but recombination between the available recombinase targeting sites can reduce the efficiency of targeted integration. We developed a new LoxP site (designated L3), which when used with the original LoxP site (designated L2), allows highly efficient and directional replacement of chromosomal DNA with incoming DNA. A total of 6 independent LoxP integration sites introduced either by homologous recombination or retroviral delivery were analyzed; 70-80% of the clones analyzed in hamster and human cells were correct recombinants. We combined the RMCE strategy with a new, tightly regulated tetracycline induction system to produce a robust, highly reliable system for inducible transgene expression. We observed stable inducible expression for over one month, with uniform expression in the cell population and between clones derived from the same integration site. This system described should find significant applications for studies requiring high level and regulated transgene expression and for determining the effects of various stresses or oncogenic conditions *in vivo* and *in vitro*.

Introduction

Many studies require the ability to compare the functional consequences of introducing mutations into genes of interest. Rigorous comparative analyses require

similar gene expression levels in each stable cell clone. Comparison between mutant genes is difficult using the common strategy of deriving stable cell lines as gene expression level is unpredictable due to variable copies of integrated DNA combined with position effects on gene expression. All of these confounding variables can be eliminated if each transgenic clone is derived by independently introducing the gene of interest into a pre-determined genomic locus (Feng et al., 1999).

Gene targeting by homologous recombination is widely applied in mouse embryonic stem cells (ES cells) and occasionally in other cell types to produce accurately modified loci (Capecchi, 1989). However, it is a sophisticated and time consuming procedure that can be compromised by the low recombination efficiency of some loci. Alternatively, the RMCE strategy uses bacterial and yeast DNA recombinases to target any DNA sequence into a predetermined genomic locus that was previously modified to contain the appropriate recombinase recognition sequences (Baer and Bode, 2001). For example, the widely used bacteriophage P1 Cre/LoxP recombination system utilizes LoxP sites consisting of two 13-base pair (bp) inverted repeats and a central 8-bp spacer sequence. The central 8-bp sequence within each LoxP site determines if a pair of LoxP sites is compatible for recombination by Cre (Hoess et al., 1986). LoxP sites containing the same 8-bp core sequences recombine, but LoxP sites differing by one or more base pairs exhibit reduced or no recombination (Hoess et al., 1986; Kolb, 2001; Lee and Saito, 1998). The success of RMCE relies on the use of two heterospecific LoxP sites (LoxP sites of different sequences) that will not recombine with each other. Thus, flanking a donor gene of interest with heterospecific sites enables it to precisely replace genomic DNA flanked

by identical sequences upon expression of Cre recombinase. However, the previously published LoxP sites (L2) and LoxP511 (L1) (Hoess et al., 1986) are not entirely heterospecific when tested in mammalian cells, and are consequently not ideal for RMCE (Feng et al., 1999; Kolb, 2001). For example, deletion of the intervening sequence occurs when L2 and L1 are placed as direct repeats on the same DNA, while inversion occurs if they are placed as inverted repeats (Feng et al., 1999). Due to the wide usage of RMCE, the development of new LoxP sites with greater specificity for directional exchange is clearly needed.

RMCE can also facilitate structure-function analyses by ensuring reproducible expression of different mutant alleles from the same locus. However, the biological significance of such studies can be compromised if the expression level does not reflect that present physiologically. For that, a reliable inducible system with low basal expression and reproducible ligand-dependent induction is required. Tight regulation of gene expression is particularly important if, for example, the gene of interest is toxic, or induces cell cycle arrest or apoptosis. The tetracycline (tet) regulatable system has proven especially valuable as it uses an inexpensive inducer (doxycycline or dox), has high dynamic range, low background in un-induced state and can be used *in vivo* and *in vitro* (Bockamp et al., 2002). Regulation in this system involves highly specific interaction between the Tet repressor (TetR) and Tet operator (*tetO*) DNA sequence (Tet response element or TRE). In the original Tet-Off system, the DNA binding domain of TetR was fused with the potent herpes simplex virus VP16 transactivation domain to form the tetracycline responsive transactivator (tTA) (Gossen and Bujard, 1992). tTA in the absence of doxycycline (dox) binds *tetO* to

initiate transcription. The Tet-On system was later developed due to its wider application *in vivo* (e.g. for gene therapy and in transgenic animals) (Bockamp et al., 2002; Gossen et al., 1995). Random mutagenesis of TetR generated a new transactivator (rtTA), which binds and transactivates gene expression in the presence of dox. Improved versions of rtTA have been developed to give tighter gene expression, increased sensitivity towards the inducer, enhanced stability and expression in mammalian cells, and more uniform transgene expression in the induced cells (Baron et al., 1997; Urlinger et al., 2000).

We incorporated the Cre/LoxP and Tet-On systems into one integrated system to enable tightly regulated induction of gene expression at reproducible levels between experiments and in different clones of mammalian cells. A new LoxP site (L3) was developed to minimize unwanted intrachromosomal recombination between heterospecific LoxP sites. When tested in two different cell lines and at 6 independent integration sites, incoming DNA was correctly targeted at high efficiencies. Expression of the reporter gene, luciferase-green fluorescence protein fusion (LucGFP) was uniformly induced across most of the RMCE clones derived from the same integration site. Such a highly efficient gene targeting approach in combination with predictable and reproducible gene expression should find wide application *in vitro* and *in vivo*.

Results

Designing a new LoxP site

The success of directional RMCE relies on the use of two heterospecific LoxP sites ideally exhibiting no recombination with each other. The natural LoxP (L2) site and the mutant LoxP511 (L1) are commonly used (Bouhassira et al., 1997; Feng et al., 1999), but they differ by only 1-bp in the central 8-bp spacer region. A plasmid bearing L1 and L2 sites (pL1L2) can recombine illegitimately when cotransfected with the Cre recombinase plasmid (compare Lane 1 and Lane 2 in Fig 2.2c). As such recombination reduces the effectiveness of RMCE, we designed a new LoxP site (designated LoxP257 or L3; see Fig 2.2a) that differs from the original LoxP site by 3 nucleotides. A plasmid carrying a pair of L3 sites (pL3L3) recombines efficiently with itself in the presence of Cre recombinase (compare lanes 3 and 5 in Fig 2.2c). More importantly, no recombination was detected in a plasmid containing L3 and the inverse L2 (2L) site (pL32L) in the presence of Cre (compare lanes 4 and 6). Thus, the newly designed L3 site paired with L2 is more ideal for RMCE than is the pair L1 and L2.

Highly efficient RMCE by L3-2L after integration into the genome

We next perform a vigorous test for the efficiency of cassette exchange mediated by L3 and L2. L3 and L2 are integrated into the genome of CHO and HeLa cells by homologous recombination or retroviral delivery. CHO was chosen because it is a commonly used cell line for the expression of recombinant proteins of pharmaceutical value (Fussenegger et al., 1998; Warner, 1999; Zang et al., 1995) and because of our ongoing studies of DNA replication control in the DHFR locus. HeLa was chosen because it is commonly used for analyses of a variety of biological

processes and is readily transfected. We made use of a chimeric hygromycin phosphotransferase-thymidine kinase (HyTK) gene for both positive and negative selections (Feng et al., 1999). The HyTK fusion gene, which confers resistance to hygromycin and sensitivity to ganciclovir, was flanked by L3 and L2 (L3HyTK2L). This cassette was first inserted into the DHFR locus in CHO cells by homologous recombination. The DHFR locus was chosen due to our interest in its replication domain and because it can be amplified to high levels in the presence of methotrexate (Alt et al., 1978), which may be used to enhance production of proteins of biological interest (Alt et al., 1978; Kellems, 1991). Also, robust procedures are available for homologous recombination between a cosmid carrying the 3' half of the DHFR coding sequence with DR-8 (a DHFR-deficient CHO cell line hemizygous for a 3'truncated DHFR gene) (Jin et al., 1995; Urlaub and Chasin, 1980) (Fig 2.3a). This reconstructs the full-length DHFR gene, which is readily identified by growth of cells in medium lacking thymidine, hypoxanthine and glycine (Kalejta et al., 1998). We modified the targeting vector to include the L3HyTK2L cassette downstream of the DHFR gene. Southern blotting using probes spanning different regions of the DHFR locus confirmed the reconstruction of the DHFR gene and a probe for HyTK confirmed the integration of the L3HyTK2L cassette (Fig 2.3b), this clone is now named 146-111.

We next used retroviruses to insert single copies of the L3HyTK2L cassette into HeLa (Fig 2.3c) or CHO cells genome (data not shown). Southern blotting using a probe against HyTK demonstrated single copy integration at random sites in the genome of different clones (Fig 2.3d). Four HeLa clones and one CHO (CHO #4) clone exhibiting high and stable expression of HyTK (assayed by western blot for TK

expression, data not shown; polyclonal antibody against TK kindly provided by Ian R Wickersham) were used for subsequent recombination experiments.

To test the efficiency of recombination at the genomic site, plasmid DNA containing L3 and L2 sites was electroporated with a Cre-expressing plasmid (O'Gorman et al., 1997) into the previously constructed CHO and HeLa parental lines containing L3HyTK2L cassette (L32L parent). LoxP sites, L3 and L2, were placed as inverted repeats to eliminate the possibility of recombination and deletion of the selection gene. Recombinants were selected based on resistance to ganciclovir after the replacement of the TK gene (Fig 2.1). A clone that is resistant to ganciclovir can either lose the TK gene by RMCE or has retained TK but silenced its expression or mutationally inactivated it. We identified recombinants that underwent RMCE using PCR to identify clones that lost the TK gene and gained the predicted recombinant junctions (Fig 2.1 and Table 2.1). Single copy integration of the incoming DNA was also confirmed by Southern blot analysis (Supplementary Data).

The overall frequency of correct recombination was 81% for CHO and 69% for HeLa cells (Table 2.1). The efficiency of recombination does not appear to be affected by the size of the incoming DNA, as fragments between the lengths of 100-bp to 4000-bp recombined with similar frequencies (Table 2.1). All clones that were negative for recombination junctions were positive for HyTK by PCR, suggesting that they arise due to silencing of the TK gene. No clone was tested positive for inversion between LoxP sites or illegitimate deletion of the TK sequence (Table 2.1).

Uniform and stable doxycycline-inducible expression of transgene by RMCE clones

It has been previously reported that gene expression is uniform between RMCE clones derived from the same parental line (Feng et al., 1999; Schubeler et al., 1998). Since it is often essential to regulate the level of gene expression, we further tested the uniformity and stability in gene expression by comparing gene induction in RMCE clones containing an integrated copy of L3-TRE-LucGFP-2L. The Tet-On system we used has been modified as follows to enable stringent on-off regulation. The transactivator (rtTA) is a modified bacterial TetR protein fused to VP16 transcriptional activation domain (rtTA2^S-M2). It activates gene transcription by binding to TRE in the presence of dox (Baron et al., 1997; Urlinger et al., 2000); in the absence of dox, a Tet-transrepressor (tTR), TetR(B/E)-KRAB, binds TRE and actively represses gene expression (Forster et al., 1999).

We tested two ways of generating rtTA and tTR expressing stable cell lines. In the first system, rtTA and tTR were linked by an IRES element in a single plasmid (pWHE134) and were transcriptionally controlled by one promoter (single plasmid Tet-On system exemplified by the M2PK HeLa and CHO 111-134 in Fig 2.4a). In the second system, rtTA and tTR genes were on separate plasmids and their expression were driven from two independent promoters (two plasmid Tet-On system in HeLa cell line M2K in Fig 5a).

Gene expression was induced at a saturating dose of dox (2 µg/ml) for 72 hours followed by a luciferase assay to determine the maximum induction attained by each RMCE clone. To compare uniformity in gene expression between clones, cells

were induced at a non-saturating dose of dox followed by single cell analysis for GFP fluorescence using flow cytometry. We first tested the dose response to dox by titrating the concentration of dox and measuring the mean fluorescence units at three days (Fig 4.4b, c) after induction. Flow cytometric analysis showed uniform GFP expression in the induced populations and the fluorescence increased in a dose-dependent manner in CHO 111-134 cells from 12.5 ng/ml to 200 ng/ml. A similar titration experiment was performed for HeLa cells (data not shown). Dox used at 50 ng/ml and 100 ng/ml for CHO 111-134 and HeLa cells, respectively, fell within the linear range of induction and was chosen to test the uniformity in gene expression in the RMCE clones.

The single plasmid Tet-On system in HeLa cells (M2PK in Fig 4.4) generates low basal luciferase activity in the un-induced state and high level of luciferase activity at high dox concentration in all the four RMCE clones tested (Fig 2.4d). The fold increase in luciferase activity ranged from $3x10^4$- to $7x10^4$-fold over the un-induced state in these clones. Three of four RMCE clones exhibited greater than 90% GFP expression while one exhibited greater than 70% expression after induction with sub-maximal dose of dox (Fig 2.4e). Three clones had mean GFP fluorescence between 90-110 and one clone had a mean GFP fluorescence of about 70. These data show that within single clones, individual cells exhibited similar expression levels, though we did detect some inter-clonal variability.

In CHO 111-134, all five clones derived by RMCE at the DHFR locus showed high luciferase activities upon induction at 2 μg/ml dox whereas the expression of luciferase was close to background in the absence of dox (Fig 2.4d). The fold increase

in luciferase activity range from $6x10^3$ to $4x10^4$. As shown in Fig 2.4e, five out of five RMCE clones were greater than 92% GFP positive after induction at sub-maximal dose. Clone 1 had the highest mean GFP fluorescence (236) while clone 3 showed the lowest mean GFP fluorescence (94). Other RMCE clones had mean GFP fluorescence 105, 107, and 138 respectively. These results indicated that the reporter gene expression in these RMCE clones derived from the L3HyTK2L CHO parental cell line had substantial inducibility and uniformity.

In the two plasmid Tet-On system (M2K HeLa cells in Fig 2.5), basal luciferase activity was relatively low and uniform across the four clones analyzed. The maximum fold induction in luciferase activity ranged from $1x10^4$ to $3x10^4$ in the clones analyzed (Fig 2.5b). Three of the four RMCE clones tested show greater than 80% green cells after induction and exhibited mean GFP fluorescence between 100 to 110 (Fig 2.5c). One of the clones showed greater than 50% green cells and mean GFP fluorescence of 86 upon induction.

The RMCE approach enables genes to be independently introduced into a single genomic locus. Comparison between genes obtained from independent RMCE experiments is possible if the level of gene expression is preserved in clones obtained from independent RMCE experiments. Using the same L32L parent (HeLa M2K), we compared GFP expression in clones obtained from 2 independent RMCE experiments performed at the same genomic locus (Fig 2.5d). Seven out of ten clones obtained in the second RMCE experiment had similar mean GFP fluorescence level as 3 out of 4 of the clones obtained in the first RMCE experiment.

We evaluated whether the inducible phenotype was stable over time using one representative RMCE clone from M2PK and one from M2K HeLa. These clones were continuously passaged for one month before analysis. The basal GFP level remained low, and dox addition produced robust GFP induction when assayed one month later. Uniformity of expression in M2PK #1 was very high over this time period (i.e., 90% of cells exhibited GFP fluorescence after one month, compared to 92% originally). (Fig 2.6). However, the mean GFP fluorescence and the percentage of GFP expressing cells after induction declined slightly in HeLa M2K #3 (Fig 2.6).

Monitoring population doubling by Tet-regulated H2BGFP expression

The highly inducible nature of this system suggested potential applications for transiently marking individual cells to "pulse label" them. As one example, we previously generated a very stable histone H2BGFP fusion protein that is readily incorporated into chromatin to generate brilliantly fluorescent chromosomes and nuclei (Kanda et al., 1998). We reasoned that if the H2BGFP gene was induced for several cell doublings to uniformly label the chromatin in each cell, and it was then turned off, the fluorescence of the cell would be diminished by a factor of two each time the cell divided since nucleosomes segregated randomly when DNA is replicated (Burhans et al., 1991). Thus, fluorescence microscopy or flow cytometry could be used to determine how many times a cell doubled by merely measuring its fluorescence intensity relative to that at the beginning of the experiment.

Figure 2.7 shows a flow cytometric analysis of the fluorescence intensity of HeLa cells followed for seven population doublings. The decrease in fluorescence per

population doubling is precisely that expected for a two-fold decrease per cell division. Importantly, there was no decrease in fluorescence observed in cells that were held in quiescence by thymidine block (Fig 2.7a). This shows that the decreased fluorescence required entry into and progression through S-phase, and was not the result of H2BGFP degradation.

Discussion

We have combined the powers of RMCE and regulated gene expression into a single highly efficient system that should facilitate structure-function studies, enable production of biopharmaceuticals, or provide a means of tracking cell proliferation in real time. The Cre/LoxP recombination system is preferred for site-specific recombination because it exhibits higher efficiency of recombination over the Flp/FRT system in specific cell types such as mouse embryonic stem cells and primary cells (Andreas et al., 2002; Ringrose et al., 1998; Seibler et al., 1998; Westerman and Leboulch, 1996). However, the system we describe could as easily be implemented using engineered Flp recombination target sequences designed not to recombine with each other. We first engineered a new LoxP site to minimize intrachromosomal exchanges that generate deletions, and to maximize exchanges between the chromosomal and plasmid donor LoxP targets. To minimize the need for drug selection markers, we introduced into the chromosomal target a HyTK fusion gene. This enables positive selection to identify clones containing the LoxP target, and then counterselection using gancyclovir to select for loss of the chromosomal target and concomitant replacement with the donor plasmid. This is especially valuable for

situations in which introduction of extraneous transcriptional control sequences needs to be avoided. We also used an optimized Tet-On system to enable robust controlled expression of the donated sequences. This should allow for analyses of phenotypic effects of the introduced gene when it is expressed at normal, sub- or supraphysiologic levels.

We tested the system by first analyzing the stringency of recombination with the newly characterized L3 LoxP site. A pair of heterospecific recombination sites that do not recombine with each other is necessary for efficient RMCE (Kolb, 2001). When used with the original LoxP site (L2), the first LoxP variant (LoxP*511* or L1) that was generated greatly enhanced the frequencies of exogenous gene integration when coupled with positive selection (Bouhassira et al., 1997). However, using negative selection as a means to enrich for recombinants, the efficiencies were markedly different (Feng et al., 1999; Kolb, 2001). Deletion of intervening sequences without replacement occurred when L2 and L1 were placed as direct repeats, suggesting interaction between L1 and L2 (Kolb, 2001). When placed as inverted repeats, inversion of the intervening sequence resulted in an equal proportion of clones in either direction (Feng et al., 1999). This is not desirable, especially when directionality of the integrant is important. We solved the problem of recombination between L2 and L1 by generating a new LoxP site, LoxP257 (L3), which was designed based on findings from *in vitro* recombination assays (Lee and Saito, 1998). L3 differs from L2 by three bases within the 8-bp spacer sequence. When used in combination with L2, L3 generated recombinants at high frequency, suggesting the feasibility of using L3 and L2 for RMCE. The finding was consistent with a previous

study showing that a modified LoxP sequence (LoxP2272) with two base changes from L2 also enabled high efficiency exchange (Kolb, 2001). Other than having a high inter-molecular recombination efficiency, the probability of selecting a recombinant clone among the ganciclovir resistant clones is increased when TK expression from the L3HyTK2L parent line is high and stable. Using this criterion for the selection of the L3HyTK2L cell line, we observed high efficiency, accurate RMCE in two different mammalian cell lines at six independent genomic loci. We also observed little size dependence on RMCE frequency or accuracy. The high frequency of correctly recombined clones expedites screening for desirable clones.

We used homologous recombination to introduce L3HyTK2L into several single copy loci, including the intergenic region of the CHO DHFR locus. Our data demonstrate that the DHFR locus was favorable for RMCE and for tightly regulated gene induction. Recombination occurred at very high efficiency (50-100%) and we readily obtained clones exhibiting robust inducible expression (up to 10^4-fold by luciferase, and >100 fold by GFP analyses). This locus offers a number of advantages for other studies. For example, it can be readily amplified using selection for methotrexate-resistance (Alt et al., 1978). As CHO cells are often used to produce biopharmaceuticals, the combination of amplification and highly regulated expression could provide substantial advantages for reducing production costs, enabling stable maintenance of transgenes, and obtaining very high level expression of potentially toxic proteins. In studies to be presented elsewhere, we found the L2 and L3 sites to be useful for generating genetically engineered ES cells, mouse embryo fibroblasts,

and mice with different p53 point mutations or fusion genes with high efficiency (F. Toledo, C. Lee, and G.M. Wahl, manuscript in preparation).

Using a strategy similar to that employed for the delivery of Flp/FRT tagged sites into the genome of mammalian cells (Schubeler et al., 1998; Wirth and Hauser, 2004), we integrated the LoxP sites at single copy into random positions in the genome of HeLa and CHO cells by retroviral delivery (Fig 2.3c). An advantage of the retroviral system is that it ensures delivery of the entire transgene at high efficiency and at single copy (Fig 2.3d) into the genome. Active transcription sites are the preferred retroviral integration sites (Scherdin et al., 1990; Schroder et al., 2002). Consistent with this, we were able to select retroviral integrations at high efficiency, an advantage over gene targeting by homologous recombination.

An important advantage of RMCE approach that is valuable for structure-function studies and production of recombinant proteins of pharmaceutical value is the ability to repeatedly obtain clones exhibiting predictable and uniform gene expression at high frequencies (Feng et al., 1999; Fukushige and Sauer, 1992; Schubeler et al., 1998). We combined that with the improved version of the Tet-On inducible system to evaluate the reproducibility of gene induction at each locus (Urlinger et al., 2000). By single cell analysis, GFP was uniformly expressed within the population and it was induced in a dose-responsive manner. The improved rtTA (rtTA2^s-M2) demonstrated many superior properties over the original rtTA. Beside the ability to induce graded transgene expression, induction exhibited a greater dynamic range, higher sensitivity to dox and faster induction rate (within 24 hours, data not shown) compared to the original rtTA system (Fig 2.4b, c) (Kringstein et al., 1998; Urlinger et al., 2000).

Recombinants derived from the same L32L parental line have the reporter gene inserted at the same genomic locus. As expected, the majority of the RMCE clones obtained in one experiment showed similar levels of expression upon induction (Fig 2.4 & 2.5). The uniformity in gene expression was also found between clones obtained from independent RMCE experiments (Fig 2.5d). Hence, clones that reproducibly induce different transgenes can be readily obtained through multiple rounds of RMCE.

Maintaining stable transgene expression is as important as high transgene expression. Since transgene expression may be subjected to silencing, especially when viral promoter is used to drive gene expression (Paterna et al., 2000; Teschendorf et al., 2002) and when expression is not maintained under selective pressure (Barnes et al., 2003). We measured the stability of expression in HeLa cells after at least 30 PD in culture. We observed that the level of inducibility, and the fraction of cells expressing the transgene, was stable over the time period studied when transcription of rtTA and tTR were coupled to that of the neomycin resistance gene by the IRES elements and by maintaining the culture under G418 selection. Hence, the use of IRES to mediate coexpression of multiple genes will gain popularity in both *in vitro* and *in vivo* applications (Salucci et al., 2002; Wong et al., 2002).

The tight and reversible gene expression regulated by the Tet-On system was further demonstrated by switching H2BGFP expression on and then off to monitor cell doubling (Fig 2.7) as a function of fluorescence units. H2BGFP is incorporated into the chromatin after synthesis, and tracks with nucleosomes that are segregated randomly to daughter cells during each division (Burhans et al., 1991). Being a stable protein, H2BGFP fluorescence should approximately halve with each division if its

expression is prevented. Consistent with this prediction, after H2BGFP expression was turned off for different numbers of population doublings, flow cytometric analysis revealed the expected twofold decay per population doubling (Fig 2.7). Hence, the inducible expression of H2BGFP can be used to measure population doublings within a defined time frame. For example, as stem cells are expected to divide fewer times than transit amplifying cells, the retention of H2BGFP fluorescence should be able to be used as a marker to localize putative stem cells *in situ* and as a means to isolate them by fluorescence based cell sorting (Clarke et al., 2005; Tumbar et al., 2004; Welm et al., 2002).

In conclusion, the LoxP/Cre recombination system offers reproducible and directional DNA integration into specific loci in the genome at high frequency. The single plasmid Tet-On system, which ensures stable expression of the transactivator and transrepressor, allows reproducible and graded induction of transgenes to a similar level in the RMCE clones derived from single and independent recombination experiments.

Materials and Methods

Construction of L3

L3 was made from two oligonucleotides that contained 16 complementary (**bold**) 3-prime residues (5'-GGA *CTC GAG* ATA ACT TCG **TAT AAA GTC TCC TAT A** and 5'-CCT ATC GAT ATA ACT TCG T**AT AGG AGA CTT TAT A**). The oligos were made duplex by 10 cycles of PCR at an annealing temperature of 42 ºC.

The result was cloned into pCR2.1 using TOPO cloning (Invitrogen) and confirmed by sequencing. The specificity of L3 derives from an internal non-repetitive eight basepair sequence (underlined) that deviates from wild-type at three positions (AT‌GTA‌TG‌C).

Plasmids construction

Naming of the wild-type and LoxP511 sites are according to previously published (Bouhassira et al., 1997). pL1L2 and L1HyTK2L were gifts of S. Fiering (Feng et al., 1999). pL32L was made by substituting L1, bounded by Xho I and Nco I in plasmid L1HyTK2L with L3 from pCR2.1-L3, bounded by Xho I (oligonucleotide restriction site in *italics* above) and BspLU11 I within pCR2.1. pL3L3 was made from pL32L. L3 was removed with Xho I and Pvu II and re-inserted in the position of 2L using Sal I and Sbf I blunted with T4 DNA polymerase.

L3HyTK2L was constructed by replacing L1 in L1HyTK2L with L3 from pL32L by Ahd I and Cla I digestion. The L3HyTK2L cassette was cloned into a retrovirus backbone by inserting L3HyTK2L restricted with Not I and Xba I into pCFB-EGSH (Stratagene) digested with the same enzymes, generating RV-L3HyTK2L.

To facilitate insertion of genes into the inducible L32L exchange vector, we constructed L3-TRE-MCSpolyA-2L by cloning the fragment containing seven *tetO* sites, multiple cloning sites and a polyadenylation signal derived from Xho I and Sap I/Klenow treated pTRE2 (BD Bioscience) into L3HyTK2L previously digested with Xho I and PshA I. The exchange plasmid, L3-TRE-LucGFP-2L (pLi028), was derived

by cloning a Bgl II-Not I fragment containing LucGFP from pLuciferase-EGFP (gift from D. Buscher) into BamH I-Not I sites of L3-TRE-MCSpolyA-2L.

A bicistronic transregulator-expressing cassette was obtained by amplifying the TetR(B/E)-KRAB (tTR or Tet-transrepressor) gene by standard PCR using the primers 5'-(B/E)-BamH I and 3'-(B/E)-Bgl II, followed by restriction with BamH I and Bgl II and ligation with BamH I-restricted and dephosphorylated pWHE120(sM2), yielding pWHE124. The polio-virus IRES element was amplified with 5'-P-IRES-Sma I and 3'-P-IRES-Sma I from pCMV-KRAB-rtTA (Forster et al., 1999), restricted with Sma I and inserted into likewise-digested and dephosphorylated pWHE124, yielding pWHE125-P. The plasmid pWHE134 containing the tricistronic transregulator-cassette with rtTA2^S-M2, tTR and a neomycin selection marker separated by two IRES elements was constructed by restricting pWHE125-P with EcoR I and Hpa I and ligating the fragment encoding the regulatory cassette with pIRESneo (BD Bioscience) containing the selection marker. pIRESneo had previously been restricted with BamH I, the 5' overhangs filled-in with T4 DNA polymerase, and then restricted with EcoR I. All primer and plasmid sequences are available upon request.

Recombination assay by transient transfection

293 HEK cells were cotransfected by electroporation with 2 µg of LoxP test plasmid and either 18 µg of GFP expressing plasmid or 18 µg of Cre expressing plasmid, pOG231 (O'Gorman et al., 1997). Extra-chromosomal DNA was harvested by Hirt extraction (Hirt, 1967) 48 hours post-transfection and examined by Southern hybridization after digestion with Ssp I or Nde I. The probe used was a 426-bp Nco I-

Sac II fragment corresponding to the hygromycin resistance gene common to all the LoxP plasmids.

Cell culture and construction of stable cell lines

Both HeLa and chinese hamster ovary (CHO) cells were cultured in Dulbecco's modified Eagle's medium (Cellgro) supplemented with 5% fetal bovine serum (Atlanta biologicals) and 1x non-essential amino acids (Invitrogen) in a humidified atmosphere containing 7% CO_2 at 37 ^{o}C.

The HeLa cell line M2K was generated by stably transfecting the cell line HRM2 (Knott et al., 2002) with pCMV-TetR(B/E)-KRAB (Forster et al., 1999) and pPUR (BD Bioscience). Details will be published elsewhere (Schätz, Knott, Hillen & Berens; manuscript in preparation). To generate the cell line M2PK, approximately 5_10^5 cells were transfected with 2 μg Pvu II-linearized pWHE134 using Lipofectamine (Invitrogen). Twenty-four hours later, cells were seeded into 15 cm plates and selected with 800 μg/ml G418 (Invitrogen) for at least two weeks. Positive clones stably producing the transfected regulators were identified by transient transfection of 0.1 μg pUHC13-3 (Gossen and Bujard, 1992), 0.6 μg pUHD16-1 for normalization of transfection efficiency, and 1.3 μg pWH802 as non-specific DNA. Clone with the highest induction of luciferase activity after incubation with 1 μg/ml dox for 24 hours was chosen. Cells were routinely maintained in medium containing 400 μg/ml G418.

For retroviral delivery of L3HyTK2L into CHO, HeLa M2K and M2PK cells, approximately $5x10^5$ cells were infected with culture supernatant containing RV-

L3HyTK2L (as described by manufacturer). Resistant clones were selected in 400 μg/ml hygromycin B (Calbiochem) for CHO and 100 μg/ml for HeLa cells.

L3HyTK2L was also integrated into the dihydrofolate reductase gene (DHFR) locus of DR-8 (a derivative of CHOK1) by homologous recombination using the strategy previously described, generating the stable clone 146-111 (Kalejta et al., 1998). For dox inducibility, pWHE134 was stably integrated into 146-111 by an approach described above, generating stable line 111-134.

Cre recombination and selection for RMCE derivatives

30 μg of exchange plasmid and 3 μg of pOG231 were electroporated into approximately 4×10^6 cells at 250V 1500 μF (Hybaid). Approximately 1×10^5 cells were re-plated onto 15 cm tissue culture plate 4 days after electroporation. Ganciclovir (Moravek Biochemicals) was added the next day to a final concentration of 2 μM. The drug-containing medium was washed off and replaced with fresh medium after 3 days. Colonies were picked between 7 to 10 days after transferring into fresh medium.

PCR screening

Clones isolated from ganciclovir selection were screened for recombinants by PCR for loss of HyTK gene and gain of specific recombination junctions. 5 ng of total genomic DNA was added to a PCR reaction mix containing 0.2 μM primers, 0.2 mM dNTP mix, 1.5 mM $MgCl_2$ and 0.05 U/μl AmpliTaq Gold polymerase (Applied Biosystems). Amplification was performed once at 94 ºC for 10 minutes, followed by 40 cycles at 94 ºC for 30 seconds, 57 ºC for 30 seconds and 72 ºC for 30 seconds,

followed by a final extension step at 72 $^{\circ}$C for 10 minutes. Refer to Figure 2.1 in Results section for the position of primer pairs used. The same strategy was employed for HeLa and CHO cells. Primer sequences are available upon request.

Reporter Assays

Cells grown on 35-mm dishes were washed once with phosphate-buffered saline (PBS) and lysed in 200 µl lysis buffer (50 mM Tris-HCl (pH 8.0), 5 mM EDTA, 150 mM NaCl, 0.5% NP-40, 1x complete protease inhibitor mix (Roche Diagnostics)) and incubated for 30 minutes at 4 $^{\circ}$C. 20 µl of cell lysate was then mixed with 100 µl of luciferase reagent (20 mM Tricine, 1.07 mM $MgCO_3$, 2.67 mM $MgSO_4$, 0.1 mM EDTA, 33.3 mM DTT, 270 µM coenzyme A (USBiological), 530 µM ATP and 470 µM luciferin (Molecular Probes)) before reading on the luminometer (Lumat LB9507). Luciferase activity was normalized to total protein content (Biorad Laboratories). GFP fluorescence was analyzed by passing single cell suspensions in PBS through the FACScan (Becton Dickenson).

Determination of population doublings

The population doubling is calculated based on the formula 3.34 ($logN_i$-$logN_f$), where N_i is the initial cell count and N_f is the final cell count.

Acknowledgements

The text of Chapter II, in full, is a reprint of the material as it appears in *Nucleic Acids Research, 33:e147(2005).* The dissertation author is the primary researcher and author, and J Kolman, YC Li, L Mesner, W Hillen and C Berens are secondary authors in this publication. Geoffrey M. Wahl directed and supervised the research that forms the basis for this chapter.

Figure 2.1: Principle of RMCE and screening strategy for recombinants

The positive-negative selection marker HyTK that confers resistance to hygromycin (Hyg^R) and sensitivity to ganciclovir (Gan^S) is flanked by a pair of heterospecific LoxP sites placed in inverted orientation (inverted triangles) and integrated as a single copy into a genomic site. In the presence of Cre recombinase and incoming DNA harboring the same pair of LoxP sites, exchange will replace the existing HyTK with DNA on the exchange plasmid. Cells that have successfully undergone RMCE can be selected based on resistance to ganciclovir. The tetracycline inducible LucGFP (TRE-LucGFP) is used as the reporter to characterize uniformity of gene expression between clones after integration into the genome. Also shown are the positions of BamH I site and Luc probe used for Southern blot and primer pairs (P1-P6) used for screening of recombinants.

Figure 2.2: Construction and characterization of new LoxP site for RMCE

a. Sequence of the 8-bp spacer found within the LoxP site. LoxP and LoxP511 are named according to previously published (Bouhassira et al., 1997). Recombination occurs efficiently between LoxP sites with identical spacer sequence. Changes to the sequence within the 8-bp spacer generates LoxP sites that recombine with themselves but not with other LoxP sites. Underlined base(s) represents the base change that differs from the original L2 sequence.

b. A schematic of the three test plasmids (or I=input DNA), pL1L2, pL3L3 and pL32L and the possible products of RMCE (R=recombinant). Shown are the positions of the LoxP sites, the restriction sites used for the Southern (S = Ssp I, N = Nde I), and the target sequence for the probe (black box). The sizes of the predicted restriction fragments are listed below. The boxed fragment corresponds to that detected by the probe. Note that only the L3L3 intramolecular recombination would be predicted to occur if L1, L2 and L3 do not recombine with each other.

c. Southern analysis of test plasmids transfected into 293 cells in the absence or presence of a Cre-expressing plasmid (pOG231, (O'Gorman et al., 1997)). Bands were detected using a probe to the hygromycin sequence common to the test plasmids. Unrecombined, input plasmids are marked with "I"; products of Cre recombination are marked with "R". Note the presence of a non-specific band in lanes 3 and 5 marked with an asterisk.

A

ATGTATGC L2 = loxP
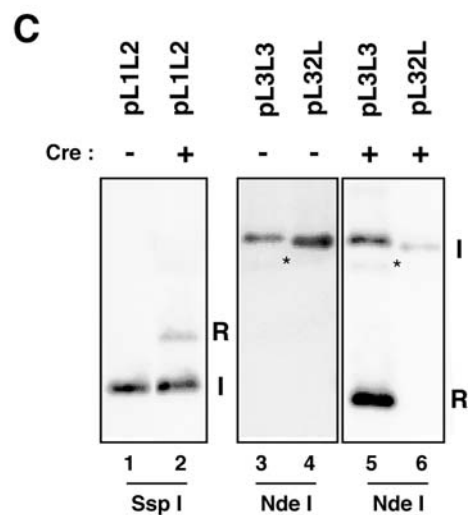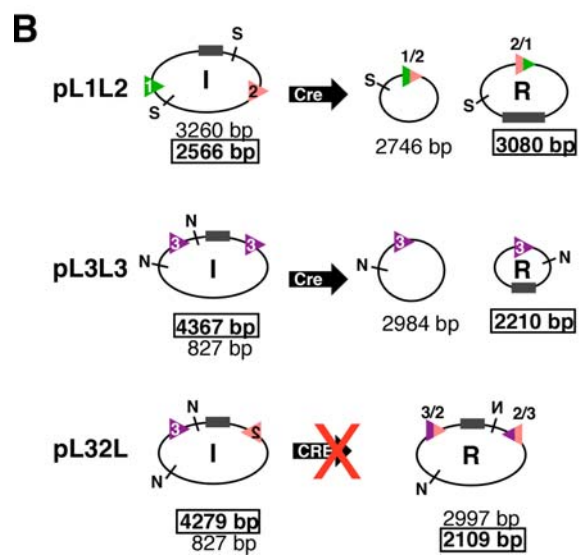ATGTATAC L1 = loxP511
AAGTCTCC L3 = loxP257

B

C

Figure 2.3: Integration and analysis of L32L introduced into the genomes of CHO and HeLa cells

   a. Engineering L32L into DR-8 cell line by homologous recombination using the strategy described by Kalejta *et al* (Kalejta et al., 1998). The diagram shows the genomic structure at the DHFR locus (wt), sizes of the fragments generated by EcoR I digestion and the positions of the probes used for Southern blot. Targeting cosmid DNA containing the 3' half of the DHFR gene is used to reconstruct the entire gene in DR-8 cell line that contains truncation at the 3' end of the DHFR gene. The L3 and L2 sites are placed in inverted orientation and flanking the HyTK positive-negative selectable marker gene. The entire cassette was inserted downstream of DHFR gene after homologous recombination.
   b. Southern blot of genomic DNA derived from CHO cells hemizygous for wildtype DHFR (WT/- or UA21 (Kalejta et al., 1998)), 3' truncated DHFR (delta/- or DR-8 (Kalejta et al., 1998)) and HyTK reconstituted cells (HyTK/- or 146-111). DNA was restricted with EcoR I before blotting and the positions of the bands generated by each probe are indicated with an arrow. Probe 121 marks the 5' flank of the cosmid DNA, probe 100 tests for reconstruction at the 3' end of the DHFR gene, probe 12/38 indicates the presence of *ori*-beta (β), probe 8 marks the 3' flank of the cosmid DNA, and probe HyTK indicates the insertion of HyTK into the genome. M, molecular weight marker.
   c. Schematic diagram of retrovirus RV-L3HyTK2L. L3 and L2 are placed in inverted orientation flanking HyTK gene. Also shown is the position of the BamH I site and the probe used for Southern. Upon integration into the genome, the expected size of the fragment generated by BamH I is 4 + x kb.
   d. Southern analysis to determine the copy number of integrated HyTK gene in the HeLa cell clones (1 to 10) derived after infection with RV-L3HyTK2L. Genomic DNA was restricted with BamH I and probed against HyTK gene. Positive control (+) is original retrovirus DNA used to generate the stable line. P, parental HeLa.
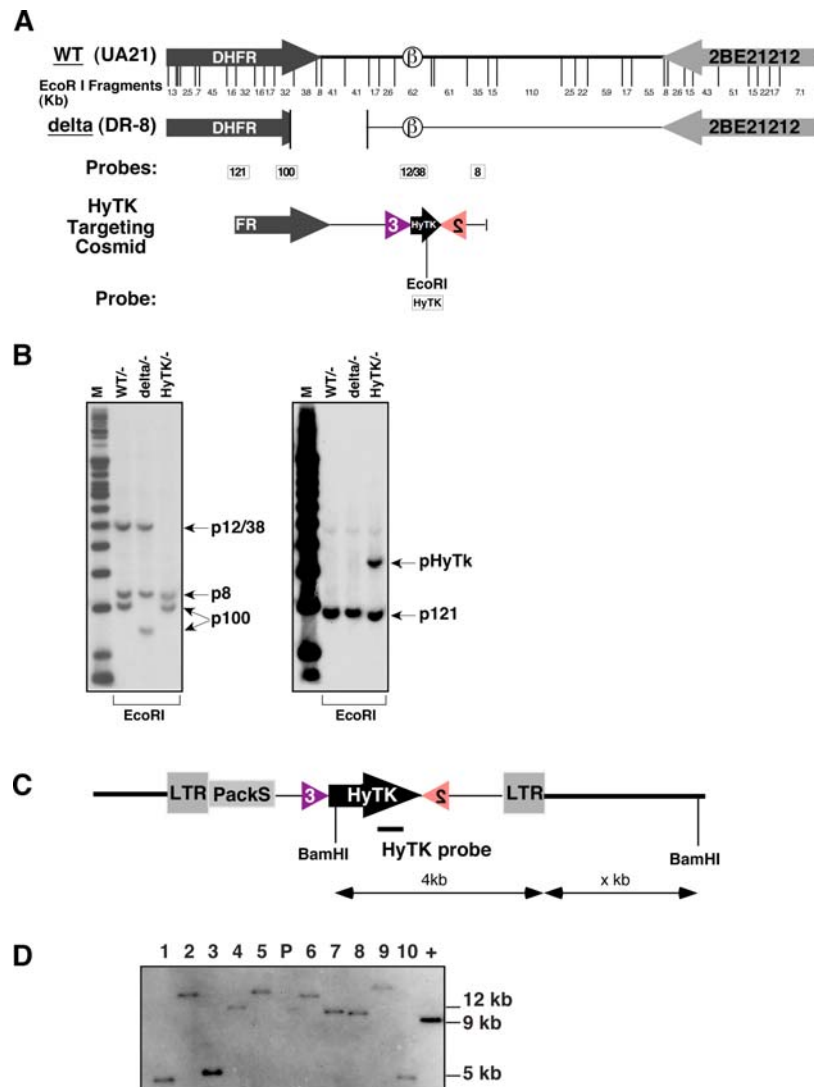
Figure 2.4: GFP induction by single plasmid Tet-On CHO 111-134 and HeLa M2PK RMCE clones. The RMCE clones were named after the L32L parent that they were derived from.

a. Schematic diagram showing the various genes that were incorporated to make up the RMCE clones. In CHO 111-134 and HeLa M2PK, rtTA and tTR genes are linked by IRES and transcriptionally driven by one promoter. Neo^R codes for neomycin/G418 resistance gene. The L3-TRE-LucGFP-2L cassette is inserted as single copy into the genome by RMCE as described in Fig 2.1.
b. Histogram plot showing green fluorescence exhibited by CHO 111-134 after induction with increasing concentration of dox for 72 hours.
c. Graph shows the mean fluorescence units exhibited by CHO 111-134 after induction with increasing dox concentrations for 72 hours. Data are obtained from two independent experiments.
d. Normalized luciferase activity to show maximum gene induction in cells before and after incubation with 2 µg/ml dox for 72 hours. Data represents mean and standard error of three independent experiments. Parental lines (P) do not have luciferase gene inserted into their genomes.
e. Histogram plots of GFP expression by RMCE derivatives before (-) and after (+) dox induction in one representative experiment. HeLa and CHO cells were induced with 0.1 µg/ml and 0.05 µg/ml dox respectively for 72 hours before harvesting for flow cytometry. Each population was gated and the percentage of the gated cells and their corresponding mean GFP fluorescence are indicated in each plot.
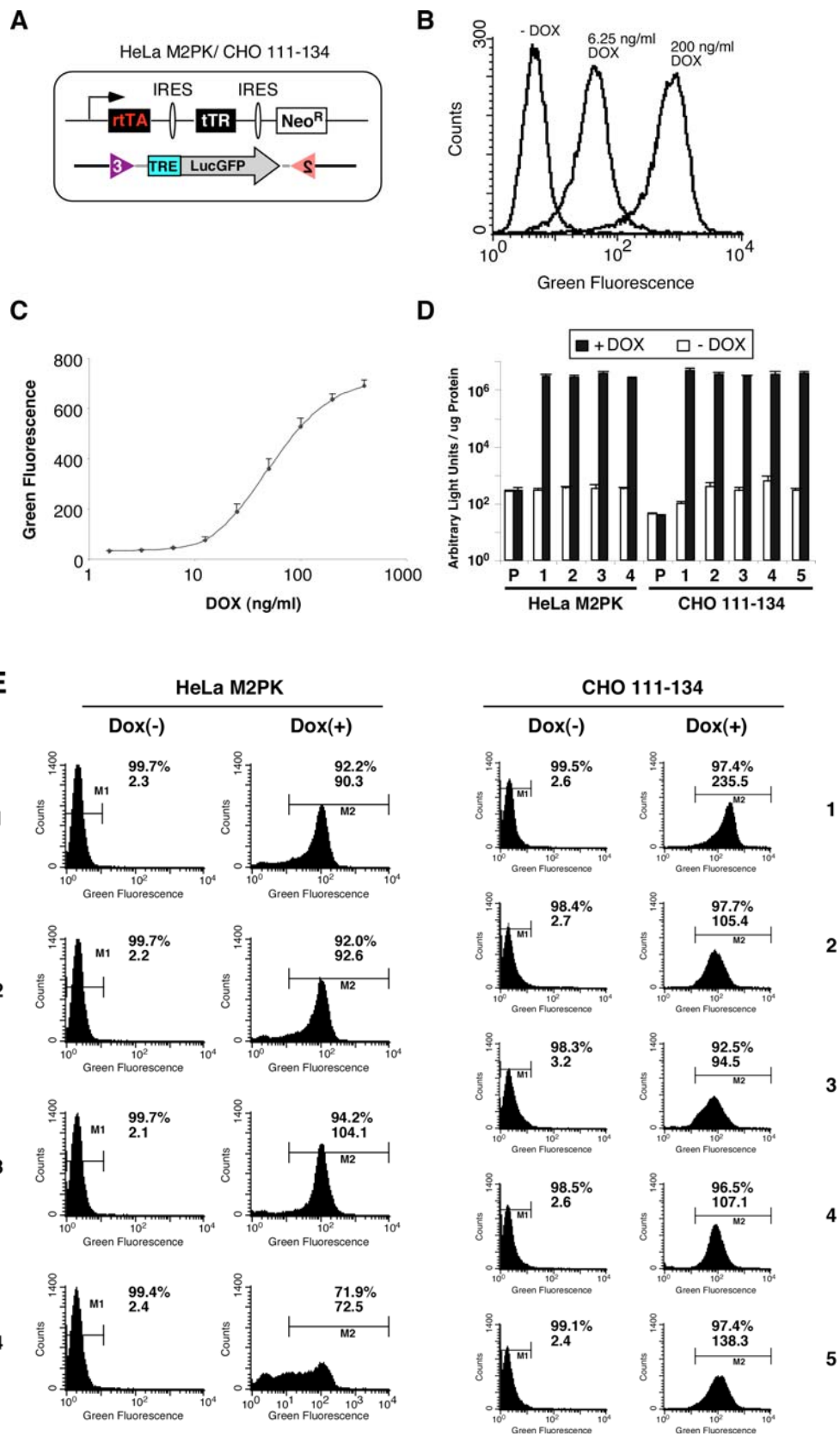
Figure 2.5: Reporter gene induction by two plasmids Tet-On stable HeLa M2K RMCE clones.

  a. Schematic diagram showing the various genes that were incorporated to make up M2K RMCE clones. Two independent promoters are used to drive the rtTA and tTR genes. The reporter gene LucGFP is inserted into the genome by RMCE.
  b. Normalized luciferase activity to show maximum gene induction in cells before and after incubation with 2 µg/ml dox for 72 hours. Data shown are mean with standard error obtained from three independent experiments.
  c. Histogram plots of GFP expression by M2K RMCE derivatives before (-) and after (+) dox induction at 0.1 µg/ml for 72 hours. Cells were harvested for flow cytometry amd each population was gated with the corresponding percentage of gated cells and mean GFP fluorescence shown in each plot.
  d. Graph shows mean GFP fluorescence of RMCE clones obtained from two independent RMCE experiments. Cells were either uninduced (-) or treated with 0.1 µg/ml dox for 72 hours.

A HeLa M2K

B

C

Dox(-)   Dox(+)

D
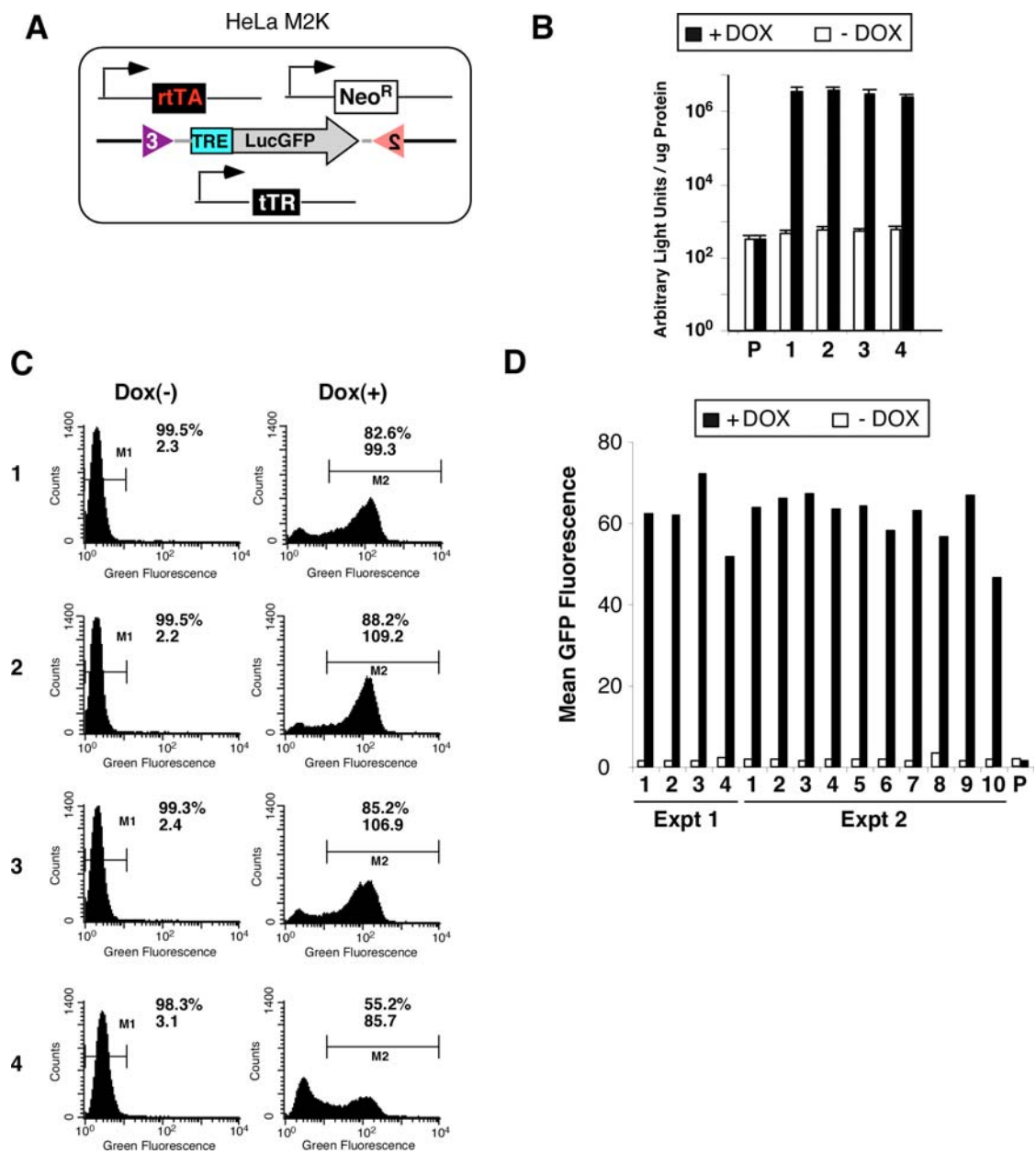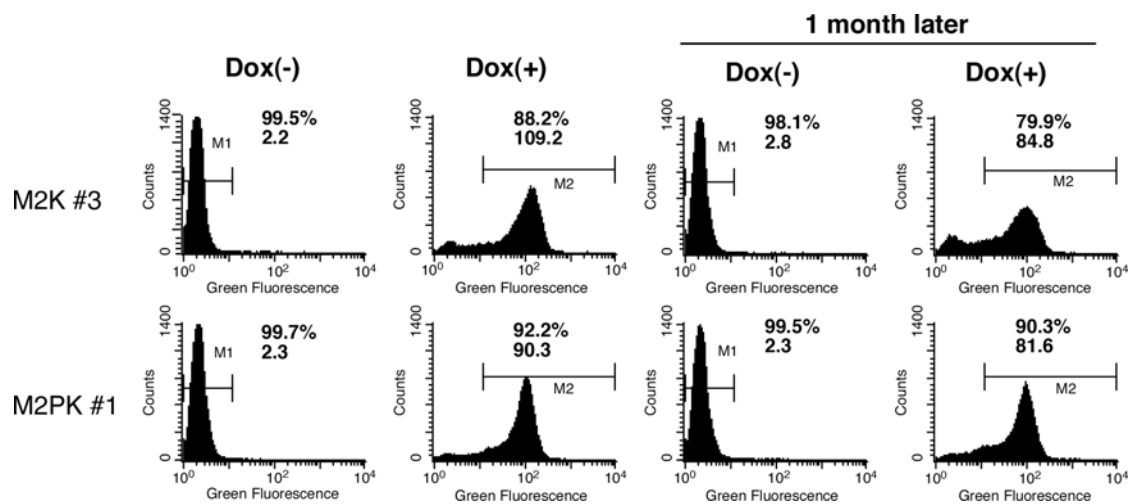
Figure 2.6: Stability of gene induction at the LoxP loci

Histogram plots showing GFP induction in M2K #3 and M2PK #1 before and after 1 month (mth) of continuous passage. Experiments were performed twice and data shown are from one experiment.
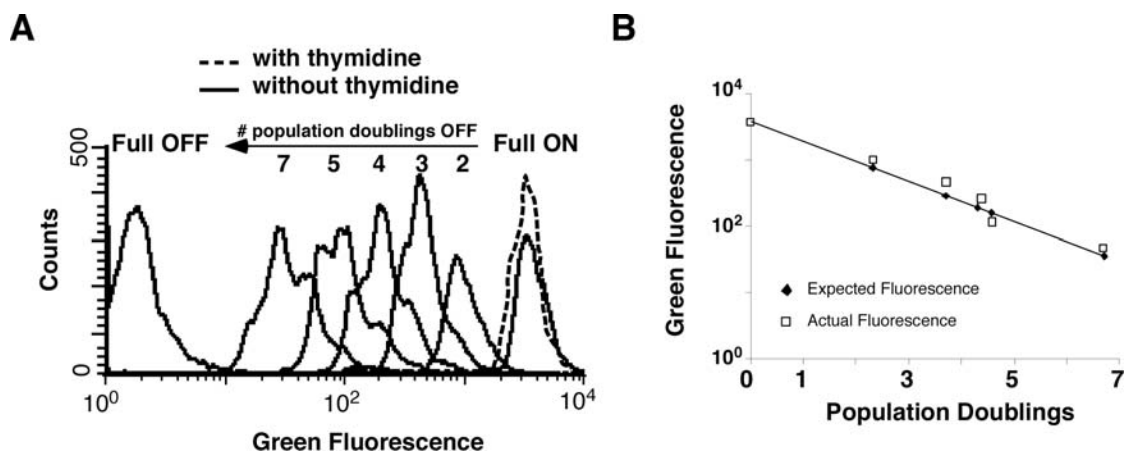
Figure 2.7: Monitoring cell doubling using inducible H2BGFP.

HeLa cells stably expressing TRE-H2BGFP were generated by L32L mediated RMCE. Cells were either not induced (- dox) or induced with 2 μg/ml dox (+ dox) for three days to achieve maximum expression before washing out the dox in the presence or absence of 2 mM thymidine. Cells were harvested each day after the removal of dox and their fluorescence monitored by flow cytometry (Actual fluorescence). The expected fluorescence is the theoretical fluorescence value assuming 50% decay after each population doubling. Experiments were performed twice and data from one experiment are shown as a histogram in (a) and as a graph in (b).

Table 2.1: RMCE efficiency in cell lines tested.

Two different loci were tested in CHO and 4 independent sites were tested in HeLa. The L32L site in CHO #4 was generated by retrovirus integration. LoxP sites in CHO 146-111 were introduced by homologous recombination into the DHFR locus. All RMCE clones were screened by PCR and scored for positive RMCE junctions (P3+P4 and P5+P6) and positive for TK (P1+P2) using primer pairs indicated in Fig 2.1. The percentage of successful recombinants is expressed as the number of positive junctions over the total number of clones tested.

Parental line	L32L clones	RMCE Exchange plasmid	Cre plasmid pOG231 (ug)	PCR for junction (no.+ve / no.tested)	PCR for HyTK gene (no.+ve / no.tested)	% Recombination
CHO	4	10ug L3-SV40bGal-2L	1	5/5	0/5	100
		30ug L3-SV40bGal-2L	3	5/5	0/5	100
		60ug L3-SV40bGal-2L	6	5/5	0/5	100
		0ug	3	0/3	3/3	0
		10ug L3-SV40bGal-2L	0	0/3	3/3	0
		30ug L3-IndbGal-2L	3	6/12	6/12	50
CHO	146-111	30ug L3 DHFR 207bp 2L	3	8/11	3/11	73
		30ug L3 DHFR 109bp 2L	3	12/12	0/12	100
		30ug L3 DHFR 101bp 2L	3	11/12	1/12	92
		30ug L3 DHFR 2400bp 2L	3	8/12	4/12	67
		30ug L3 DHFR 2299bp 2L	3	12/12	0/12	100
		30ug L3 DHFR 2291bp 2L	3	8/10	2/10	73
		30ug L3-TRE-LucGFP-2L	3	7/12	5/12	58
Overall Frequencies in CHO						**81**
HeLa	M2K2	30ug L3-TRE-LucGFP-2L	3	4/7	3/7	57
	M2K3	30ug L3-TRE-LucGFP-2L	3	6/8	2/8	67
	M2PK7	30ug L3-TRE-LucGFP-2L	3	5/8	3/8	63
	M2PK10	30ug L3-TRE-LucGFP-2L	3	3/3	0/3	100
Overall Frequencies in HeLa						**69**

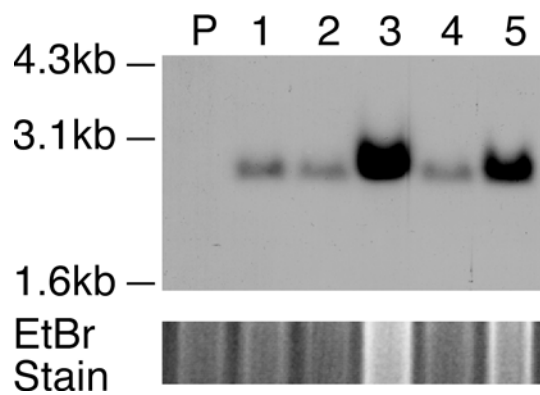Figure S2.1: Southern analysis of CHO 111-134 clones after RMCE to confirm single copy integration of TRE-LucGFP.

Genomic DNA were digested with BamH I and probed with Luc probe (upper panel) according to the schematic in Fig 2.1. Lower panel is ethidium bromide (EtBr) stain of the digested DNA before Southern blotting.

References

Alt, F. W., Kellems, R. E., Bertino, J. R., and Schimke, R. T. (1978). Selective multiplication of dihydrofolate reductase genes in methotrexate-resistant variants of cultured murine cells. J Biol Chem *253*, 1357-1370.

Andreas, S., Schwenk, F., Kuter-Luks, B., Faust, N., and Kuhn, R. (2002). Enhanced efficiency through nuclear localization signal fusion on phage PhiC31-integrase: activity comparison with Cre and FLPe recombinase in mammalian cells. Nucleic Acids Res *30*, 2299-2306.

Baer, A., and Bode, J. (2001). Coping with kinetic and thermodynamic barriers: RMCE, an efficient strategy for the targeted integration of transgenes. Curr Opin Biotechnol *12*, 473-480.

Barnes, L. M., Bentley, C. M., and Dickson, A. J. (2003). Stability of protein production from recombinant mammalian cells. Biotechnol Bioeng *81*, 631-639.
Baron, U., Gossen, M., and Bujard, H. (1997). Tetracycline-controlled transcription in eukaryotes: novel transactivators with graded transactivation potential. Nucleic Acids Res *25*, 2723-2729.

Bockamp, E., Maringer, M., Spangenberg, C., Fees, S., Fraser, S., Eshkind, L., Oesch, F., and Zabel, B. (2002). Of mice and models: improved animal models for biomedical research. Physiol Genomics *11*, 115-132.

Bouhassira, E. E., Westerman, K., and Leboulch, P. (1997). Transcriptional behavior of LCR enhancer elements integrated at the same chromosomal locus by recombinase-mediated cassette exchange. Blood *90*, 3332-3344.

Burhans, W. C., Vassilev, L. T., Wu, J., Sogo, J. M., Nallaseth, F. S., and DePamphilis, M. L. (1991). Emetine allows identification of origins of mammalian DNA replication by imbalanced DNA synthesis, not through conservative nucleosome segregation. Embo J *10*, 4351-4360.

Capecchi, M. R. (1989). Altering the genome by homologous recombination. Science *244*, 1288-1292.

Clarke, R. B., Spence, K., Anderson, E., Howell, A., Okano, H., and Potten, C. S. (2005). A putative human breast stem cell population is enriched for steroid receptor-positive cells. Dev Biol *277*, 443-456.

Feng, Y. Q., Seibler, J., Alami, R., Eisen, A., Westerman, K. A., Leboulch, P., Fiering, S., and Bouhassira, E. E. (1999). Site-specific chromosomal integration in mammalian cells: highly efficient CRE recombinase-mediated cassette exchange. J Mol Biol *292*, 779-785.

Forster, K., Helbl, V., Lederer, T., Urlinger, S., Wittenburg, N., and Hillen, W. (1999). Tetracycline-inducible expression systems with reduced basal activity in mammalian cells. Nucleic Acids Res *27*, 708-710.

Fukushige, S., and Sauer, B. (1992). Genomic targeting with a positive-selection lox integration vector allows highly reproducible gene expression in mammalian cells. Proc Natl Acad Sci U S A *89*, 7905-7909.

Fussenegger, M., Schlatter, S., Datwyler, D., Mazur, X., and Bailey, J. E. (1998). Controlled proliferation by multigene metabolic engineering enhances the productivity of Chinese hamster ovary cells. Nat Biotechnol *16*, 468-472.

Gossen, M., and Bujard, H. (1992). Tight control of gene expression in mammalian cells by tetracycline-responsive promoters. Proc Natl Acad Sci U S A *89*, 5547-5551.
Gossen, M., Freundlieb, S., Bender, G., Muller, G., Hillen, W., and Bujard, H. (1995). Transcriptional activation by tetracyclines in mammalian cells. Science *268*, 1766-1769.

Hirt, B. (1967). Selective extraction of polyoma DNA from infected mouse cell cultures. J Mol Biol *26*, 365-369.

Hoess, R. H., Wierzbicki, A., and Abremski, K. (1986). The role of the loxP spacer region in P1 site-specific recombination. Nucleic Acids Res *14*, 2287-2300.
Jin, Y., Yie, T. A., and Carothers, A. M. (1995). Non-random deletions at the dihydrofolate reductase locus of Chinese hamster ovary cells induced by alpha-particles simulating radon. Carcinogenesis *16*, 1981-1991.

Kalejta, R. F., Li, X., Mesner, L. D., Dijkwel, P. A., Lin, H. B., and Hamlin, J. L. (1998). Distal sequences, but not ori-beta/OBR-1, are essential for initiation of DNA replication in the Chinese hamster DHFR origin. Mol Cell *2*, 797-806.

Kanda, T., Sullivan, K. F., and Wahl, G. M. (1998). Histone-GFP fusion protein enables sensitive analysis of chromosome dynamics in living mammalian cells. Curr Biol *8*, 377-385.

Kellems, R. E. (1991). Gene amplification in mammalian cells: strategies for protein production. Curr Opin Biotechnol *2*, 723-729.

Knott, A., Garke, K., Urlinger, S., Guthmann, J., Muller, Y., Thellmann, M., and Hillen, W. (2002). Tetracycline-dependent gene regulation: combinations of transregulators yield a variety of expression windows. Biotechniques *32*, 796, 798, 800 passim.

Kolb, A. F. (2001). Selection-marker-free modification of the murine beta-casein gene using a lox2272 [correction of lox2722] site. Anal Biochem *290*, 260-271.

Kringstein, A. M., Rossi, F. M., Hofmann, A., and Blau, H. M. (1998). Graded transcriptional response to different concentrations of a single transactivator. Proc Natl Acad Sci U S A *95*, 13670-13675.

Lee, G., and Saito, I. (1998). Role of nucleotide sequences of loxP spacer region in Cre-mediated recombination. Gene *216*, 55-65.

O'Gorman, S., Dagenais, N. A., Qian, M., and Marchuk, Y. (1997). Protamine-Cre recombinase transgenes efficiently recombine target sequences in the male germ line of mice, but not in embryonic stem cells. Proc Natl Acad Sci U S A *94*, 14602-14607.

Paterna, J. C., Moccetti, T., Mura, A., Feldon, J., and Bueler, H. (2000). Influence of promoter and WHV post-transcriptional regulatory element on AAV-mediated transgene expression in the rat brain. Gene Ther *7*, 1304-1311.

Ringrose, L., Lounnas, V., Ehrlich, L., Buchholz, F., Wade, R., and Stewart, A. F. (1998). Comparative kinetic analysis of FLP and cre recombinases: mathematical models for DNA binding and recombination. J Mol Biol *284*, 363-384.

Salucci, V., Scarito, A., Aurisicchio, L., Lamartina, S., Nicolaus, G., Giampaoli, S., Gonzalez-Paz, O., Toniatti, C., Bujard, H., Hillen, W.*, et al.* (2002). Tight control of gene expression by a helper-dependent adenovirus vector carrying the rtTA2(s)-M2 tetracycline transactivator and repressor system. Gene Ther *9*, 1415-1421.

Scherdin, U., Rhodes, K., and Breindl, M. (1990). Transcriptionally active genome regions are preferred targets for retrovirus integration. J Virol *64*, 907-912.

Schroder, A. R., Shinn, P., Chen, H., Berry, C., Ecker, J. R., and Bushman, F. (2002). HIV-1 integration in the human genome favors active genes and local hotspots. Cell *110*, 521-529.

Schubeler, D., Maass, K., and Bode, J. (1998). Retargeting of retroviral integration sites for the predictable expression of transgenes and the analysis of cis-acting sequences. Biochemistry *37*, 11907-11914.

Seibler, J., Schubeler, D., Fiering, S., Groudine, M., and Bode, J. (1998). DNA cassette exchange in ES cells mediated by Flp recombinase: an efficient strategy for repeated modification of tagged loci by marker-free constructs. Biochemistry *37*, 6229-6234.

Teschendorf, C., Warrington, K. H., Jr., Siemann, D. W., and Muzyczka, N. (2002). Comparison of the EF-1 alpha and the CMV promoter for engineering stable tumor cell lines using recombinant adeno-associated virus. Anticancer Res *22*, 3325-3330.

Tumbar, T., Guasch, G., Greco, V., Blanpain, C., Lowry, W. E., Rendl, M., and Fuchs, E. (2004). Defining the epithelial stem cell niche in skin. Science *303*, 359-363.

Urlaub, G., and Chasin, L. A. (1980). Isolation of Chinese hamster cell mutants deficient in dihydrofolate reductase activity. Proc Natl Acad Sci U S A *77*, 4216-4220.

Urlinger, S., Baron, U., Thellmann, M., Hasan, M. T., Bujard, H., and Hillen, W. (2000). Exploring the sequence space for tetracycline-dependent transcriptional activators: novel mutations yield expanded range and sensitivity. Proc Natl Acad Sci U S A *97*, 7963-7968.

Warner, T. G. (1999). Enhancing therapeutic glycoprotein production in Chinese hamster ovary cells by metabolic engineering endogenous gene control with antisense DNA and gene targeting. Glycobiology *9*, 841-850.

Welm, B. E., Tepera, S. B., Venezia, T., Graubert, T. A., Rosen, J. M., and Goodell, M. A. (2002). Sca-1(pos) cells in the mouse mammary gland represent an enriched progenitor cell population. Dev Biol *245*, 42-56.

Westerman, K. A., and Leboulch, P. (1996). Reversible immortalization of mammalian cells mediated by retroviral transfer and site-specific recombination. Proc Natl Acad Sci U S A *93*, 8971-8976.

Wirth, D., and Hauser, H. (2004). Flp-mediated integration of expression cassettes into FRT-tagged chromosomal loci in mammalian cells. Methods Mol Biol *267*, 467-476.

Wong, E. T., Ngoi, S. M., and Lee, C. G. (2002). Improved co-expression of multiple genes in vectors containing internal ribosome entry sites (IRESes) from human genes. Gene Ther *9*, 337-344.

Zang, M., Trautmann, H., Gandor, C., Messi, F., Asselbergs, F., Leist, C., Fiechter, A., and Reiser, J. (1995). Production of recombinant proteins in Chinese hamster ovary cells using a protein-free cell culture medium. Biotechnology (N Y) *13*, 389-392.

III

Cell architecture can affect the biologic outcome of the P53 stress response pathway

through Hdmx regulation.

Summary

Extracellular matrix (ECM) and tissue architecture provide cell survival signals that can influence therapeutic efficacy. We therefore analyzed the responses of human mammary epithelial cells grown either as two dimensional (2D) monolayers or three dimensional (3D) acini to genotoxic and non-genotoxic P53 activators. Activation kinetics were similar in both growth states, but acinar structures were more resistant to apoptosis induced by a combination of genotoxic and non-genotoxic agents. This correlated with decreased down-regulation of Hdmx, a negative regulator of P53 transactivation. shRNA knockdown of Hdmx sensitized cells to apoptosis, indicating that Hdmx contributes to a threshold for P53 biological output. The data indicate that signals derived from tissue architecture influence Hdmx levels, which affects P53 activation and cell survival.

Significance

Most studies on P53 regulation are performed in fibroblasts and cancer cell lines growing as 2D sheets on non-physiological matrices. However, most cancers arise from the transformation of epithelial cells and normal epithelial cells are naturally attached on ECM and are organized into 3D structures *in vivo*. We found that a critical negative regulator of P53, Hdmx, is downregulated to a lesser extent in cells that exhibit normal cell architecture. This correlates with lower sensitivity to apoptosis. Reducing Hdmx expression sensitized cells to apoptosis. This study identifies a previously unrecognized link between cell architecture and Hdmx

regulation and supports the importance of cell architecture and Hdmx level in the influence of cell response to P53 activation during cancer therapy.

Introduction

Approaches to cancer treatment have broadened significantly over the past decade. Conventional therapy typically involves the use of clastogenic agents such as irradiation and DNA damaging drugs. However, the major drawbacks such as toxic side effects, mutagenic effects and the emergence of multi-drug resistance have fueled the search for less toxic alternatives. The enhanced understanding of the genetic and biochemical mechanisms by which cancers arise is enabling the development of target-selective agents exhibiting remarkable specificity for cancer cells (Hanahan and Weinberg, 2000; Vogelstein and Kinzler, 2004). One attractive approach is to re-activate the tumor suppressor P53 with the cis-imadazoline compound (Nutlin) in the numerous cancers that over-express the P53 negative regulator Hdm2 (Vassilev et al., 2004).

P53 is one determinant of the response to classical cancer therapies. P53 induces cell cycle arrest, apoptosis or DNA repair upon activation (Vogelstein et al., 2000). It is inactive under basal unstressed conditions, and is activated by diverse stresses including DNA damage, oncogene activation and metabolic stresses (Wahl, 2006). Thus, P53 activation limits the proliferation of cells with unrepaired DNA damage, and cells experiencing metabolic challenges or supra-physiological oncogene expression. Consequently, strong selective pressures exist for the outgrowth of cells that have *p53* inactivated by one of several mechanisms. For example, *p53* gene

mutations occur in about 50% of sporadic human cancers (Hollstein et al., 1991; Levine et al., 1991). Alternatively, wildtype P53 is functionally disabled in the remaining 50% of tumors by overexpression of its negative regulators, Hdm2 and Hdmx (the human orthologs of mouse Mdm2 and Mdm4), or loss of the Hdm2 antagonist P14Arf (Danovi et al., 2004; Kamijo et al., 1997; Momand et al., 1998; Riemenschneider et al., 1999).

Mdm2 and Mdm4 are essential negative regulators of P53, as deletion of either leads to early embryonic lethality, rescuable by P53 deficiency (Jones et al., 1995; Montes de Oca Luna et al., 1995). Mdm4 is a major antagonist of P53 transcriptional output. Mdm2 seems less able to antagonize P53 transactivation, but is the major determinant of P53 abundance and stability (Francoz et al., 2006; Toledo et al., 2006; Xiong et al., 2006). The contemporary view of P53 activation emphasizes that pathways that modulate the level and activity of Hdm2 and Hdmx should influence P53 downstream biological responses. In unstressed cells, Hdm2 stability depends on its interaction with the ubiquitin-specific protease HAUSP (herpes virus associated ubiquitin specific protease) (Cummins et al., 2004; Li et al., 2004) and phosphorylation by AKT (Ashcroft et al., 2002; Gottlieb et al., 2002), while mitogenic signals (eg Erk) and P53 modulate Hdm2 gene transcription (Ries et al., 2000a) Less is known about Hdmx regulation other than its stability is controlled by the balance of ubiquitination and deubiquitination by interaction with Hdm2 and HAUSP, which can be affected by phosphorylations introduced by damage activated kinases (Li et al., 2004; Meulmeester et al., 2005; Pereg et al., 2005).

The majority of studies on P53 regulation have employed fibroblasts or cancer cell lines growing on non-physiological matrices (e.g., coated plastic). However, cancers typically originate from epithelial cells, and the survival of epithelial cells and their responses to cancer therapies can be profoundly influenced by tissue architecture, cell-cell and cell-ECM attachment (Zahir and Weaver, 2004). Yet, it is unknown if the activation and output of the P53 pathway is affected by 3D structural organization. Interestingly, some reports have suggested that P53 activation can be affected by cell adhesion (Ilic et al., 1998; Lewis et al., 2002; Nigro et al., 1997; Seewaldt et al., 2001; Stromblad et al., 2002; Truong et al., 2003). The functional significance of cellular architecture on P53 functional output remain unclear as previous studies employed non-physiological rigid substrata or showed conflicting results in different cell types used.

This report describes the influence of 3D architecture and ECM adhesion on the ability of P53 to activate the cell cycle and apoptotic programs. We compared the responses of *p53* wildtype human mammary epithelial cells to genotoxic and non-genotoxic activators of P53 when grown in 2D and 3D. We show that cell architecture can affect the relative abundance of P53 and its key regulators. Interestingly, although P53 levels were higher, and Hdmx level was lower in 3D, the functional output of the pathway was similar in 2D and 3D cells. This implies the existence of factors beyond Hdm2 and Hdmx that are affected by cellular architecture to modulate P53 output. Nutlin did not induce apoptosis, while the commonly used chemotherapeutic agent doxorubicin (Dox) induced apoptosis in both 2D and 3D cells. Importantly, Nutlin and doxorubicin showed enhanced apoptotic activity in cells cultured in 2D, while

cells in 3D responded as if treated with doxorubicin alone. We show that the Hdmx level underlies the relative resistance of 3D cells to combined doxorubicin and Nutlin therapy. Thus, Hdmx is an important determinant of the biological outcome of the P53 pathway in cells growing in 3D, and signals from cell architecture appear to regulate Hdmx levels.

Results

The kinetics of ATM signaling to P53 and P53 activation are similar in 2D and 3D mammary epithelial cells

IR and doxorubicin are commonly used as adjuvant therapies in breast cancer patients. A comprehensive sequencing study revealed approximately 80% of all breast cancers express wildtype *p53* (Pharoah et al., 1999), suggesting that P53 function may be attenuated by mechanisms other than gene mutation. Since DNA damage activates P53, and the level and activity of P53 can be affected by ECM attachment (Lewis et al., 2002; Nigro et al., 1997; Truong et al., 2003), we used MCF10A cells to provide an *in vitro* model for evaluating the impact of cellular architecture on the kinetics of damage signaling and P53 activation.

MCF10A cells are an immortalized mammary epithelial cell line that retains wildtype *p53* but showed genetic alterations (eg. loss of *p14ARF* and *p16INK4a* and overexpression of *c-myc*) often seen in cells at the early stages of carcinogenesis (Crawford et al., 2004; Shimada et al., 2005; Silva et al., 2001). Through the use of MCF10A cells in 2D and 3D, we investigated the influence of cell architecture on P53 activation in these early initiated cells. The cells form polarized 3D structures when

grown on a commercially available basement membrane-like ECM extracted from Engelbreth-Holm-Swarm tumors (matrigel) (Debnath et al., 2003). By contrast, cells in 2D exhibit no cellular polarity (Figure S3.1A). Cells in 2D and 3D were predominantly in GO/G1 prior to analysis (Figure S3.1B). This controls for mitogenic signaling that can influence Hdm2 and P53 activity (Ashcroft et al., 2002; Gottlieb et al., 2002; Ries et al., 2000a), and for cell cycle phase that can influence cell survival (Dikomey and Brammer, 2000; Pawlik and Keyomarsi, 2004; Sak et al., 2000).

We first determined the kinetics of DNA damage induction and transmission of the damage signal to P53 (Figure 3.1A). Erk is used as loading control instead of actin as it is constant in 2D and 3D cells as shown in multiple western blots (see subsequent blots). ATM phosphorylation at Ser1981 is a surrogate marker for induction of DNA double strand breaks as it occurs very soon after their generation (Bakkenist and Kastan, 2003). ATM protein was more abundant in 2D cells, but as judged by S1981 phosphorylation, ATM was activated rapidly and with similar kinetics in cells growing in 2D and 3D after exposure to 6 Gy IR. Even though it appears that a greater proportion of ATM is phosphorylated in 3D cells, it is unclear if ATM is more active in 3D cells since phosphorylation of S1981 is not sufficient for ATM activation (Lee and Paull, 2005). Despite the significant difference in ATM level, there is paradoxically more S15-phosphorylated P53 in 3D cells. P53 was phosphorylated with similar kinetics in 2D and 3D cultures. We also measured ATM phosphorylation at lower IR doses (0.1 - 0.5 Gy) to determine if 2D and 3D cells exhibit a difference in their activation thresholds. The extent of ATM phosphorylation induced by low dose

IR was similar between the two growth states (data not shown), indicating that 2D and 3D cells are equally sensitive to activation by low amounts of DNA damage.

We next evaluated the levels of P53 and several proteins known to play key roles in P53 activation (Figure 3.1B). Hdm2 levels were similar, or somewhat higher in 2D cells, while Hdmx levels were consistently greater in 2D cells. P53 levels were higher in 3D cells, perhaps because the lower HAUSP levels destabilize Hdm2 to reduce its abundance. HAUSP levels did not change after DNA damage. Given higher level of P53 and S15-P53 in 3D cells, we predict stronger P53 activation in these cells. Since phosphorylation of P53 alone is not sufficient for activation, we further analyzed P53 activity by measuring the induction of P53 target gene products. Kinetic analysis showed that at early time points following IR (0-2 hours), levels of P53 increased, while Hdm2 declined in both 2D and 3D cultures, consistent with accelerated Hdm2 auto-degradation as an early step in P53 activation (Meulmeester et al., 2005; Stommel and Wahl, 2004). At later times, increases Hdm2 and P21CIP protein abundance occurred with similar kinetics in 2D and 3D cultures, though 2D cells accumulated more Hdm2 and P21CIP protein. Hdmx levels decreased after IR in cells growing in both 2D and 3D, and correlated with a time at which Hdm2 levels increased most significantly. This is consistent with recent studies reporting DNA damage induced degradation of Hdmx as an important contributor to P53 activation (Kawai et al., 2003; Meulmeester et al., 2005; Pan and Chen, 2003; Pereg et al., 2005).

The architectural differences created in cells growing in 3D can impact on nuclear processes such as transcription to influence the structure and function of the acini formed (Myers et al., 1998; Plachot and Lelievre, 2004; Roskelley et al., 1994).

Since P21CIP and Hdm2 can be regulated post-transcriptionally, we performed dose and kinetic analyses of the transactivation of one gene in each class of P53 target genes involved in cell cycle arrest, auto-regulation and apoptosis (Figure 3.1C). The transactivation of *p21CIP* in 2D and 3D cells and *hdm2* induction in 2D cells occurred in an IR dose-dependent manner. The fold accumulation of *p21CIP* and *hdm2* transcripts was similar in 2D and 3D cells following 3 and 6 Gy IR. However at 12 Gy, *hdm2* increase was weaker while *p21CIP* was higher and more sustained in 3D cells. The apoptotic gene *puma*, which is important for IR-induced apoptosis (Jeffers et al., 2003), was weakly transcribed and did not show significant differences in 2D and 3D cells (data not shown).

These data show that relative to 2D cells, despite higher proportion of phosphorylated ATM, more P53 and similar or lower levels of Hdm2 and Hdmx, P53 did not induce the examined target genes more efficiently in 3D cells. This reveals a lack of concordance between P53 abundance and activity, and suggests that factors beyond Hdm2 and Hdmx levels are regulated by growth conditions to affect P53 output.

The contribution of cell architecture to P53 activation induced by genotoxic agent and a direct P53 activator

In approximately 25% of breast cancers retaining wildtype *p53*, increased Hdm2 and Hdmx levels could compromise P53 function (Al-Kuraya et al., 2004; Danovi et al., 2004; Ho et al., 2001; Marchetti et al., 1995). Recently, small molecules that activate P53 in the absence of DNA damage have become available (Chen et al.,

2005; Galatin and Abraham, 2004; Issaeva et al., 2004; Vassilev et al., 2004). One such molecule, Nutlin, activates P53 by specifically preventing Hdm2-P53 interaction (Patton et al., 2006; Vassilev et al., 2004), Wade *et al*, in press). We therefore evaluated the impact of 3D architecture in regulating Hdm2 and Hdmx levels and the response of cells growing in 2D and 3D to Nutlin alone, and combination treatments with Nutlin and DNA damaging agent.

We assessed apoptosis induction in 3D cells by staining for active caspase 3. Only positively stained cells found in the periphery of the acini were counted (Figure 3.2A, white arrow heads). We excluded apoptotic cells in the center of the lumen as they result from a P53-independent process associated with lumen formation (Debnath et al., 2002; Muthuswamy et al., 2001) (Figure 3.2A, yellow arrow heads). No significant increase in the apoptotic population in the lumen was observed after the drug treatments. The predominant phenotype after Nutlin treatment in MCF10A cells is cell cycle arrest or senescence in the short or long-term, respectively (Figure S3.2). The topoisomerase II-dependent DNA damaging agent doxorubicin is frequently used in human breast cancer therapy, but serious side effects limit its use at high concentrations in humans. As doxorubicin and Nutlin activate P53 by different mechanisms, we determined whether their combined use might enable doxorubicin to be used at lower doses to elicit greater toxicity. At the stated concentration, doxorubicin-induced death in 2D cells is largely P53-dependent as apoptosis was significantly inhibited by a dominant negative C-terminal P53 fragment referred to as "DD" (Shaulian et al., 1992) (Figure 3.2B). When doxorubicin and Nutlin were used simultaneously on 2D cells, enhanced killing was observed as measured by caspase 3

positivity and confirmed by TUNEL and sub-G1 content (data not shown). By contrast, cell death induced by doxorubicin is P53-independent in 3D cells and the doxorubicin-Nutlin combination did not exhibit increased toxicity in 3D cultures. Hence, cells in 3D appear to be protected from apoptosis induced by this drug combination.

Attachment to the ECM induces changes in cell polarity, tissue architecture and downstream signal transduction to protect cells against cell death induced by diverse stresses (Weaver et al., 2002). We therefore determined whether ECM attachment per se, rather than generation of 3D architecture, generates survival signals that attenuate cell death induced by doxorubicin and Nutlin. We confirmed that communication with the ECM had taken place by determining the extent of activation of the focal adhesion kinase (FAK), which was higher in cells attached on plastic than matrigel (Figure 3.2C), as expected from previous reports (Paszek et al., 2005). We then evaluated the effects of doxorubicin and/or Nutlin applied soon after cell attachment to either matrix, and before formation of acini in the matrigel culture. Cells grown on tissue culture plastic or matrigel were equally sensitive to apoptosis induced by doxorubicin and Nutlin (Figure 3.2D). This indicates that ECM attachment and the cell shape change associated with attachment (Figure 3.2C) are not sufficient to confer protection against apoptosis induced by P53 activation. Instead, as suggested previously, 3D organization may play a more important role in determining cell survival after stress (Weaver et al., 2002).

P53-dependent transactivation of most target genes is similar between 2D and 3D cells

We next evaluated whether the difference in cell death induced by combined doxorubicin and Nutlin treatment derives from changes in P53, its upstream regulators and its transcriptional output. We first analyzed the P53 pathway in unstressed cells. The levels of P53 were higher, while HAUSP and Hdmx were lower in 3D cells compared to 2D cells (Figures 3.1, 3.3A). HAUSP is a relatively stable protein, as it did not increase after proteasome inhibitor (MG132) treatment. Lower HAUSP expression likely derives from decreased HAUSP transcription in 3D cells (Figure 3.3B). The increase in P53 is likely post-transcriptional as no significant increase in its mRNA was observed (data not shown). *p21CIP* mRNA was higher in unstressed 3D cells, but the increase is likely P53-independent as DD expressing 3D cells had a similar 2-fold increase in *p21CIP* transcript level. However, P21CIP protein level was similar or increased in 3D cells compared to 2D cells (Figures 3.1B, 3.3A, 3.3C). Hdm2 protein levels were similar or marginally reduced in 3D cells (Figures 3.1B, 3.3A). Hence, even though there are changes in the levels of P53 and its upstream regulators, P53 activity is similar in unstressed 2D and 3D cells.

Hdm2 negatively regulates P53 stability and its transcription function. We used Nutlin to specifically evaluate the extent to which Hdm2 controls P53 activation in 2D and 3D cells as it prevents Hdm2-P53, but not Hdmx-P53 interactions (Patton et al., 2006), Wade *et al*, in press). Nutlin activated P53 similarly in 2D and 3D cells, as determined by the increase in Hdm2 and P21CIP protein levels (Figure 3.3C). We investigated by immunostaining the possibility that heterogeneity in the 3D population

and differences in drug penetration could have led us to underestimate P53 activation in 3D cells (Figures S3.4A, B). There were slightly more P53-positive cells in 3D under basal conditions, while most of the cells were positive for P53 in 2D and 3D cultures after Nutlin treatment. The percentages of P21CIP and Hdm2 positive cells were similar in untreated and Nutlin-treated cells growing in both 2D and 3D.

We next extended the QPCR analysis to additional P53 target genes, as cell type and stress can affect the kinetics and spectrum of P53 target genes activated (Espinosa et al., 2003; Fei et al., 2002; Szak et al., 2001) (Figures 3.4A, S3.4C, D). The non-apoptotic genes (*p21CIP*, *hdm2*) and a gene coding for a secreted protein (*MIC-1*) generally exhibited greater induction than apoptotic genes (*bax*, *pig3*, *puma*) by Nutlin treatment. Interestingly, Nutlin induced other P53 pro-apoptotic target genes *noxa* and *bid* very poorly. Kinetics and dose response studies indicated that the induction of most target genes was similar between 2D and 3D cells with the exception of MIC-1, which was induced better in 2D cells at a late time point (24 hour). Taken together, these data demonstrate that P53 transcriptional output after Nutlin treatment is similar in 2D and 3D cells and is not sufficient for apoptosis induction. Therefore, Nutlin antagonizes Hdm2-P53 interaction similarly regardless of cellular architecture, with similar effects on P53 transcriptional output.

Since Nutlin synergizes with doxorubicin to induce cell death in 2D but not in 3D cells, and both drugs are P53 activators, we next determined if the transcriptional output of P53 differs between 2D and 3D cells after combined drug treatment (Figure 3.4B). Like Nutlin, doxorubicin turned on all the P53 target genes examined except with differences in the efficiency for *hdm2* and *MIC-1*. Combined drug treatments did

not lead to further P53 transactivation of target genes in 2D or 3D cells when compared to Nutlin treatment alone. This suggests that Nutlin-induced P53 target gene activation is saturated under the conditions we used. Among the target genes analyzed, *p21CIP*, *MIC-1* and *PUMA* induction were similar between 2D and 3D cells while *hdm2* and *bax* genes were induced better in 3D cells after doxorubicin and Nutlin treatment. Consistent with the mRNA data, the level of Hdm2 and P21CIP proteins did not further increase using a combination of two drugs compared to each drug singly (Figures 3.5A, B). We have not observed a direct correlation between the induction of the P53-target genes examined and sensitivity to apoptosis.

Cell survival signaling in 2D and 3D cells

Figure 3.2 indicates that cells growing in 3D are significantly more resistant to death induced by doxorubicin and Nutlin than cells growing in monolayer. Engagement of appropriate cell-ECM and cell-cell adhesion molecules can generate pro-survival signaling (Bates et al., 1994; Frisch and Screaton, 2001; Meredith et al., 1993). We therefore tested whether differences in the response of 2D and 3D cells to P53 activation may be attributed to alterations in cell survival signaling.

Akt and NFκB are two important pro-survival pathways that either work in conjunction with, or moderate the P53 pathway (Ashcroft et al., 2002; Gottlieb et al., 2002; Tergaonkar et al., 2002). We therefore determined whether their regulation is affected in 2D and 3D cells (Figure S3.3). The Akt pathway is commonly activated upon engagement of integrin and growth factor receptors (Kumar, 1998). However, growth-arrested 2D and 3D cells exhibited low mitogenic signaling through Erk and

Akt as demonstrated by the low abundance of P-Akt and P-Erk relative to an asynchronous population of dividing cells. The NFκB pathway may also be activated by 3D cell architecture-dependent signaling to protect cells in 3D against apoptosis (Weaver et al., 2002). We evaluated NFκB activation by determining the degradation of NFκB negative regulator IκBα and the activity of NFκB-responsive luciferase reporter. Doxorubicin, but not Nutlin, activated NFκB. Combined doxorubicin and Nutlin treatment did not further enhance NFκB activity, and NFκB activity was not significantly different between 2D and 3D cells. Hence, even though 3D cells were more resistant to apoptosis induced by combined doxorubicin and Nutlin treatment, cells growing in 3D did not manifest increased survival signaling through the Akt or NFκB pathways.

Hdmx is preferentially down regulated in 2D cells after doxorubicin and Nutlin treatment

The following studies were done to determine whether Hdmx could be a determinant of the relative resistance of 3D cells to apoptosis induced by doxorubicin and Nutlin. Hdmx levels remained unchanged following Nutlin treatment in both 2D and 3D MCF10A cells, but decreased in both growth conditions following doxorubicin treatment (Figures 3.5A, B). Interestingly, the Hdmx level was further reduced after combination treatment in 2D, but the extent of Hdmx decrease was significantly less in 3D cells.

We then tested whether Hdmx levels could affect the outcome of P53 activation. We used an shRNA against Hdmx to determine if decreasing Hdmx

abundance sensitizes 3D cells to doxorubicin and Nutlin-induced cell death. Following lentiviral delivery of Hdmx-specific shRNA into MCF10A cells, the Hdmx protein level was reduced to approximately 20% of basal level in the pooled and GFP sorted population as demonstrated by western analysis (Figure 3.5B). The reduction in Hdmx level by shRNA is uniform in the population as demonstrated by immunofluorescence analysis (data not shown). The basal levels of P21CIP and Hdm2 were slightly increased when Hdmx levels were reduced, consistent with Hdmx being a transcriptional antagonist of P53. Since cell architecture can influence the sensitivity of 3D cells to doxorubicin and Nutlin induced cell death, we first evaluated if Hdmx knockdown affected the cells ability to form polarized acini by staining 3D cells for protein markers indicative of polarized structures. Cells expressing control and Hdmx shRNA in matrigel culture localized α6-integrin to the basal side of the acini and β-catenin at cell-cell junctions as indicated by IF staining (Figure 3.5C). Therefore, lowering Hdmx level does not influence organization into acini. Hdmx knockdown did not sensitize cells to Nutlin-induced cell death, but increased cell death by approximately 2-fold in 2D cells in response to doxorubicin and combined doxorubicin-Nutlin treatment (Figure 3.5D). In contrast to control shRNA, Hdmx shRNA significantly sensitized 3D cells to apoptosis induced by the combination of doxorubicin and Nutlin. Reducing Hdmx levels made the cells so sensitive to apoptosis that they were harvested 24 hours post-treatment instead of 48 hours as used previously. Hence, the differential sensitivity of 2D and 3D cells to doxorubicin and Nutlin-induced apoptosis is significantly affected by the endogenous level of Hdmx.

Since Hdmx is a transcriptional antagonist of P53, we next evaluated the transcriptional output of P53 after Hdmx knock down. The influence of Hdmx reduction on P53 target gene induction appeared to be target gene and stress specific (Figure S3.5). Relative to control shRNA treated cells, shRNA-Hdmx treated cells in 2D and 3D exhibited higher levels of *p21CIP* and *MIC-1* but *bax* was not affected. Importantly, the increased apoptosis exhibited by shRNA-Hdmx expressing 3D cells did not correlate with increased transactivation of the pro-apoptotic target analysed. In summary, while P53-dependent transcriptional output can be increased by Hdmx knockdown, we did not observe a difference in the genes analyzed sufficient to explain the substantial increase in apoptotic sensitivity of 3D cells.

Discussion

P53 has recently been implicated in responding to, as well as modulating, cellular energy balance and metabolism (Bensaad et al., 2006; Crighton et al., 2006; Jones et al., 2005; Matoba et al., 2006). Consistent with these observations, P53 activation can be affected by mitogenic signaling through effects on Hdm2 (Ashcroft et al., 2002; Gottlieb et al., 2002; Ries et al., 2000b). It is reasonable to conjecture, therefore, that the rigidity of the ECM and effects of 3D cellular architecture might also affect the kinetics or consequences of P53 activation since they profoundly influence signaling pathways affecting cell growth and survival (Bissell et al., 1999; Boudreau and Bissell, 1998; Ingber, 2003; Weaver et al., 2002). Here, we show that the signals generated from DNA damage to activate P53 are dominant to potential mitigating influences of 3D cellular architecture and ECM engagement in a mammary

epithelial cell model. Importantly, we also show that organization within a 3D acinar structure can significantly attenuate death signaling mediated by a combination of a genotoxic agent and Nutlin. The data reveal that Hdmx is one important determinant of the consequences of P53 activation in cells growing as a 3D structure, and they emphasize the importance of cell architecture in influencing the outcome of therapeutic regimens.

DNA damage signaling and P53 transcriptional output are dominant to signals from cell architecture

ECM adhesion and cell architecture can significantly alter intracellular signal transduction, nuclear organization and gene transcription profiles (Bissell et al., 1999; Ingber, 2003; Ingber, 2006; Lelievre et al., 1998; Maniotis et al., 1997). Like other epithelial and endothelial cells, MCF10A requires ECM attachment for survival (Reginato et al., 2003). However, unlike endothelial cells (Ilic et al., 1998; Stromblad et al., 2002), death from detachment is P53-independent as DD expressing cells cleared the lumens of acini as effectively as parental cells (data not shown). Attachment of MCF10A cells onto various ECMs stimulated mitogenic signaling and Hdm2 accumulation to different extent. However, attachment on plastic or matrigel does not impact on the ability of P53 to transactivate *p21CIP* or induce cell cycle arrest after IR (data not shown). This emphasizes that DNA damage induced P53 activation is dominant to potential mitigating mitogenic signals from the ECM (Hosokawa et al., 1998).

Molecular connections between cell adhesion molecules, cytoskeletal filaments, and nuclear scaffolds generate the 3D cellular superstructures that comprise functional units within organs. The question of whether 3D organization also impacts DNA damage signaling to P53 has not been addressed. Our analyses (in MCF10A and 184A1, data not shown) reveal a striking similarity of P53 activation in cells growing in 2D or 3D. Thus, the early events triggered upon DNA damage such as ATM activation, transduction of the damage signal to P53, and P53 transcriptional activation were not detectably affected by signals from cell organization.

Previous studies showed a strong correlation between the stabilization and accumulation of P53 after stress with increased transactivation of P53 target genes in cells growing in 2D (Kubbutat et al., 1997; Li et al., 2002b; Stommel and Wahl, 2005). Interestingly, P53 levels were substantially higher, while Hdmx were significantly lower in 3D cells. Yet, transcriptional activation of the six P53 target genes analyzed was remarkably similar in DNA damaged or Nutlin treated 2D and 3D cells. Furthermore, there was no correlation between target gene activation of *bax*, *PIG3* or *PUMA* and apoptosis, suggesting that activation of these three classic apoptotic activators identified in 2D cells do not determine apoptotic sensitivity in 3D cells. A more comprehensive analysis by microarray will be required to identify P53 target gene targets that determine the differing sensitivity to Nutlin and doxorubicin in cells growing with correct architecture in 3D.

Our data indicate that P53 is far less efficient transcriptional regulator in 3D acini than in 2D monolayers. *In vitro* footprinting and chromatin immunoprecipitation (ChIP) assays demonstrate that P53 binds chromatin constitutively even without stress

(Espinosa and Emerson, 2001; Kaeser and Iggo, 2002; Szak et al., 2001). The lower amount of acetylated histone H4, and increased amount of heterochromatin protein HP1 γ and chromatin associated methyl binding proteins (MeCP2) are indicative of a more repressed chromatin state in 3D cells (Plachot and Lelievre, 2004). Since P53 exhibited similar nuclear localization in cells growing in both conditions, it is conceivable that a smaller fraction of P53 is chromatin associated in 3D cells. Although this possibility can be addressed by ChIP, the limited material available from 3D cultures has thus far prevented such studies. Alternatively, the efficiency of transcription by P53 may be lower in 3D cells due to their repressive chromatin structure.

3D cell architecture promotes cell survival in response to P53 activation and cytotoxic stress by a mechanism involving Hdmx

The tissue microenvironment has been implicated in tumor resistance to therapy (Paszek et al., 2005). The experimental model we used offered a route to examining strategies to preferentially kill tumor cells in specific microenvironmental contexts as well as the potential mechanisms underlying therapy resistance. Consistent with previous studies using normal skin cells, fibroblasts and hematopoietic cells (Secchiero et al., 2006; Vassilev et al., 2004), Nutlin alone did not kill MCF10A cells growing in 2D or 3D. However, the commonly used chemotherapeutic agent doxorubicin and an inducer of the extrinsic apoptotic pathway (TRAIL, Figure S3.6) were equally effective in killing MCF10A cells growing in both conditions. The sensitivity of 3D cells to TRAIL- or doxorubicin-induced apoptosis

contrasts with a previous study showing that 3D tissue organization enhanced survival signaling to counteract death signals induced by death receptor ligation and etoposide treatment (Weaver et al., 2002). This discrepancy may be explained by the use of different cell lines (the cell line used in this study is wildtype for *p53*) and different classes of drugs used in the two studies.

Combination drug therapy is often employed to increase tumor cell killing and decrease resistance. Consistent with previous observations, doxorubicin and Nutlin treatment enhanced cell death compared to drugs used singly in 2D cells (Patton et al., 2006). By contrast, such additive cytotoxicity was not observed in 3D cells. The difference in drug sensitivity is not likely due to differences in drug penetration or variation in responses within a sub-population of cells in 3D since immunofluorescence analysis revealed equal proportions of cells exhibiting P53 activation. Tumors grow as 3D cluster of cells that exhibit no cell polarity. Tumor cells grown as 3D mass are more resistant to therapy compared to monolayer cultures (Desoize and Jardillier, 2000; Durand and Sutherland, 1972; Frank et al., 1993; Kwok and Sutherland, 1991; Rodriguez et al., 1988). Our findings suggest the importance of cellular context and tissue organization in influencing chemotherapeutic responses. Hence it is important to extent the finding to determine if 3D per se affects P53 activity in *p53* wildtype cancer cells.

Hdmx has emerged as an important regulator of P53 transactivation in both unstressed and stressed cells, but Hdmx has not previously been linked to regulating P53 output in response to architectural cues. Our data show that Hdmx is an important contributor to the relative resistance of 3D cells to apoptosis induced by doxorubicin

and Nutlin. Cells in 3D degraded Hdmx with lower efficiency than cells in 2D when exposed to this drug combination. Full P53 activation by Nutlin requires that the P53 abundance must increase to exceed that of Hdmx. In normal cells and many tumor cell lines, DNA damage induces Hdmx degradation, which contributes to P53 activation. Thus, lack of Hdmx degradation in 3D cells should attenuate P53 activation. Strikingly, shRNA against Hdmx reduced Hdmx levels by 70-80% and stimulated cell death induced by doxorubicin and Nutlin more in 3D than in 2D cells. These data are consistent with other recent studies showing that lowering Hdmx levels sensitizes cells to Nutlin-induced cell killing (Patton et al., 2006), Wade *et al*, in press).

Based on the above information, it would be reasonable to infer that the mechanism by which reduced Hdmx levels augment the P53 response is through increased P53 transactivation. However, the transcriptional effects on the genes analysed was surprisingly modest. Interestingly, we also observed P53 transactivation following Hdmx knockdown, but in a stress- and target gene-specific manner, with the most significant increases being in *p21CIP* and *MIC-1*. Importantly, none of the apoptotic target genes analyzed increased after Hdmx knockdown, and their levels did not correlate with sensitivity of 2D and 3D cells to apoptosis. Hence, it remains possible that Hdmx regulates a specific subset of pro-apoptotic genes that remains to be identified to differentially regulate the sensitivity of 2D and 3D cells to apoptosis. Another intriguing possibility is that Hdmx has effects in both the nucleus and the cytoplasm since it is far more abundant in the cytoplasm of 2D and 3D cells (E-t Wong, unpublished observations and (Li et al., 2002a; Pan and Chen, 2003).

Our data show that Hdmx functions as a buffer against P53-dependent cell death, and they reveal the importance of cell architecture in influencing the survival outcome of cells upon P53 activation. Differential regulation of Hdmx degradation by changes in tissue organization clearly influences the functional output of P53 activation, and suggests that genetically similar cells in different architectural contexts may respond very differently to drug treatment. This could constitute a novel mechanism of resistance to cytotoxic and biologically targeted therapies. On the other hand, strategies that induce Hdmx degradation or down-regulation in cancer cells expressing wild type *p53* may be able to achieve a favorable therapeutic index when used in combination with drugs such as Nutlin that appear to exhibit remarkably little toxicity towards normal cells *in vivo* (Vassilev et al., 2004).

Experimental Procedures

Cell culture

MCF10A cells were from ATCC and Matrigel™ was from Trevigen. The media and culture conditions used for regular maintenance and acini culture were as described (Debnath et al., 2003) and supplementary data). 2D cells were allowed to grow to 80-90 % confluence in growth medium before growth arrest in assay medium for two days prior to drug treatment. 3D cells grown on matrigel in differentiation medium for 5-6 days were transferred to assay medium containing 2 % matrigel for 2 days prior to drug treatment. For acute attachment, MCF10A cells were resuspended in assay medium containing a final concentration of 5 ng/ml EGF and replated onto tissue culture plates that were either uncoated or pre-coated with 300 μl matrigel at a

density of $1 \times 10^5 / 35$ mm dish. Cells were allowed to attach for 3-4 hours prior to drug treatments.

Drug treatments

Nutlin was a kind gift of Dr Lyubomir Vassilev (Hoffman-La Roche) and was used at a final concentration of 2.5 μM unless otherwise stated. Doxorubicin and MG132 (Calbiochem) were used at final concentrations of 0.6 μg/ml and 10 μM respectively. TRAIL (Peprotech) was used at final concentration of 50 ng/ml.

γ-irradiation

Growth medium was removed and cells were irradiated using a Co-60 source at 500 Rad/min. Growth medium was replaced and cells were returned to 37ºC.

Lentiviral-mediated gene delivery

The construction of lentivirus expressing shRNA against Hdmx or MKP (chicken MAPK phosphatase) was described elsewhere (Wade *et al*, in press). The lentivirus construct containing the NFκB responsive luciferase reporter was provided by Dr Inder M. Verma (Tergaonkar et al., 2003). Virus production and titering were performed as described (Wade *et al*, in press). Virus particles were concentrated by pelleting culture supernatant at 50, 000 g for 2 hours. Cells were infected overnight at multiplicity of infection of 10 and cultured for one week before performing all other experiments. Cells were sorted for GFP using the Becton-Dickinson FACS Vantage

SE DiVa cell sorter to isolate cells expressing high level of shRNA against Hdmx or MKP.

Indirect IF and image acquisition

Cells in 3D culture were processed into 7 µM thick cryosections before immunostaining (Gudjonsson et al., 2003). Immunostaining was performed using procedures as previously described (Debnath et al., 2003). Images were captured using the Leica TCS SP2 AOBS Confocal microscope.

Western blot

Proteins were extracted from 3D cells as previously described (Debnath et al., 2003). Western blot procedure and antibodies used were as described (Stommel and Wahl, 2004). Antibody against IκBα was a kind gift from Dr Inder M. Verma. For quantitation of band intensity using the Odyssey infrared imaging system (LiCor system), PVDF membrane (Immobilon-FL, Millipore), Odyssey blocking solution at 1:1 mix with PBS, IRDye™800 (Rockland Immunochemicals) and AlexaFluor 680 (Molecular Probes) conjugated secondary antibodies (1:20000) were used. Bands were scanned and analyzed using the Odyssey imaging software provided.

Real time quantitative PCR

Total RNA extraction (Qiagen RNeasy Kit), reverse transcription (Invitrogen SuperScript III) and QPCR (SYBR green or Taqman (for PUMA), Invitrogen) were performed as described (Stommel and Wahl, 2004). With the exception of RNA

isolated from doxorubicin-treated samples, transcript levels obtained from all other samples were normalized to 18S rRNA. As the level of 18S rRNA was repressed in doxorubicin treated samples, transcript levels were normalized to β-glucuronidase instead.

Luciferase assay

Luciferase assay was performed as described previously (Wong et al., 2002).

Cell Cycle and flow cytometry

Cells were labeled with 10 μM bromodeoxyuridine (BrdU) for 1 hour before harvesting. Briefly, cells were harvested from matrigel by treating with dispase for 10-15 minutes (Roche) before dissociation into single cells by trypsinization. Cells were fixed at 4°C overnight in 70% ethanol. Cells were stained with fluorescein isothiocyanate-conjugated anti-BrdU antibody according to the manufacturer's protocol (Discovery labware) and propidium iodide and analysis was performed using FACScan flow cytometer (Discovery labware).

Detection of senescent cells

Cells were stained for acidic β-galactosidase according to (Dimri et al., 1995).

Statistical analysis

Paired t-test using Microsoft Excel was performed on QPCR and IF data.

Acknowledgements

We thank Dr Tony Hunter, Lesley Ellies, Mark Wade, Kurt Krummel, Vivian Wang, Ettienne Danis and Leo YC Li for thoughtful readings of the manuscript. We also thank Dr Mina Bissell, Aylin Rizki and Jimmie E Fata for assistance with 3D matrigel culture, Dr David Chambers, Quan Zhu and Chun Li Zhang for assistance with confocal microscopy, Dr Inder Verma for providing NFκB reporter constructs, Dr Lyubomir Vassilev for providing Nutlin. This work was supported by grants from the NIH (CA61449 and CA10845-04) to GMW. This material is based upon work supported under an A*STAR Oversea Graduate Fellowship awarded to E.Wong.

The dissertation author is the primary researcher and author and Geoffrey M. Wahl directed and supervised the research that forms the basis for this chapter.

Figure 3.1: The kinetics of DNA damage signaling to and P53 activation are similar between growth arrested 2D and 3D cells

a. Cells were subjected to 6 Gy IR before harvest at the indicated time points for western analysis. "L" and "H" represent lower and higher exposures, respectively. The corresponding exposures in 3D were omitted, as they were either too faint or too dark to be suitable for display.
b. Western blot to demonstrate changes in the level of P53 upstream regulators and induction of downstream targets following 6 Gy IR.
c. *p21$^{CIP/KIP}$* and *hdm2* mRNA induction following 3, 6 and 12 Gy IR. Transcripts were quantified by QPCR and fold inductions relative to the untreated were expressed as mean ± SEM.

A

2D   3D

6Gy IR (hr)   0 0.5 1 2 4 8 10   0 0.5 1 2 4 8 10

P-ATM
ATM
ATM (L)
S15-P53
S15-P53(H)
P53
Erk

B

2D   3D

6 Gy IR (hr)   0 0.5 1 2 4 8 10   0 0.5 1 2 4 8 10

HAUSP
Hdm2
Hdmx
Hdmx (L)
P53
P21CIP
Erk

C

p21^{CIP} Induction

Fold Induction

P<0.6   P<0.1   P<0.6

2D 3D   2D 3D   2D 3D
3Gy   6Gy   12Gy

□ 0hr
■ 4hr
■ 8hr
■ 12hr

hdm2 Induction

Fold Induction

P<0.2   P<0.1   P<0.007
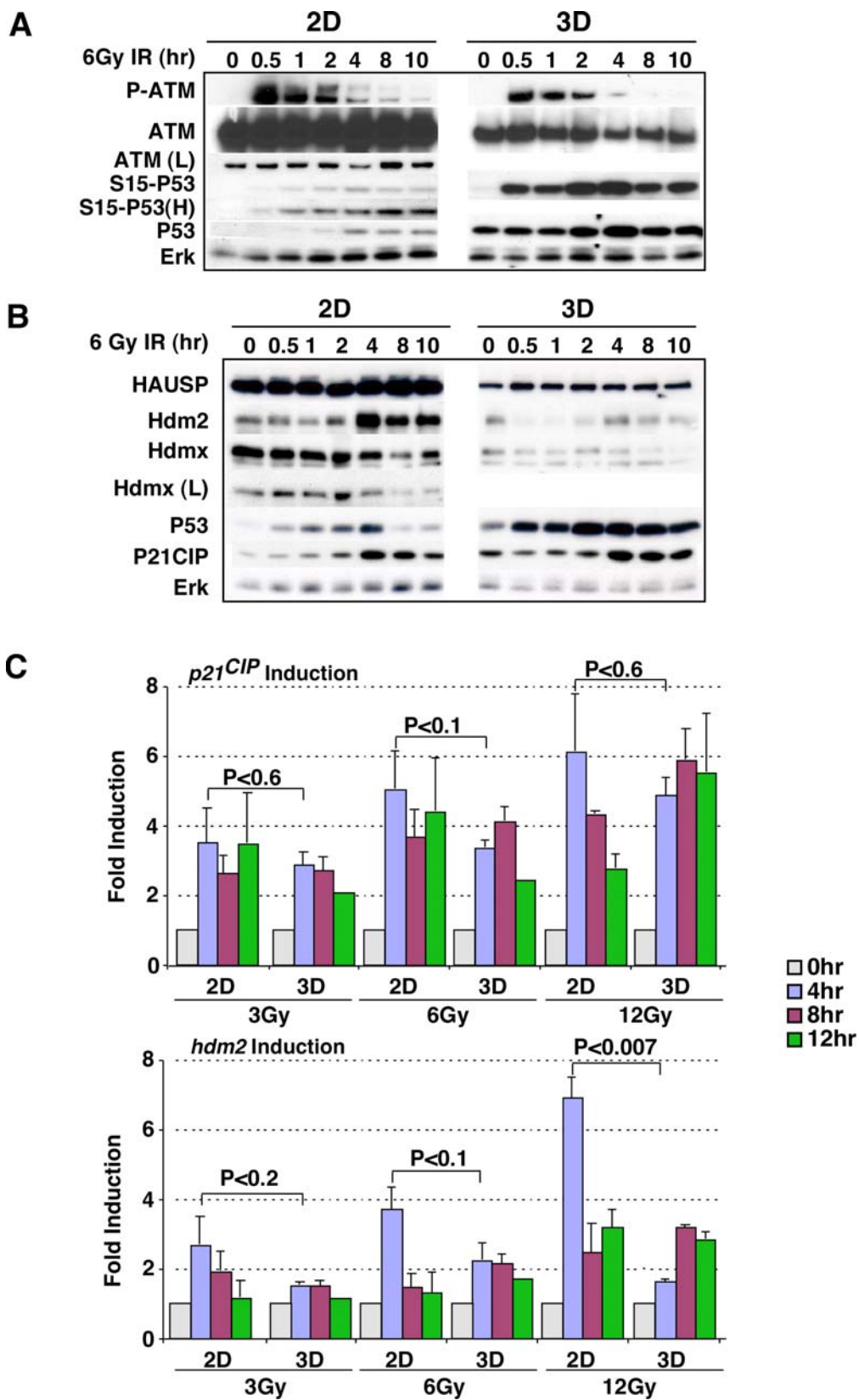
2D 3D   2D 3D   2D 3D
3Gy   6Gy   12Gy

Figure 3.2: P53-dependent apoptosis induced by a combination of Nutlin and doxorubicin is attenuated in 3D cells.

a. IF demonstrating active caspase 3 (casp 3) staining in growth arrested MCF10A cells in 3D following Nutlin (Nut), doxorubicin (Dox) or combination of doxorubicin and Nutlin (Dox+Nut) treatment. Cells were harvested 48 hours after treatment and processed as 7 μm thick frozen sections for immunostaining. Casp 3 positive cells that are located at the periphery of an acinus (white arrow heads) were counted while casp 3 positive cells located within the central lumen of an acinus (yellow arrow heads) were not counted for experiments described in (b).

b. Cell death in P53 wild-type and P53 dominant negative (DD) expressing MCF10A cells 48 hours after drug treatment. A minimum of at least 100 cells were counted and expressed as a percentage of total cell count before plotting the mean ± SEM from 3 independent experiments.

c. MCF10A cells were trypsinized and replated at low density onto either tissue culture plastic (plastic) or matrigel-coated plate (matrigel). Top panel: phase contrast picture to demonstrate cell shape change at 2 and 10 hours following attachment. Bottom panel: IF staining to demonstrate signaling to FAK at 2 hours post-attachment.

d. Growing MCF10A cells were seeded at low density onto plastic or matrigel and allowed to attach for 3 hours before addition of drugs. Cell death was assessed by casp 3 staining 24 hours after drug treatment.
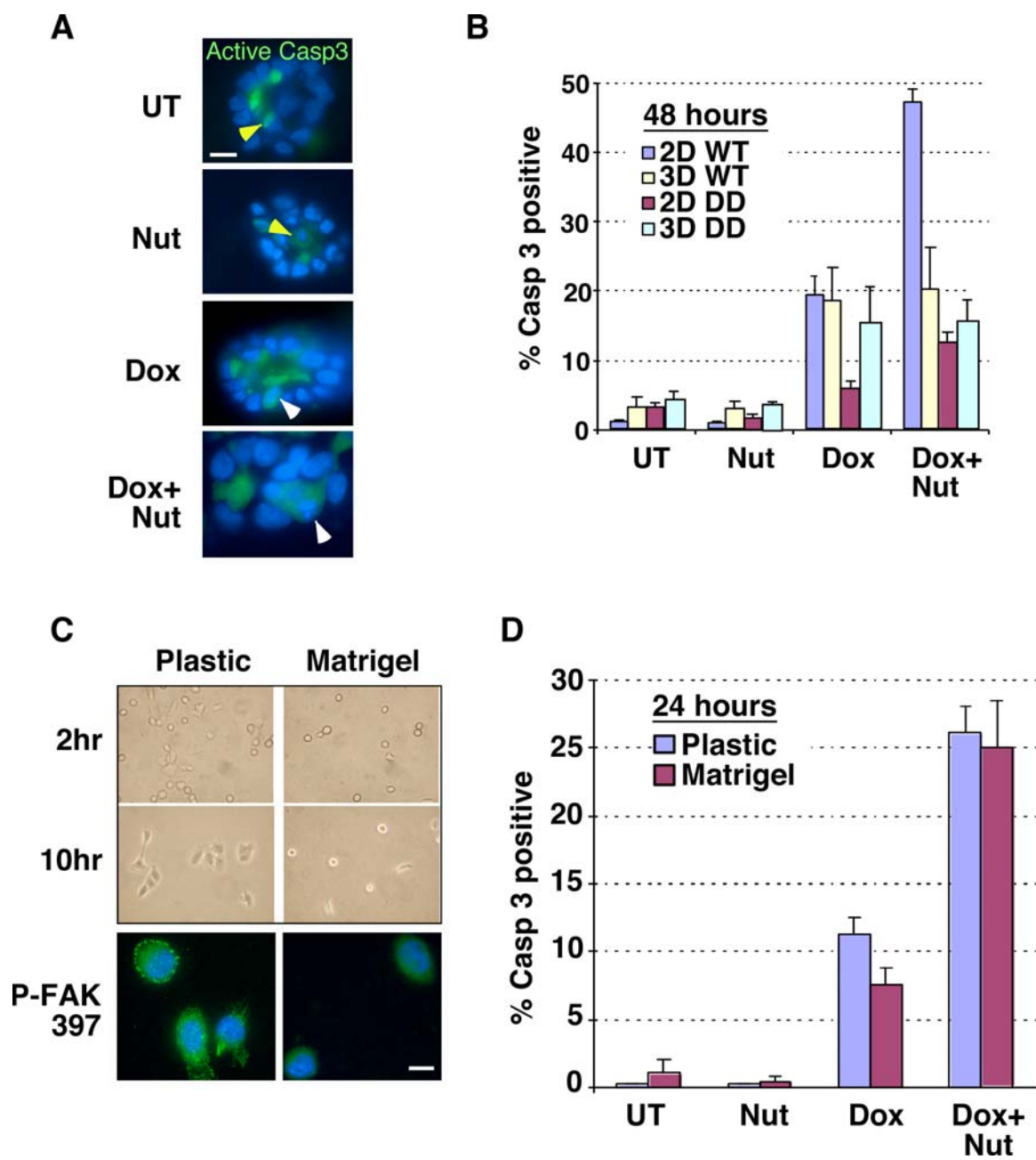
Figure 3.3: Transactivation of most P53-dependent target genes is similar between growth arrested 2D and 3D cells.

a. 2D and 3D cells were either left untreated (-) or treated with MG132 (+) for 8 hours before harvesting for western blot. Erk is used as the loading control.
b. Steady state transcript levels in 3D relative to 2D cells. Transcripts were quantified by QPCR and are mean ± SEM obtained from at least 3 independent experiments.
c. Western analysis to show the time course of P53 stabilization and Hdm2 and P21CIP induction after Nutlin treatment in 2D and 3D cells
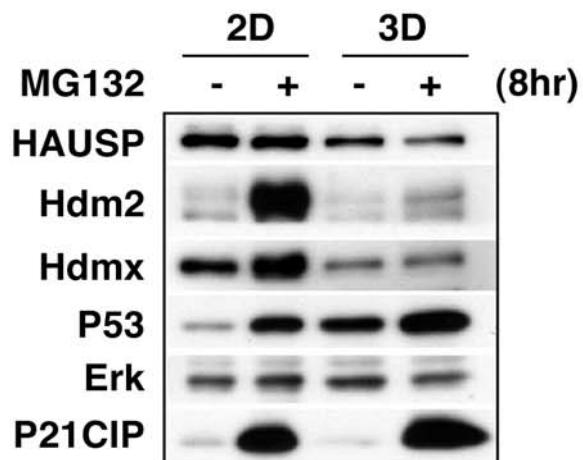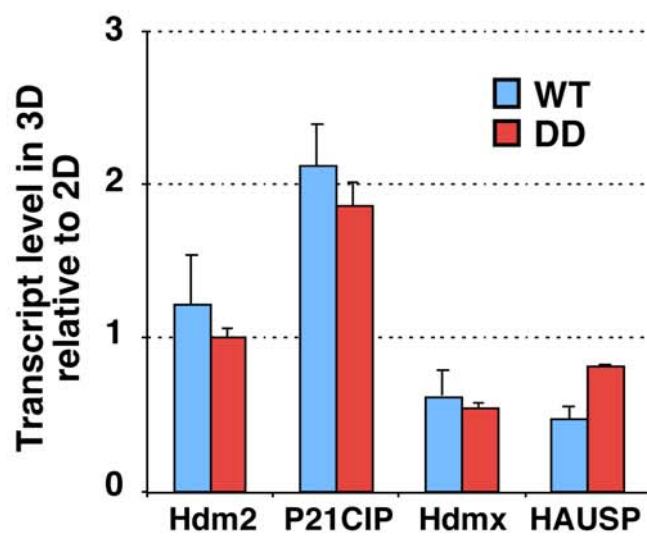
A

B

C
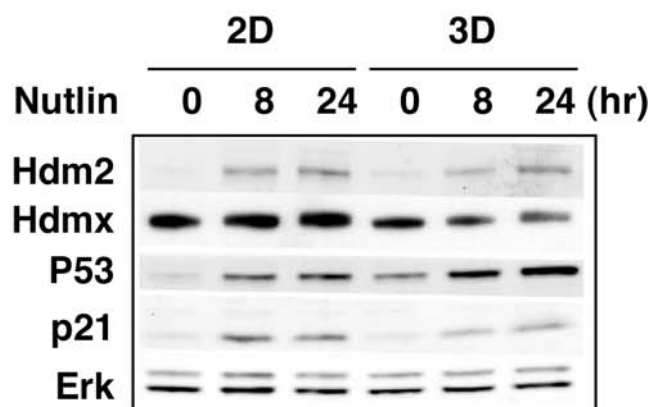
Figure 3.4: P53 activation of target genes after Nutlin and doxorubicin treatment

a. QPCR data demonstrating the time course of P53-responsive transcripts induction after Nutlin treatment. The data were mean ± SEM of the fold induction expressed relative to 2D untreated cells obtained from 3 independent experiments.
b. P53-responsive transcripts induction 24 hours after drug treatment. The data were mean ± SEM of the fold induction expressed relative to 2D untreated cells obtained from 3 independent experiments.

Figure 3.5: Hdmx is preferentially down regulated by doxorubicin and Nutlin treatment in 2D cells

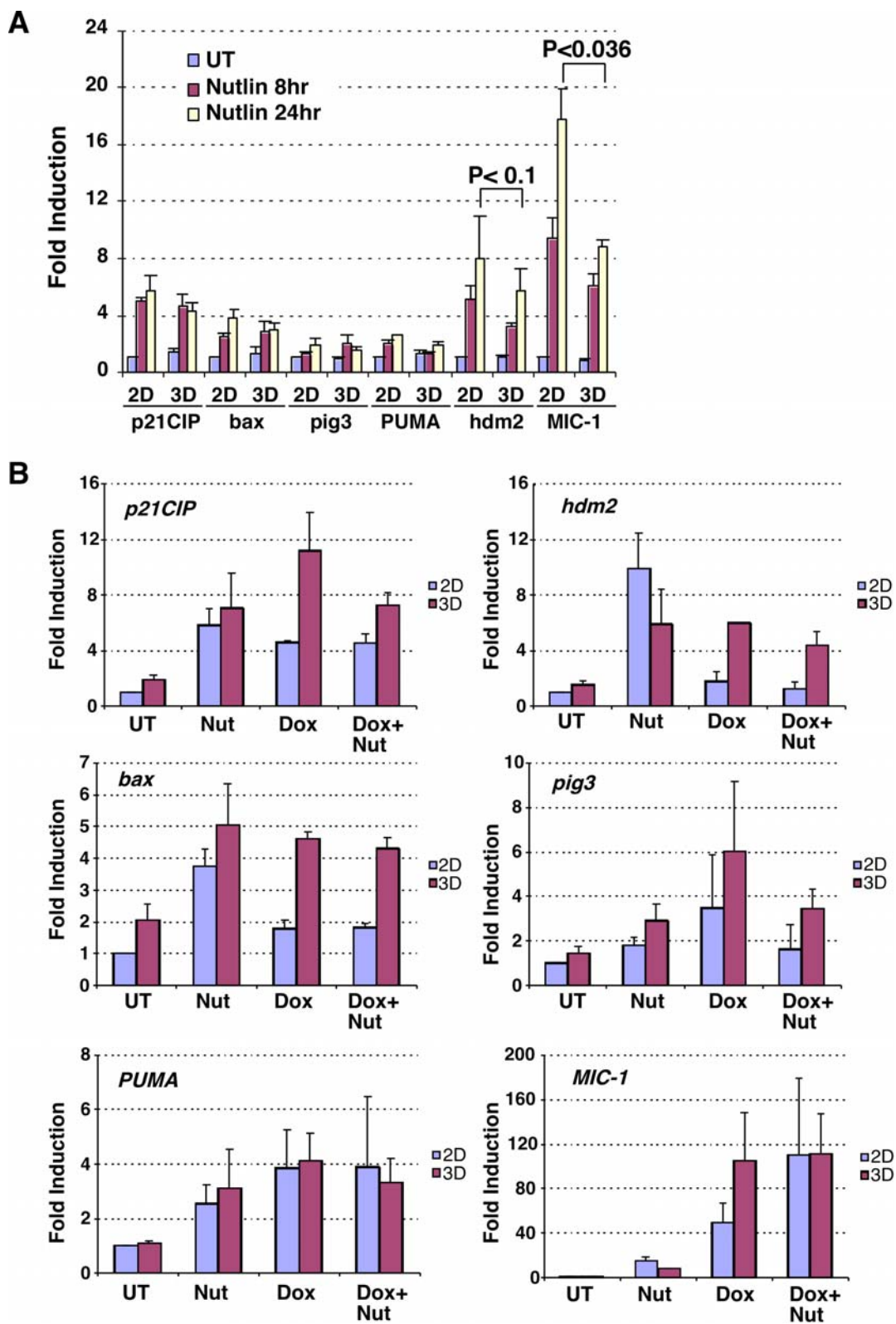a. P53 activation and decrease in Hdmx level in growth arrested 2D and 3D cells 24 hours post drug treatment as analyzed by western blot. Band intensities were quantified by LiCor and normalized to loading control (Erk) and expressed as fold induction relative to the untreated.
b. Western blot to demonstrate the efficiency of Hdmx knockdown by shRNA. Cells were infected with lentivirus expressing control shRNA (against MKP) or Hdmx specific shRNA and harvested for western analysis 5 days post infection.
c. IF staining of control and Hdmx shRNA expressing MCF10A cells in 3D culture. Cells were stained for basal marker α6-integrin and cell junction marker β-catenin. The ruler represents 50 μm in length.
d. Cell death in MKP and Hdmx shRNA expressing 2D and 3D MCF10A cells at 24 hours post drug treatment.

A

B

C

D
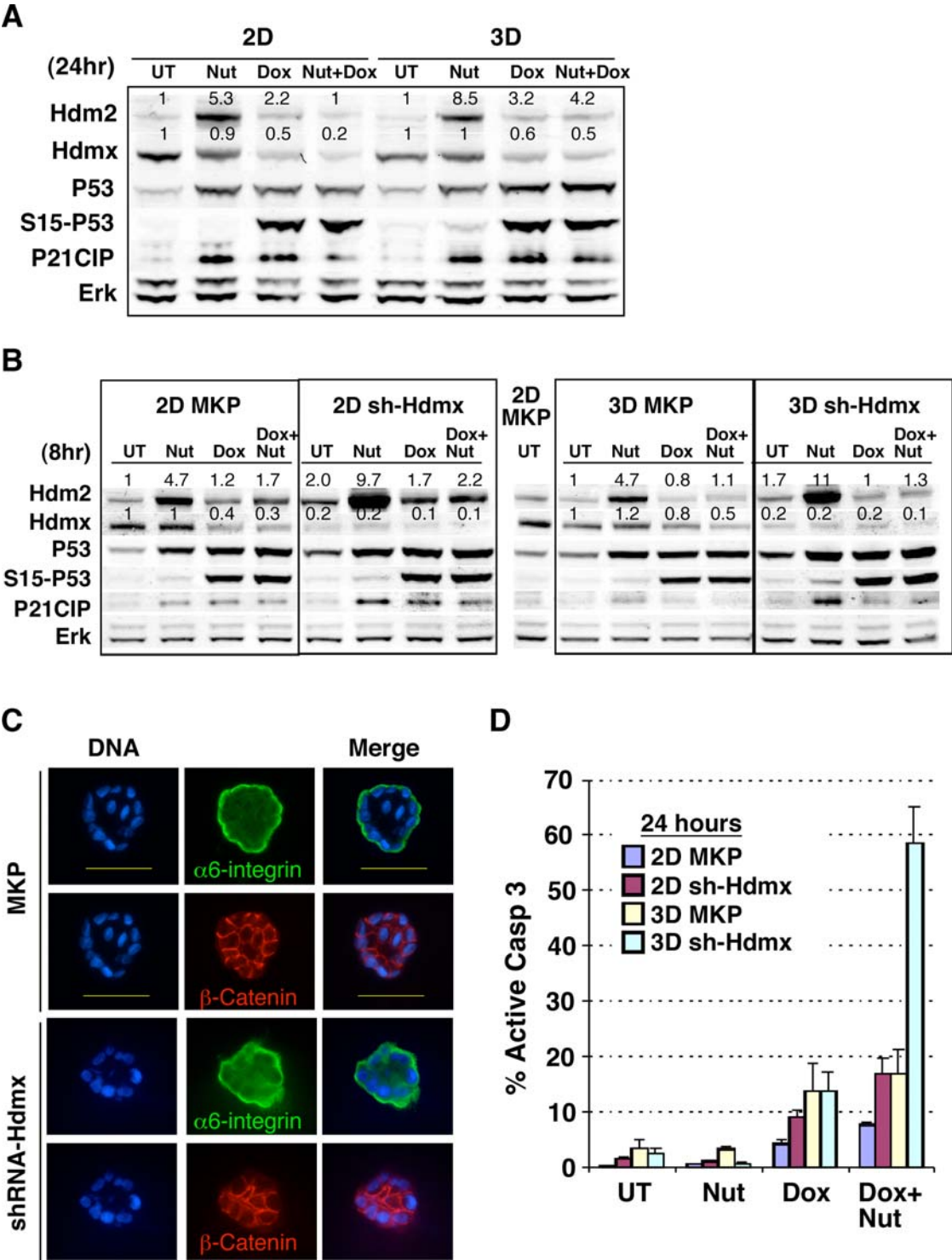
Supplemental procedure

MCF10A culture media

The media used were as follows: growth medium (20 ng/ml EGF, 100 ng/ml cholera, 10 µg/ml insulin, 0.5 µg/ml hydrocortisone, 5% horse serum); assay medium (100 ng/ml cholera, 10 µg/ml insulin, 0.5 µg/ml hydrocortisone, 5% horse serum); differentiation medium (5 ng/ml EGF, 100 ng/ml cholera, 10 µg/ml insulin, 0.5 µg/ml hydrocortisone, 2% horse serum, 2% matrigel).

Antibody dilutions for IF

Antibodies used were P53 (FL393, 1:1000, Santa Cruz), P21CIP (Clone 70, 1:400, Transduction Lab), β-catenin (1:1000, USBiological), Hdm2 (2A9, 5B10 at 1:500, Oncogene Science), active caspase 3 (1:500, Cell Signaling Technology), phosphoY397-FAK (1:1000, Biosource International) and α6-integrin (1:2000, Cymbus).

Primers and probe sequences used in QPCR

β-glucuronidase: sense: GAA CGC CCT GCC TAT CTG TAT T, antisense: CAG ACA CAG GCC CCA GTG A; BID: sense: GCT TGG GAA GAA TAG AGG CAG AT, antisense: GCG AGG TGC CTG GCA AT; GADD45a: sense: GAA GAC CGA AAG GAT GGA TAA GG, antisense: CAG GGC TTT GCT GAG CAC TT; Noxa: sense: GCA AGT AGC TGG AAG TCG AGT GT, antisense: TTC TGC CGG AAG TTC AGT TTG; PUMA: sense: TGC ACT GAC GGA GAT GCG, antisense:

TTC CGA TGC TGA GTC CAT CA, PUMA probe: FAM CGT CCC TCT CCT GGC

TTC TTG GC TAMRA and MIC-1 (Yang et al., 2003).

Supplemental figures
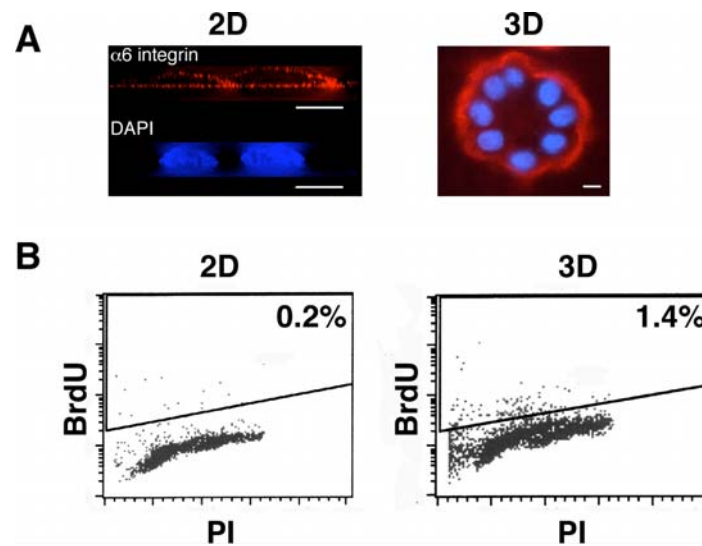
Figure S3.1: Cells in matrigel culture are polar and growth arrested.

a. Immunofluorescence images showing α6-integrin expression across the middle of an acinus structure in 3D cells and across the Y-Z-plane of 2D cells. Ruler represents 10 μm.
b. FACS profile and BrdU incorporation by cells in 2D and 3D. Cells were cultured in the absence of EGF for 2 days, pulsed with BrdU for 1 hour before harvesting for analysis. PI: propidium iodide stain for DNA content
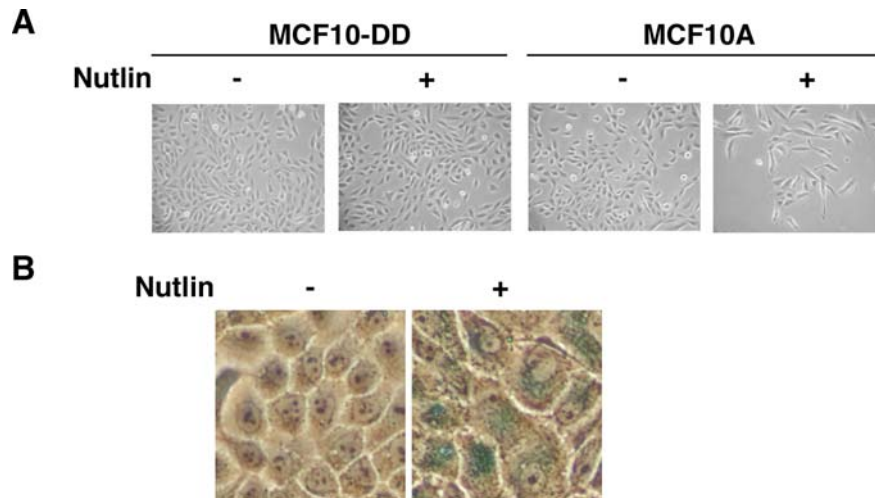
Figure S3.2: Nutlin induces cell cycle arrest or senescence in MCF10A.

a. Phase contrast pictures demonstrating the cell density of parental or DD-expressing MCF10A that were either left untreated (-) or treated with Nutlin (+) for 2 days.
b. Phase contrast pictures demonstrating acidic β-galactosidase staining in growth arrested MCF10A (-) and cells treated with Nutlin (+) for 16 days.

Figure S3.3: Cell survival signaling in 2D and 3D cells

a. Western blot showing signaling through Erk and Akt in asynchronously dividing (Asy) 2D culture and growth arrested 2D and 3D cells.

b. IκBα degradation after drug treatment. Growth arrested cells in 2D and 3D were harvested 24 hours after drug treatment and processed for western blot. Band intensities were quantified by LiCor and normalized to that of actin and expressed as fold changes relative to the untreated.

c. NFκB activation after drug treatment. MCF10A cells were stably infected with lentivirus expressing luciferase reporter gene linked either to NFκB responsive promoter (κB-Luc) or mutated NFκB promoter (mut-κB-Luc). Cells were plated as 2D or 3D, growth arrested before drug treatment and harvested for luciferase assay 24 hours after drug treatment. NFκB activation is expressed as κB-Luc activity normalized to mut-κB-Luc activity and total protein content before expressing it as fold induction relative to the untreated samples. Data are mean ± SEM obtained from 3 independent experiments.

A

P-Akt
(S473)

P-Erk
(T202/Y204)

Erk

	Asy	2D	3D

B

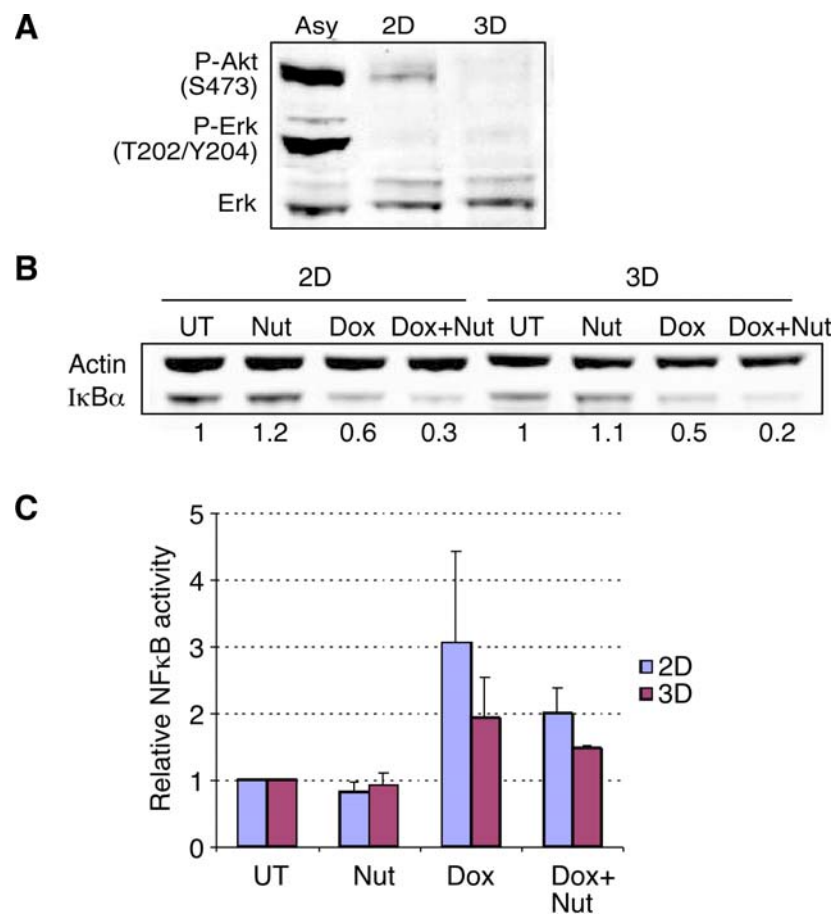|	2D				3D			
	UT	Nut	Dox	Dox+Nut	UT	Nut	Dox	Dox+Nut
Actin								
IκBα								
	1	1.2	0.6	0.3	1	1.1	0.5	0.2

C

Figure S3.4: P53 is activated similarly in 2D and 3D cells after Nutlin treatment

a. Plot tabulating the average ± SEM of the percentage of cells positively stained for P53, Hdm2 and P21CIP obtained from 3 independent experiments before and after Nutlin treatment for 24 hours. The staining intensity in the untreated samples was arbitrally set as the background value and all cells exhibiting a signal above the background were counted. A minimum of at least 100 cells were counted and expressed as a percentage of the total count.

b. IF demonstrating P53, P21CIP and Hdm2 accumulation before and 24 hours after Nutlin treatment in 2D (top panel) and 3D (bottom panel) cells. Staining for α6-integrin indicates the polarized nature of acini in 3D culture. Ruler represents 50 μm.

c. Induction of P53 target genes after 8 hours of Nutlin treatment in P53 wild type and DD-expressing MCF10A. Transcripts were normalized to 18S rRNA and expressed as fold induction relative to the untreated.

d. P53 target genes induction after treatment with increasing concentration of Nutlin for 8 hours. Transcripts were quantified by QPCR and normalized to the level of 18S rRNA housekeeping gene and expressed as fold induction relative to the untreated 2D cells.
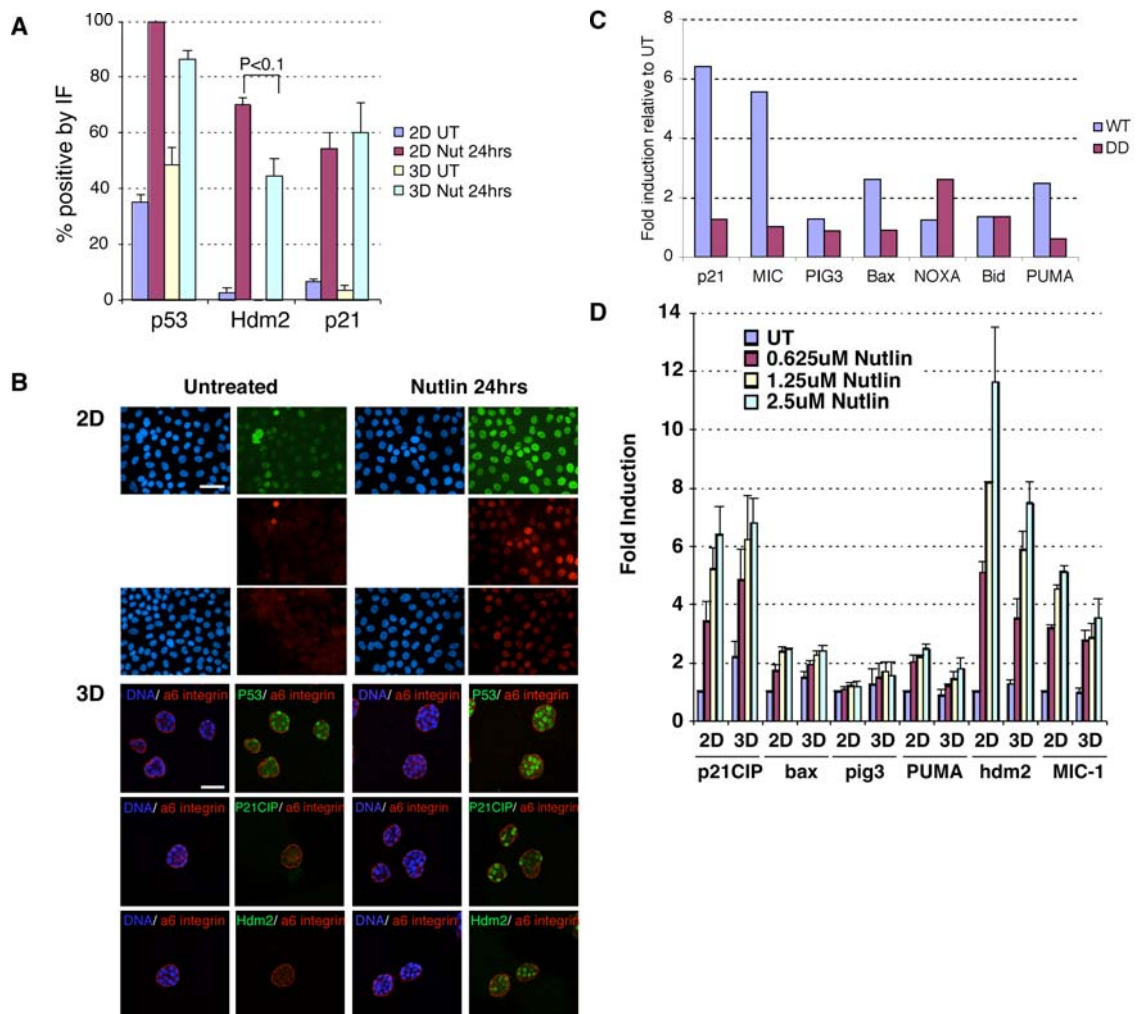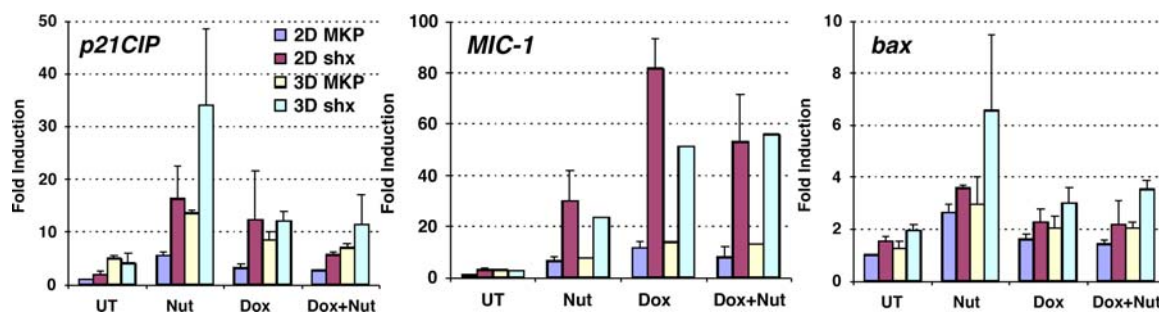
Figure S3.5: Influence of Hdmx knockdown on P53 target gene expression

Tabulation of P53 target genes induction in control shRNA and Hdmx specific shRNA expressing 2D and 3D cells at 8 hours post drug treatment. Transcripts were normalized to housekeeping gene and expressed as fold induction relative to 2D untreated cells.

Figure S3.6: Induction of apoptosis by TRAIL and Nutlin in 2D and 3D cells
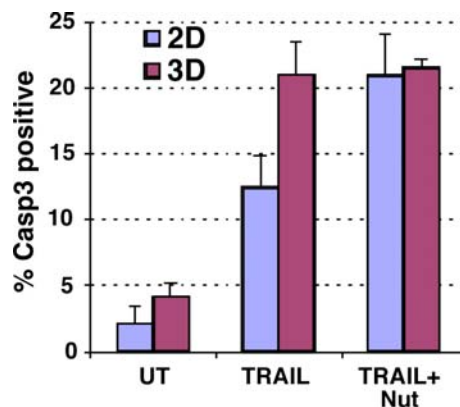
Graph shows the tabulation of caspase 3 positive cells induced by Nutlin alone, TRAIL alone or combination of TRAIL and Nutlin 48 hours after treatment in 2D and 3D cells.

References

Al-Kuraya, K., Schraml, P., Torhorst, J., Tapia, C., Zaharieva, B., Novotny, H., Spichtin, H., Maurer, R., Mirlacher, M., Kochli, O., *et al*. (2004). Prognostic relevance of gene amplifications and coamplifications in breast cancer. Cancer Res *64*, 8534-8540.

Ashcroft, M., Ludwig, R. L., Woods, D. B., Copeland, T. D., Weber, H. O., MacRae, E. J., and Vousden, K. H. (2002). Phosphorylation of HDM2 by Akt. Oncogene *21*, 1955-1962.

Bakkenist, C. J., and Kastan, M. B. (2003). DNA damage activates ATM through intermolecular autophosphorylation and dimer dissociation. Nature *421*, 499-506.

Bates, R. C., Buret, A., van Helden, D. F., Horton, M. A., and Burns, G. F. (1994). Apoptosis induced by inhibition of intercellular contact. J Cell Biol *125*, 403-415.

Bensaad, K., Tsuruta, A., Selak, M. A., Vidal, M. N., Nakano, K., Bartrons, R., Gottlieb, E., and Vousden, K. H. (2006). TIGAR, a p53-inducible regulator of glycolysis and apoptosis. Cell *126*, 107-120.

Bissell, M. J., Weaver, V. M., Lelievre, S. A., Wang, F., Petersen, O. W., and Schmeichel, K. L. (1999). Tissue structure, nuclear organization, and gene expression in normal and malignant breast. Cancer Res *59*, 1757-1763s; discussion 1763s-1764s.

Boudreau, N., and Bissell, M. J. (1998). Extracellular matrix signaling: integration of form and function in normal and malignant cells. Curr Opin Cell Biol *10*, 640-646.

Chen, L., Yin, H., Farooqi, B., Sebti, S., Hamilton, A. D., and Chen, J. (2005). p53 alpha-Helix mimetics antagonize p53/MDM2 interaction and activate p53. Mol Cancer Ther *4*, 1019-1025.

Crawford, Y. G., Gauthier, M. L., Joubel, A., Mantei, K., Kozakiewicz, K., Afshari, C. A., and Tlsty, T. D. (2004). Histologically normal human mammary epithelia with silenced p16(INK4a) overexpress COX-2, promoting a premalignant program. Cancer Cell *5*, 263-273.

Crighton, D., Wilkinson, S., O'Prey, J., Syed, N., Smith, P., Harrison, P. R., Gasco, M., Garrone, O., Crook, T., and Ryan, K. M. (2006). DRAM, a p53-induced modulator of autophagy, is critical for apoptosis. Cell *126*, 121-134.

Cummins, J. M., Rago, C., Kohli, M., Kinzler, K. W., Lengauer, C., and Vogelstein, B. (2004). Tumour suppression: disruption of HAUSP gene stabilizes p53. Nature *428*, 1 p following 486.

Danovi, D., Meulmeester, E., Pasini, D., Migliorini, D., Capra, M., Frenk, R., de Graaf, P., Francoz, S., Gasparini, P., Gobbi, A., *et al*. (2004). Amplification of Mdmx (or Mdm4) directly contributes to tumor formation by inhibiting p53 tumor suppressor activity. Mol Cell Biol *24*, 5835-5843.

Debnath, J., Mills, K. R., Collins, N. L., Reginato, M. J., Muthuswamy, S. K., and Brugge, J. S. (2002). The role of apoptosis in creating and maintaining luminal space within normal and oncogene-expressing mammary acini. Cell *111*, 29-40.

Debnath, J., Muthuswamy, S. K., and Brugge, J. S. (2003). Morphogenesis and oncogenesis of MCF-10A mammary epithelial acini grown in three-dimensional basement membrane cultures. Methods *30*, 256-268.

Desoize, B., and Jardillier, J. (2000). Multicellular resistance: a paradigm for clinical resistance? Crit Rev Oncol Hematol *36*, 193-207.

Dikomey, E., and Brammer, I. (2000). Relationship between cellular radiosensitivity and non-repaired double-strand breaks studied for different growth states, dose rates and plating conditions in a normal human fibroblast line. Int J Radiat Biol *76*, 773-781.

Dimri, G. P., Lee, X., Basile, G., Acosta, M., Scott, G., Roskelley, C., Medrano, E. E., Linskens, M., Rubelj, I., Pereira-Smith, O., and et al. (1995). A biomarker that identifies senescent human cells in culture and in aging skin in vivo. Proc Natl Acad Sci U S A *92*, 9363-9367.

Durand, R. E., and Sutherland, R. M. (1972). Effects of intercellular contact on repair of radiation damage. Exp Cell Res *71*, 75-80.

Espinosa, J. M., and Emerson, B. M. (2001). Transcriptional regulation by p53 through intrinsic DNA/chromatin binding and site-directed cofactor recruitment. Mol Cell *8*, 57-69.

Espinosa, J. M., Verdun, R. E., and Emerson, B. M. (2003). p53 functions through stress- and promoter-specific recruitment of transcription initiation components before and after DNA damage. Mol Cell *12*, 1015-1027.

Fei, P., Bernhard, E. J., and El-Deiry, W. S. (2002). Tissue-specific induction of p53 targets in vivo. Cancer Res *62*, 7316-7327.

Francoz, S., Froment, P., Bogaerts, S., De Clercq, S., Maetens, M., Doumont, G., Bellefroid, E., and Marine, J. C. (2006). Mdm4 and Mdm2 cooperate to inhibit p53 activity in proliferating and quiescent cells in vivo. Proc Natl Acad Sci U S A *103*, 3232-3237.

Frank, C., Weber, K. J., Fritz, P., and Flentje, M. (1993). Increased dose-rate effect in V79-multicellular aggregates (spheroids). Relation to initial DNA lesions and repair. Radiother Oncol *26*, 264-270.

Frisch, S. M., and Screaton, R. A. (2001). Anoikis mechanisms. Curr Opin Cell Biol *13*, 555-562.

Galatin, P. S., and Abraham, D. J. (2004). A nonpeptidic sulfonamide inhibits the p53-mdm2 interaction and activates p53-dependent transcription in mdm2-overexpressing cells. J Med Chem *47*, 4163-4165.

Gottlieb, T. M., Leal, J. F., Seger, R., Taya, Y., and Oren, M. (2002). Cross-talk between Akt, p53 and Mdm2: possible implications for the regulation of apoptosis. Oncogene *21*, 1299-1303.

Gudjonsson, T., Ronnov-Jessen, L., Villadsen, R., Bissell, M. J., and Petersen, O. W. (2003). To create the correct microenvironment: three-dimensional heterotypic collagen assays for human breast epithelial morphogenesis and neoplasia. Methods *30*, 247-255.

Hanahan, D., and Weinberg, R. A. (2000). The hallmarks of cancer. Cell *100*, 57-70.
Ho, G. H., Calvano, J. E., Bisogna, M., Abouezzi, Z., Borgen, P. I., Cordon-Cardo, C., and van Zee, K. J. (2001). Genetic alterations of the p14ARF -hdm2-p53 regulatory pathway in breast carcinoma. Breast Cancer Res Treat *65*, 225-232.

Hollstein, M., Sidransky, D., Vogelstein, B., and Harris, C. C. (1991). p53 mutations in human cancers. Science *253*, 49-53.

Hosokawa, K., Aharoni, D., Dantes, A., Shaulian, E., Schere-Levy, C., Atzmon, R., Kotsuji, F., Oren, M., Vlodavsky, I., and Amsterdam, A. (1998). Modulation of Mdm2 expression and p53-induced apoptosis in immortalized human ovarian granulosa cells. Endocrinology *139*, 4688-4700.

Ilic, D., Almeida, E. A., Schlaepfer, D. D., Dazin, P., Aizawa, S., and Damsky, C. H. (1998). Extracellular matrix survival signals transduced by focal adhesion kinase suppress p53-mediated apoptosis. J Cell Biol *143*, 547-560.

Ingber, D. E. (2003). Tensegrity II. How structural networks influence cellular information processing networks. J Cell Sci *116*, 1397-1408.

Ingber, D. E. (2006). Cellular mechanotransduction: putting all the pieces together again. Faseb J *20*, 811-827.

Issaeva, N., Bozko, P., Enge, M., Protopopova, M., Verhoef, L. G., Masucci, M., Pramanik, A., and Selivanova, G. (2004). Small molecule RITA binds to p53, blocks p53-HDM-2 interaction and activates p53 function in tumors. Nat Med *10*, 1321-1328. Jeffers, J. R., Parganas, E., Lee, Y., Yang, C., Wang, J., Brennan, J., MacLean, K. H., Han, J., Chittenden, T., Ihle, J. N., *et al.* (2003). Puma is an essential mediator of p53-dependent and -independent apoptotic pathways. Cancer Cell *4*, 321-328.

Jones, R. G., Plas, D. R., Kubek, S., Buzzai, M., Mu, J., Xu, Y., Birnbaum, M. J., and Thompson, C. B. (2005). AMP-activated protein kinase induces a p53-dependent metabolic checkpoint. Mol Cell *18*, 283-293.

Jones, S. N., Roe, A. E., Donehower, L. A., and Bradley, A. (1995). Rescue of embryonic lethality in Mdm2-deficient mice by absence of p53. Nature *378*, 206-208.

Kaeser, M. D., and Iggo, R. D. (2002). Chromatin immunoprecipitation analysis fails to support the latency model for regulation of p53 DNA binding activity in vivo. Proc Natl Acad Sci U S A *99*, 95-100.

Kamijo, T., Zindy, F., Roussel, M. F., Quelle, D. E., Downing, J. R., Ashmun, R. A., Grosveld, G., and Sherr, C. J. (1997). Tumor suppression at the mouse INK4a locus mediated by the alternative reading frame product p19ARF. Cell *91*, 649-659.

Kawai, H., Wiederschain, D., Kitao, H., Stuart, J., Tsai, K. K., and Yuan, Z. M. (2003). DNA damage-induced MDMX degradation is mediated by MDM2. J Biol Chem *278*, 45946-45953.

Kubbutat, M. H., Jones, S. N., and Vousden, K. H. (1997). Regulation of p53 stability by Mdm2. Nature *387*, 299-303.

Kumar, C. C. (1998). Signaling by integrin receptors. Oncogene *17*, 1365-1373.

Kwok, T. T., and Sutherland, R. M. (1991). The influence of cell-cell contact on radiosensitivity of human squamous carcinoma cells. Radiat Res *126*, 52-57.

Lee, J. H., and Paull, T. T. (2005). ATM activation by DNA double-strand breaks through the Mre11-Rad50-Nbs1 complex. Science *308*, 551-554.

Lelievre, S. A., Weaver, V. M., Nickerson, J. A., Larabell, C. A., Bhaumik, A., Petersen, O. W., and Bissell, M. J. (1998). Tissue phenotype depends on reciprocal interactions between the extracellular matrix and the structural organization of the nucleus. Proc Natl Acad Sci U S A *95*, 14711-14716.

Levine, A. J., Momand, J., and Finlay, C. A. (1991). The p53 tumour suppressor gene. Nature *351*, 453-456.

Lewis, J. M., Truong, T. N., and Schwartz, M. A. (2002). Integrins regulate the apoptotic response to DNA damage through modulation of p53. Proc Natl Acad Sci U S A *99*, 3627-3632.

Li, C., Chen, L., and Chen, J. (2002a). DNA damage induces MDMX nuclear translocation by p53-dependent and -independent mechanisms. Mol Cell Biol *22*, 7562-7571.

Li, M., Brooks, C. L., Kon, N., and Gu, W. (2004). A dynamic role of HAUSP in the p53-Mdm2 pathway. Mol Cell *13*, 879-886.

Li, M., Chen, D., Shiloh, A., Luo, J., Nikolaev, A. Y., Qin, J., and Gu, W. (2002b). Deubiquitination of p53 by HAUSP is an important pathway for p53 stabilization. Nature *416*, 648-653.

Maniotis, A. J., Chen, C. S., and Ingber, D. E. (1997). Demonstration of mechanical connections between integrins, cytoskeletal filaments, and nucleoplasm that stabilize nuclear structure. Proc Natl Acad Sci U S A *94*, 849-854.

Marchetti, A., Buttitta, F., Girlando, S., Dalla Palma, P., Pellegrini, S., Fina, P., Doglioni, C., Bevilacqua, G., and Barbareschi, M. (1995). mdm2 gene alterations and mdm2 protein expression in breast carcinomas. J Pathol *175*, 31-38.

Matoba, S., Kang, J. G., Patino, W. D., Wragg, A., Boehm, M., Gavrilova, O., Hurley, P. J., Bunz, F., and Hwang, P. M. (2006). p53 regulates mitochondrial respiration. Science *312*, 1650-1653.

Meredith, J. E., Jr., Fazeli, B., and Schwartz, M. A. (1993). The extracellular matrix as a cell survival factor. Mol Biol Cell *4*, 953-961.

Meulmeester, E., Maurice, M. M., Boutell, C., Teunisse, A. F., Ovaa, H., Abraham, T. E., Dirks, R. W., and Jochemsen, A. G. (2005). Loss of HAUSP-mediated deubiquitination contributes to DNA damage-induced destabilization of Hdmx and Hdm2. Mol Cell *18*, 565-576.

Momand, J., Jung, D., Wilczynski, S., and Niland, J. (1998). The MDM2 gene amplification database. Nucleic Acids Res *26*, 3453-3459.

Montes de Oca Luna, R., Wagner, D. S., and Lozano, G. (1995). Rescue of early embryonic lethality in mdm2-deficient mice by deletion of p53. Nature *378*, 203-206.

Muthuswamy, S. K., Li, D., Lelievre, S., Bissell, M. J., and Brugge, J. S. (2001). ErbB2, but not ErbB1, reinitiates proliferation and induces luminal repopulation in epithelial acini. Nat Cell Biol *3*, 785-792.

Myers, C. A., Schmidhauser, C., Mellentin-Michelotti, J., Fragoso, G., Roskelley, C. D., Casperson, G., Mossi, R., Pujuguet, P., Hager, G., and Bissell, M. J. (1998). Characterization of BCE-1, a transcriptional enhancer regulated by prolactin and extracellular matrix and modulated by the state of histone acetylation. Mol Cell Biol *18*, 2184-2195.

Nigro, J. M., Aldape, K. D., Hess, S. M., and Tlsty, T. D. (1997). Cellular adhesion regulates p53 protein levels in primary human keratinocytes. Cancer Res *57*, 3635-3639.

Pan, Y., and Chen, J. (2003). MDM2 promotes ubiquitination and degradation of MDMX. Mol Cell Biol *23*, 5113-5121.

Paszek, M. J., Zahir, N., Johnson, K. R., Lakins, J. N., Rozenberg, G. I., Gefen, A., Reinhart-King, C. A., Margulies, S. S., Dembo, M., Boettiger, D., *et al.* (2005). Tensional homeostasis and the malignant phenotype. Cancer Cell *8*, 241-254.

Patton, J. T., Mayo, L. D., Singhi, A. D., Gudkov, A. V., Stark, G. R., and Jackson, M. W. (2006). Levels of HdmX expression dictate the sensitivity of normal and transformed cells to Nutlin-3. Cancer Res *66*, 3169-3176.

Pawlik, T. M., and Keyomarsi, K. (2004). Role of cell cycle in mediating sensitivity to radiotherapy. Int J Radiat Oncol Biol Phys *59*, 928-942.

Pereg, Y., Shkedy, D., de Graaf, P., Meulmeester, E., Edelson-Averbukh, M., Salek, M., Biton, S., Teunisse, A. F., Lehmann, W. D., Jochemsen, A. G., and Shiloh, Y. (2005). Phosphorylation of Hdmx mediates its Hdm2- and ATM-dependent degradation in response to DNA damage. Proc Natl Acad Sci U S A *102*, 5056-5061.

Pharoah, P. D., Day, N. E., and Caldas, C. (1999). Somatic mutations in the p53 gene and prognosis in breast cancer: a meta-analysis. Br J Cancer *80*, 1968-1973.

Plachot, C., and Lelievre, S. A. (2004). DNA methylation control of tissue polarity and cellular differentiation in the mammary epithelium. Exp Cell Res *298*, 122-132.

Reginato, M. J., Mills, K. R., Paulus, J. K., Lynch, D. K., Sgroi, D. C., Debnath, J., Muthuswamy, S. K., and Brugge, J. S. (2003). Integrins and EGFR coordinately regulate the pro-apoptotic protein Bim to prevent anoikis. Nat Cell Biol *5*, 733-740.

Riemenschneider, M. J., Buschges, R., Wolter, M., Reifenberger, J., Bostrom, J., Kraus, J. A., Schlegel, U., and Reifenberger, G. (1999). Amplification and overexpression of the MDM4 (MDMX) gene from 1q32 in a subset of malignant gliomas without TP53 mutation or MDM2 amplification. Cancer Res *59*, 6091-6096.

Ries, S., Biederer, C., Woods, D., Shifman, O., Shirasawa, S., Sasazuki, T., McMahon, M., Oren, M., and McCormick, F. (2000a). Opposing effects of Ras on p53: transcriptional activation of mdm2 and induction of p19ARF. Cell *103*, 321-330.

Ries, S., Biederer, C., Woods, D., Shifman, O., Shirasawa, S., Sasazuki, T., McMahon, M., Oren, M., and McCormick, F. (2000b). Opposing effects of Ras on p53: transcriptional activation of mdm2 and induction of p19ARF. Cell *103*, 321-330.

Rodriguez, A., Alpen, E. L., Mendonca, M., and DeGuzman, R. J. (1988). Recovery from potentially lethal damage and recruitment time of noncycling clonogenic cells in 9L confluent monolayers and spheroids. Radiat Res *114*, 515-527.

Roskelley, C. D., Desprez, P. Y., and Bissell, M. J. (1994). Extracellular matrix-dependent tissue-specific gene expression in mammary epithelial cells requires both physical and biochemical signal transduction. Proc Natl Acad Sci U S A *91*, 12378-12382.

Sak, A., Stuschke, M., Wurm, R., and Budach, V. (2000). Protection of DNA from radiation-induced double-strand breaks: influence of replication and nuclear proteins. Int J Radiat Biol *76*, 749-756.

Secchiero, P., Barbarotto, E., Tiribelli, M., Zerbinati, C., di Iasio, M. G., Gonelli, A., Cavazzini, F., Campioni, D., Fanin, R., Cuneo, A., and Zauli, G. (2006). Functional integrity of the p53-mediated apoptotic pathway induced by the nongenotoxic agent nutlin-3 in B-cell chronic lymphocytic leukemia (B-CLL). Blood *107*, 4122-4129.

Seewaldt, V. L., Mrozek, K., Sigle, R., Dietze, E. C., Heine, K., Hockenbery, D. M., Hobbs, K. B., and Caldwell, L. E. (2001). Suppression of p53 function in normal human mammary epithelial cells increases sensitivity to extracellular matrix-induced apoptosis. J Cell Biol *155*, 471-486.

Shaulian, E., Zauberman, A., Ginsberg, D., and Oren, M. (1992). Identification of a minimal transforming domain of p53: negative dominance through abrogation of sequence-specific DNA binding. Mol Cell Biol *12*, 5581-5592.

Shimada, M., Imura, J., Kozaki, T., Fujimori, T., Asakawa, S., Shimizu, N., and Kawaguchi, R. (2005). Detection of Her2/neu, c-MYC and ZNF217 gene amplification during breast cancer progression using fluorescence in situ hybridization. Oncol Rep *13*, 633-641.

Silva, J., Dominguez, G., Silva, J. M., Garcia, J. M., Gallego, I., Corbacho, C., Provencio, M., Espana, P., and Bonilla, F. (2001). Analysis of genetic and epigenetic processes that influence p14ARF expression in breast cancer. Oncogene *20*, 4586-4590.

Stommel, J. M., and Wahl, G. M. (2004). Accelerated MDM2 auto-degradation induced by DNA-damage kinases is required for p53 activation. Embo J *23*, 1547-1556.

Stommel, J. M., and Wahl, G. M. (2005). A new twist in the feedback loop: stress-activated MDM2 destabilization is required for p53 activation. Cell Cycle *4*, 411-417. Stromblad, S., Fotedar, A., Brickner, H., Theesfeld, C., Aguilar de Diaz, E., Friedlander, M., and Cheresh, D. A. (2002). Loss of p53 compensates for alpha v-integrin function in retinal neovascularization. J Biol Chem *277*, 13371-13374.

Szak, S. T., Mays, D., and Pietenpol, J. A. (2001). Kinetics of p53 binding to promoter sites in vivo. Mol Cell Biol *21*, 3375-3386.

Tergaonkar, V., Bottero, V., Ikawa, M., Li, Q., and Verma, I. M. (2003). IkappaB kinase-independent IkappaBalpha degradation pathway: functional NF-kappaB activity and implications for cancer therapy. Mol Cell Biol *23*, 8070-8083.

Tergaonkar, V., Pando, M., Vafa, O., Wahl, G., and Verma, I. (2002). p53 stabilization is decreased upon NFkappaB activation: a role for NFkappaB in acquisition of resistance to chemotherapy. Cancer Cell *1*, 493-503.

Toledo, F., Krummel, K. A., Lee, C. J., Liu, C. W., Rodewald, L. W., Tang, M., and Wahl, G. M. (2006). A mouse p53 mutant lacking the proline-rich domain rescues Mdm4 deficiency and provides insight into the Mdm2-Mdm4-p53 regulatory network. Cancer Cell *9*, 273-285.

Truong, T., Sun, G., Doorly, M., Wang, J. Y., and Schwartz, M. A. (2003). Modulation of DNA damage-induced apoptosis by cell adhesion is independently mediated by p53 and c-Abl. Proc Natl Acad Sci U S A.

Vassilev, L. T., Vu, B. T., Graves, B., Carvajal, D., Podlaski, F., Filipovic, Z., Kong, N., Kammlott, U., Lukacs, C., Klein, C., *et al*. (2004). In vivo activation of the p53 pathway by small-molecule antagonists of MDM2. Science *303*, 844-848.

Vogelstein, B., and Kinzler, K. W. (2004). Cancer genes and the pathways they control. Nat Med *10*, 789-799.

Vogelstein, B., Lane, D., and Levine, A. J. (2000). Surfing the p53 network. Nature *408*, 307-310.

Wahl, G. M. (2006). Mouse bites dogma: how mouse models are changing our views of how P53 is regulated in vivo. Cell Death Differ *13*, 973-983.

Weaver, V. M., Lelievre, S., Lakins, J. N., Chrenek, M. A., Jones, J. C., Giancotti, F., Werb, Z., and Bissell, M. J. (2002). beta4 integrin-dependent formation of polarized

three-dimensional architecture confers resistance to apoptosis in normal and malignant mammary epithelium. Cancer Cell *2*, 205-216.

Wong, E. T., Ngoi, S. M., and Lee, C. G. (2002). Improved co-expression of multiple genes in vectors containing internal ribosome entry sites (IRESes) from human genes. Gene Ther *9*, 337-344.

Xiong, S., Van Pelt, C. S., Elizondo-Fraire, A. C., Liu, G., and Lozano, G. (2006). Synergistic roles of Mdm2 and Mdm4 for p53 inhibition in central nervous system development. Proc Natl Acad Sci U S A *103*, 3226-3231.

Yang, H., Filipovic, Z., Brown, D., Breit, S. N., and Vassilev, L. T. (2003). Macrophage inhibitory cytokine-1: a novel biomarker for p53 pathway activation. Mol Cancer Ther *2*, 1023-1029.

Zahir, N., and Weaver, V. M. (2004). Death in the third dimension: apoptosis regulation and tissue architecture. Curr Opin Genet Dev *14*, 71-80.

IV

Influence of stromal fibroblasts on epithelial cell morphogenesis and P53 activation

Abstract

Crosstalk between multiple cell types occurs frequently during carcinogenesis. For example, while luminal epithelial cells are the target of transformation and constitute the main component in breast cancer, neighboring cells such as fibroblasts, endothelial cells and immune cells facilitate epithelial cell proliferation, survival and metastasis. Data presented in this chapter demonstrate that mammary fibroblasts isolated from breast cancer patients and their conditioned culture media disrupt acini formation by MCF10A cells in matrigel culture but P53 activation by DNA damage is unaffected. Hence, paracrine signaling from fibroblasts can disrupt the normal tissue architecture of epithelial cells in culture. Targeting stromal fibroblasts with the aim of normalizing the aberrant paracrine signaling holds great potential to enhance the efficacy of existing anti-cancer therapies.

Introduction

Histological view of breast Cancer

Breast cancer is the most common cancer type among women and is also the leading cause of cancer related deaths worldwide (refer to American Cancer Society website). Improved diagnostic tools and treatments have significantly reduced the mortality rates in recent years. However, due to heterogeneity of the disease, each sub-type of breast cancer differs in their recurrence rates, their tendencies for metastasis and their response to therapy. Hence, approximately a quarter of the breast cancer patients still die of the disease. Therefore, new and effective molecular based therapies are needed to improve the prognosis.

Breast cancer progresses through histologically distinct stages starting with atypical hyperproliferation, followed by ductal carcinoma *in situ* (DCIS), then an invasive phase and finally metastatic disease (Beckmann et al., 1997). Cancer is a multi-step process characterized by the progressive accumulation of genetic and epigenetic changes in the tumor compartment. Advances in diagnostic tools have made it possible to detect breast cancers at the hyperplastic preinvasive DCIS stage. An understanding of the underlying deregulated processes during the hyperplastic phase may provide new drug targets that promote tumor regression prior to onset of fatal metastases.

DCIS can be subdivided into 3 categories based on its nuclear grade. The nuclear grade of hyperplastic cells is correlated to the clinical outcome and tumor recurrence rate (Badve et al., 1998). High-grade DCIS (cells are variable in size and have high mitotic counts) has the highest rate of local recurrence (25-30%), intermediate-grade tumors have a recurrence rate of 10-15% while low-grade DCIS (small and uniform sized cells with low mitotic counts) has a recurrence rate of 0-5%. Low-grade DCIS is more frequently well differentiated, estrogen receptor (ER) and progesterone receptor (PR) positive, has no *her*2 (Epidermal growth factor receptor 2) amplification and has wild-type *p53*. On the other hand, high-grade DCIS is frequently poorly differentiated, exhibits collagen and fibroblast rich stroma, is ER and PR negative, and often has *her*2 amplification and *p53* gene mutation.

An emerging perspective of tumorigenesis

Other than progressive changes in the epithelial compartment, the microenvironment also undergoes progressive and dynamic changes. There is degradation of basement membrane and deposition of new types of ECM not typically seen in normal tissues. Immune cells are recruited and new blood vessels are formed. Surrounding fibroblasts are activated and a myriad of growth factors, and cytokines and proteolytic enzymes participate in paracrine and autocrine signaling between the tumor and its microenvironment. As a reciprocal and dynamic communication exists between the tumor and its environment, cancer is now being viewed as a "disease of the organ" (Mueller and Fusenig, 2004; Radisky et al., 2001; Wiseman and Werb, 2002).

Many findings are consistent with the emerging theme that "normal stroma" restrains tumor progression by acting as a natural barrier while "activated" stroma is associated with higher risk for cancer development and can stimulate and support the progression of initiated and tumor cells (Bissell and Radisky, 2001; Elenbaas and Weinberg, 2001; Mueller and Fusenig, 2004). For example, high mammographic breast density in humans is associated with increased breast cancer risk (Boyd et al., 2005). Women with high density in more than 75% of the breast are at four to five times greater risk of getting breast cancer than women with little or no density in their breast. While fat appears radiolucent or dark on a mammogram, epithelial cells, fibroblasts and ECM (such as collagen deposits) constitute the mammographic dense areas. Furthermore, extensive gene expression and epigenetic changes are observed in both the epithelial and stromal compartments of normal mammary tissue and in *in situ* and invasive breast carcinomas (Allinen et al., 2004; Hu et al., 2005). Patients whose

tumors exhibit a gene expression profile consistent with activated stroma or a wound-response signature have shorter overall and disease-free survival (Chang et al., 2005; Chang et al., 2004). In addition, pregnancy is thought to provide long-term protection against breast cancers in young women. However, recent studies indicate an association between pregnancy, increased breast cancer risk and poor prognosis. The post-lactational involuting mammary gland exhibits higher matrix metalloproteinase activity, increased fibrillar collagen and bioactive fibronectin and increased laminin fragment deposition. Compared to nulliporous glands, ECM isolated from involuting glands fails to support normal ductal development but supports the invasion and metastasis of tumor cells (McDaniel et al., 2006). Lastly, changes in the microenvironment associated with wound healing and inflammation (eg, Helicobacter pylori infection or Crohn's disease) are correlated with increased risk of developing stomach and colon cancer (Mueller and Fusenig, 2004). Activated cells in the proinflammatory environment secrete cytokines, growth factors, matrix metalloproteinases (MMP) and ECM molecules that facilitate the growth and invasion of the tumor cells.

In vitro coculture and *in vivo* mouse models have helped us identify key signaling molecules involved in the epithelial-fibroblast crosstalk. Senescent fibroblasts secrete MMPs and disrupt the normal morphogenesis of epithelial cells in coculture and induces matrix invasion of breast cancer cells (Parrinello et al., 2005; Tsai et al., 2005). Stromal cell-derived factor-1 (SDF-1), a chemokine overexpressed in cancer associated fibroblasts (CAF) promote tumor cell growth and metastasis (Orimo et al., 2005). In mouse models, mammary stroma activated by irradiation

(Barcellos-Hoff and Ravani, 2000) or chemical carcinogen (Maffini et al., 2004) promotes tumor formation by implanted nontumorigenic mammary epithelial cells in part through activated transforming growth factor-β (TGF-β). Consistent with the role of paracrine signalings in the promoting of tumor formation, human mammary fibroblasts overexpressing TGF-β or hepatocyte growth factor (HGF) promote tumor formation when co-implanted with human mammary epithelial cells into nude mice (Kuperwasser et al., 2004). Interestingly, conditional inactivation of TGFβ-Type II receptor in murine fibroblasts leads to the expansion of the fibroblast population and development of intraepithelial neoplasia of the prostate and invasive carcinoma of the forestomach (Bhowmick et al., 2004). Excessive paracrine signaling in part through HGF is implicated in the promotion of epithelial cell proliferation. Other than the role of an altered microenvironment in the promotion of cancer development, a transgenic mouse model overexpressing MMP3 in the mammary gland suggests the role of aberrant ECM remodeling and signaling in tumor initiation and induction of genetic instability (Radisky and Bissell, 2006; Sternlicht et al., 1999). Furthermore, increased deposition of collagen I by the fibroblasts and an increase in interstitial fluid pressure as a result of contractive forces from the fibroblasts contribute to the impediment of drug uptake and hence reduce the efficacies of chemotherapeutic agents (Gabbiani, 2003; Heldin et al., 2004).

Loss of P53 function fuels genetic instability and resistance to chemotherapy. Consistent with this, mutation of p53 or overexpression of its negative regulators Hdm2 and Hdmx are frequently found in human cancers. The level of Hdm2 is affected by mitogenic signaling (Feng et al., 2004; Mayo et al., 2002; Ries et al., 2000)

and the results in Chapter 2 show that cell architecture can influence Hdmx degradation. Therefore, we investigated whether paracrine signaling from stromal fibroblasts could also influence mammary epithelial cell acini formation and if changes in the morphology of acini formed impact on P53 activation upon DNA damage. We co-cultured MCF10A cells on matrigel with normal fibroblasts from healthy individuals (NF), senescent fibroblasts (SF), cancer-associated fibroblasts (CAF) or their normal counterparts (NCF, from cancer patients) or with the corresponding conditioned culture media. We found that CAF or their conditioned media disrupted acini formation most efficiently. Senescent and normal fibroblasts affected acini formation only after a longer period of co-culture. We also evaluated the impact of conditioned media isolated from these stromal cells on P53-dependent cell cycle arrest in response to ionizing radiation (IR). These studies revealed that epithelial cells cultured alone or with conditioned media from stromal fibroblasts arrested with equal efficiencies, indicating that paracrine signaling from neighboring fibroblasts does not influence P53 activation by IR. Clearly, stromal fibroblasts can influence some cellular processes to promote progression of epithelial cells and may be an important target for inhibition to achieve maximal regression of the tumor.

Results

Normal mammary fibroblasts (NF) were isolated from individuals undergoing reduction mammoplasty. We also obtained fibroblasts isolated from human breast tumor samples (cancer associated fibroblast or CAF) and fibroblasts isolated from the same patient but from an area away from the cancerous area (normal counterpart

fibroblasts or NCF). CAFs were distinguished from NF by smooth muscle actin expression (SMA) and epithelial cells were identified based on their cytokeratin expression (Fig 4.1A). NF were induced to undergo senescence *in vitro* by subjecting them to high dose IR. The senescent fibroblasts (SF) displayed the classical feature of acidic β-galactosidase staining (Dimri et al., 1995) while serum-deprived fibroblasts (quiescent fibroblasts) do not (Fig 4.1B).

MCF10A cells form spherical balls when cultured on matrigel. However, co-culture with NCF or CAF disrupts spheroid formation. There were no spherical balls formed in the CAF co-culture; instead, flat sheets or "rods" of cells were observed (Fig 4.2A). The ability of NCF to disrupt epithelial morphogenesis is surprising since NCF were removed from an area away from the tumor, an area not suppose to contain activated fibroblasts. To determine if the effect observed is mediated by soluble factors secreted by the fibroblasts, MCF10A cells were cultured with conditioned media from these fibroblasts. The disruption of epithelial structures was observed but was not as effective as the co-culture, since some spheroids were formed (Fig 4.2A). Hence, soluble factors secreted by fibroblasts are partially responsible for the disruption of normal morphogenesis of epithelial cells. Senescent fibroblasts were weaker in their ability to inhibit epithelial spheroid formation as clear disruption of structures was only observed on day 8 of the co-culture (Fig 4.2B). Together, these results indicate that epithelial morphogenesis can be modulated by certain types of stromal fibroblasts in a time-dependent manner.

In order to disrupt spheroid formation, fibroblasts may secrete factors that stimulate excessive proliferation of the epithelial cells. However, the percentage of

proliferating cells was not significantly higher in the fibroblast co-cultures or conditioned media culture compared to MCF10A grown alone (Fig 4.3). Dividing epithelial cultures growing in fresh media or fibroblast-conditioned media were subjected to IR to evaluate the influence of stromal fibroblasts on the efficiency of DNA damage-induced cell cycle arrest, which is a P53-dependent process. The percentage of BrdU incorporation by the epithelial cells was reduced upon IR treatment (Fig 4.3). The efficiency of cell cycle arrest also appears similar in MCF10A cultured in fibroblast-conditioned media (Fig 4.3). Hence, DNA damage signaling to P53, and P53-dependent cell cycle arrest in epithelial cells, are unaffected by soluble factors secreted from the various stromal fibroblasts tested.

Discussion

The microenvironment of a tumor plays an active role in the development of the cancer (Bissell and Radisky, 2001; Elenbaas and Weinberg, 2001; Mueller and Fusenig, 2004). Stromal fibroblasts constitute the predominant cell type in the tumor microenvironment and can participate in the generation of "reactive" stroma via excessive secretion of collagen and other ECM, soluble factors and matrix metalloproteinases. CAF can promote the growth of an immortalized, non-tumorigenic epithelial cell line when co-injected into nude mice (Olumi et al., 1999). Consistent with this, *in vitro* co-culture of CAF with MCF10A lead to the disruption of normal acini formation. Surprisingly, NCF also produced the same effect when co-cultured with MCF10A. Fibroblasts-conditioned media produced a weaker effect on epithelial

cell morphogenesis than co-culture, indicating that soluble and insoluble factors are likely to act cooperatively to inhibit the normal morphogenesis of epithelial cells.

Senescent cells are those which have permanently growth arrested after sustaining noxious stresses such as DNA damage. Naturally, the proportion of these cells accumulates with age. Despite the role of senescence in tumor suppression, senescent cells can secrete high levels of matrix metalloproteinases, growth factors and inflammatory cytokines to alter the normal epithelial tissue structure and function to produce the effects of aging (Campisi, 2005). Consistent with this and previous reports (Parrinello et al., 2005; Tsai et al., 2005), we found that co-culture of SF with MCF10A disrupts normal acini formation in matrigel culture. Hence, the *in vitro* co-culture system when used in combination with chemical inhibitors or neutralizing antibodies is a very useful system to study the role and mechanism of paracrine signaling in cancer development.

Our preliminary experiments using conditioned media from fibroblasts did not show a significant effect on epithelial cell cycle arrest compared to normal media following IR. However, stromal fibroblasts play an active role in promoting cancer progression, and our data indicate that co-culture produces a more pronounced effect on acini formation than conditioned media. Therefore, it will be informative to repeat the IR experiment with epithelial cells co-cultured with fibroblasts. Results in chapter 3 suggest that combination of Nutlin and adriamycin treatment may work better on cancerous cells due to their loss of normal 3D architecture. Due to their ability to disrupt normal acini formation, the impact of stromal cells on P53-dependent apoptosis such as that induced by adriamycin and Nutlin needs to be investigated since

changes in epithelial tissue architecture may impact on the cell's decision to die or live. Data from such experiments will help determine whether stromal fibroblasts have a negative impact on epithelial cell genetic stability or P53 function.

In general, the stromal fibroblasts play an active role in various aspects of tumor development and progression. Being genetically more stable than the cancer cells, the stromal cells are attractive candidates for therapies to block tumor-stroma interaction and when used in combination with standard cancer therapies to enhance the efficiency and killing of the tumor cells.

Materials and Methods

Cell culture and conditioned media

NF, NCF, CAF were kind gifts from Robert Weinberg. Cells were cultured in DMEM containing 10% calf serum. Fibroblasts were induced to undergo senescence by treatment with 15 Gy IR. Conditioned media was MCF10A differentiation media (5 ng/ml EGF, 100 ng/ml cholera, 10 μg/ml insulin, 0.5 μg/ml hydrocortisone, 2% horse serum) that had been placed over a confluent plate of fibroblasts for 48 hours.

For coculture, 1.3×10^4 NF /CAF or 1.8×10^4 SF were seeded with 1×10^4 MCF10A in differentiation media containing 2% matrigel on 4-wells chamber slide that was previously coated with 100 μl of 3:1 mix of matrigel and collagen I (final concentration of collagen I is 2 mg/ml). Cells were harvested at regular days interval for morphogensis check.

Indirect immunofluorescence

Antibodies against smooth muscle actin (1A4) and pan-cytokeratin (C-11) were from Sigma. *In situ* BrdU staining was performed according to manufacturer's instructions (Amersham Biosciences). Immunostaining was performed using procedures as previously described (Debnath et al., 2003).

Acknowledgements

We thank Dr Robert Weinberg for providing NCF and CAF. We also thank Dr Akira Orimo for assistance with co-cultures. The dissertation author is the primary researcher and author and Geoffrey M. Wahl directed and supervised the research that forms the basis for this chapter.
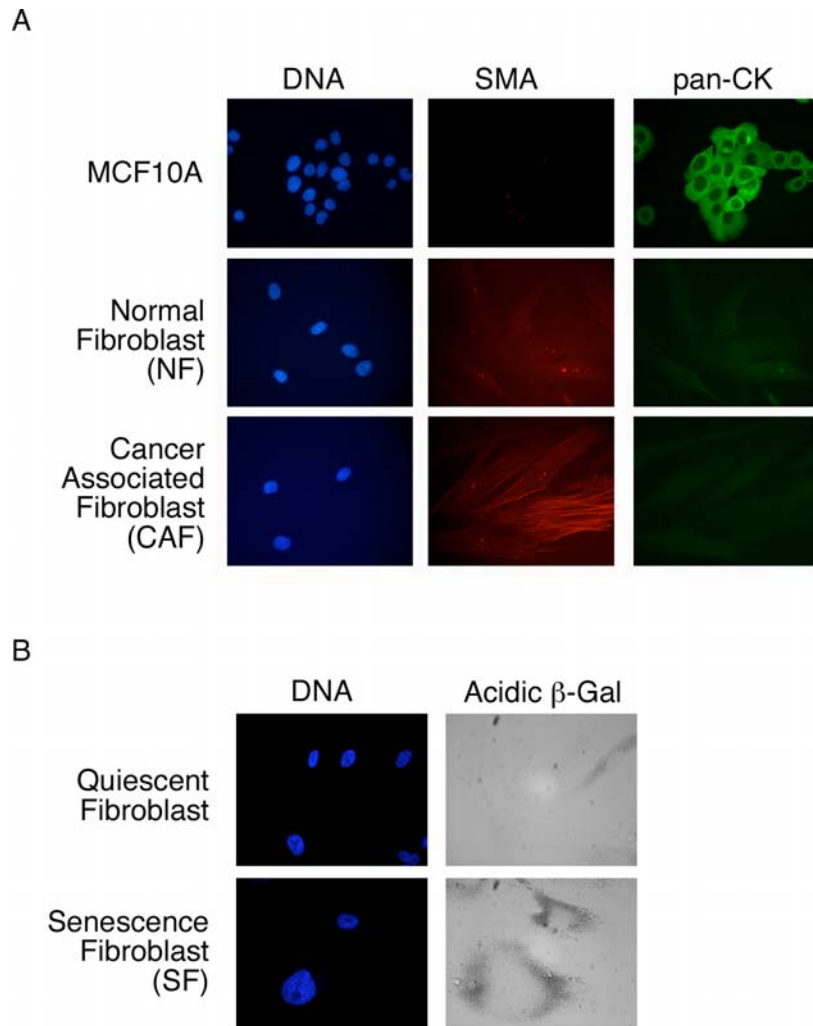
Figure 4.1: Characterization of mammary fibroblasts

a. Immunofluorescence staining of MCF10A, normal mammary fibroblasts (NF) and mammary cancer-associated fibroblasts (CAF) for smooth-muscle actin (SMA) and general cytokeratin (pan-CK) expression.
b. Distinction of serum starved fibroblasts (quiescent fibroblasts) from senescent fibroblasts by staining for acidic β-galactosidase (β-gal). Senescence in mammary fibroblasts was induced by exposing cells to 12Gy IR.

Figure 4.2: Influence of epithelial cell morphogenesis by mammary fibroblasts in matrigel culture

a. MCF10A cells were cultured on matrigel alone or co-cultured with NCF, CAF or cultured in conditioned media from NCF and CAF. Immunofluorescence staining shows epithelial cells stained for pan-CK (epithelial cells) or BrdU after 3 days in culture. Two different epithelial morphologies were shown for the fibroblast-epithelial co-cultures.

b. Fluorescence picture shows progressive changes in the morphology of H2BGFP-expressing MCF10A cells cultured alone or with NF or SF in matrigel culture.

A

Day 3

	DNA	pan-CK	BrdU	DNA	pan-CK	BrdU
MCF10A						
MCF10A+ NCF						
MCF10A+ CAF						
MCF10A+ cNCF						
MCF10A+ cCAF						

B

	MCF10A	MCF10A+ NF	MCF10A+ SF
Day 2			
Day 4			
Day 8			
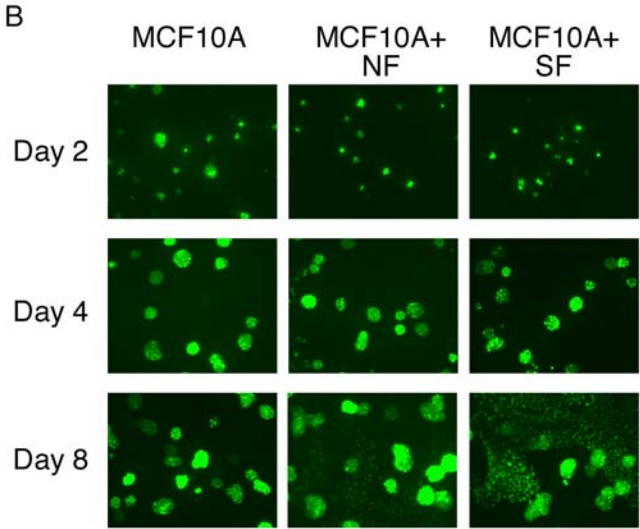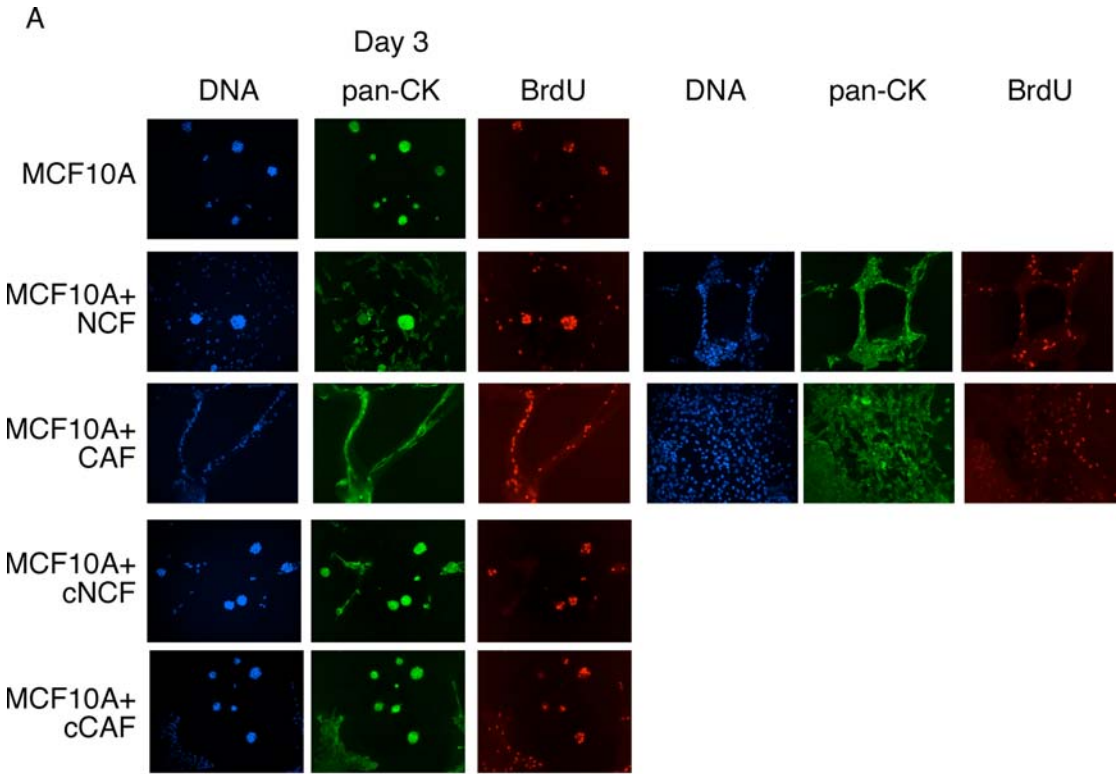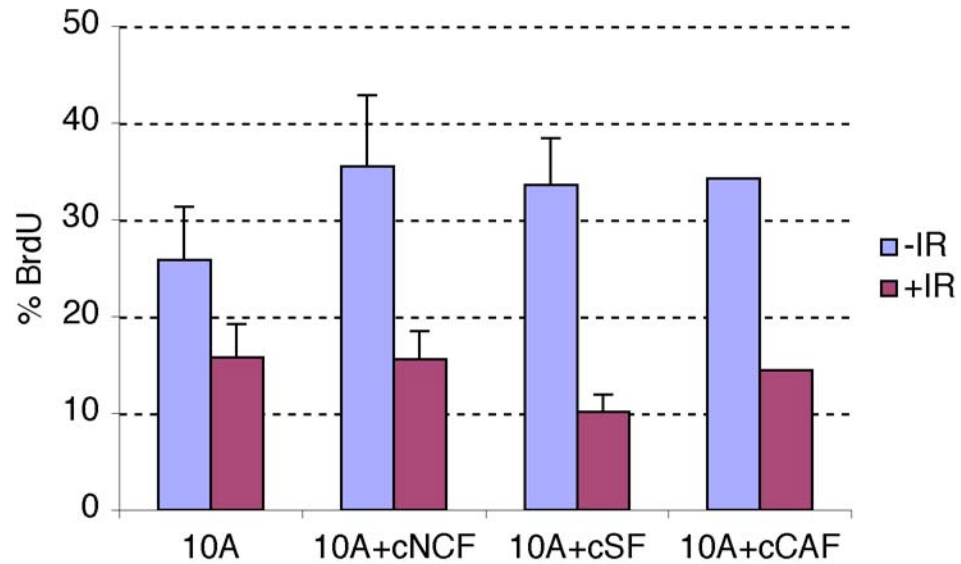
Figure 4.3: IR-induced cell cycle arrest is similar in MCF10A cells cultured in fibroblast-conditioned media.

MCF10A were cultured in normal differentiation media or in media conditioned by mammary fibroblasts (NCF, SF, CAF) for 24 hours in 2D before plating onto matrigel. Cells were irradiated with 5 Gy IR 3 hours after plating and harvested for BrdU analysis 48 hours after IR treatment. Graph shows the percentage of BrdU incorporation in MCF10A before and after IR.

References

Allinen, M., Beroukhim, R., Cai, L., Brennan, C., Lahti-Domenici, J., Huang, H., Porter, D., Hu, M., Chin, L., Richardson, A., *et al.* (2004). Molecular characterization of the tumor microenvironment in breast cancer. Cancer Cell *6*, 17-32.

Badve, S., A'Hern, R. P., Ward, A. M., Millis, R. R., Pinder, S. E., Ellis, I. O., Gusterson, B. A., and Sloane, J. P. (1998). Prediction of local recurrence of ductal carcinoma in situ of the breast using five histological classifications: a comparative study with long follow-up. Hum Pathol *29*, 915-923.

Barcellos-Hoff, M. H., and Ravani, S. A. (2000). Irradiated mammary gland stroma promotes the expression of tumorigenic potential by unirradiated epithelial cells. Cancer Res *60*, 1254-1260.

Beckmann, M. W., Niederacher, D., Schnurch, H. G., Gusterson, B. A., and Bender, H. G. (1997). Multistep carcinogenesis of breast cancer and tumour heterogeneity. J Mol Med *75*, 429-439.

Bhowmick, N. A., Chytil, A., Plieth, D., Gorska, A. E., Dumont, N., Shappell, S., Washington, M. K., Neilson, E. G., and Moses, H. L. (2004). TGF-beta signaling in fibroblasts modulates the oncogenic potential of adjacent epithelia. Science *303*, 848-851.
Bissell, M. J., and Radisky, D. (2001). Putting tumours in context. Nat Rev Cancer *1*, 46-54.

Boyd, N. F., Rommens, J. M., Vogt, K., Lee, V., Hopper, J. L., Yaffe, M. J., and Paterson, A. D. (2005). Mammographic breast density as an intermediate phenotype for breast cancer. Lancet Oncol *6*, 798-808.

Campisi, J. (2005). Senescent cells, tumor suppression, and organismal aging: good citizens, bad neighbors. Cell *120*, 513-522.

Chang, H. Y., Nuyten, D. S., Sneddon, J. B., Hastie, T., Tibshirani, R., Sorlie, T., Dai, H., He, Y. D., van't Veer, L. J., Bartelink, H., *et al.* (2005). Robustness, scalability, and integration of a wound-response gene expression signature in predicting breast cancer survival. Proc Natl Acad Sci U S A *102*, 3738-3743.

Chang, H. Y., Sneddon, J. B., Alizadeh, A. A., Sood, R., West, R. B., Montgomery, K., Chi, J. T., van de Rijn, M., Botstein, D., and Brown, P. O. (2004). Gene expression signature of fibroblast serum response predicts human cancer progression: similarities between tumors and wounds. PLoS Biol *2*, E7.

Dimri, G. P., Lee, X., Basile, G., Acosta, M., Scott, G., Roskelley, C., Medrano, E. E., Linskens, M., Rubelj, I., Pereira-Smith, O., and et al. (1995). A biomarker that identifies senescent human cells in culture and in aging skin in vivo. Proc Natl Acad Sci U S A *92*, 9363-9367.

Elenbaas, B., and Weinberg, R. A. (2001). Heterotypic signaling between epithelial tumor cells and fibroblasts in carcinoma formation. Exp Cell Res *264*, 169-184.

Feng, J., Tamaskovic, R., Yang, Z., Brazil, D. P., Merlo, A., Hess, D., and Hemmings, B. A. (2004). Stabilization of Mdm2 via decreased ubiquitination is mediated by protein kinase B/Akt-dependent phosphorylation. J Biol Chem.

Gabbiani, G. (2003). The myofibroblast in wound healing and fibrocontractive diseases. J Pathol *200*, 500-503.

Heldin, C. H., Rubin, K., Pietras, K., and Ostman, A. (2004). High interstitial fluid pressure - an obstacle in cancer therapy. Nat Rev Cancer *4*, 806-813.

Hu, M., Yao, J., Cai, L., Bachman, K. E., van den Brule, F., Velculescu, V., and Polyak, K. (2005). Distinct epigenetic changes in the stromal cells of breast cancers. Nat Genet *37*, 899-905.

Kuperwasser, C., Chavarria, T., Wu, M., Magrane, G., Gray, J. W., Carey, L., Richardson, A., and Weinberg, R. A. (2004). Reconstruction of functionally normal and malignant human breast tissues in mice. Proc Natl Acad Sci U S A *101*, 4966-4971.

Maffini, M. V., Soto, A. M., Calabro, J. M., Ucci, A. A., and Sonnenschein, C. (2004). The stroma as a crucial target in rat mammary gland carcinogenesis. J Cell Sci *117*, 1495-1502.

Mayo, L. D., Dixon, J. E., Durden, D. L., Tonks, N. K., and Donner, D. B. (2002). PTEN protects p53 from Mdm2 and sensitizes cancer cells to chemotherapy. J Biol Chem *277*, 5484-5489.

McDaniel, S. M., Rumer, K. K., Biroc, S. L., Metz, R. P., Singh, M., Porter, W., and Schedin, P. (2006). Remodeling of the mammary microenvironment after lactation promotes breast tumor cell metastasis. Am J Pathol *168*, 608-620.

Mueller, M. M., and Fusenig, N. E. (2004). Friends or foes - bipolar effects of the tumour stroma in cancer. Nat Rev Cancer *4*, 839-849.

Olumi, A. F., Grossfeld, G. D., Hayward, S. W., Carroll, P. R., Tlsty, T. D., and Cunha, G. R. (1999). Carcinoma-associated fibroblasts direct tumor progression of initiated human prostatic epithelium. Cancer Res *59*, 5002-5011.

Orimo, A., Gupta, P. B., Sgroi, D. C., Arenzana-Seisdedos, F., Delaunay, T., Naeem, R., Carey, V. J., Richardson, A. L., and Weinberg, R. A. (2005). Stromal fibroblasts present in invasive human breast carcinomas promote tumor growth and angiogenesis through elevated SDF-1/CXCL12 secretion. Cell *121*, 335-348.

Parrinello, S., Coppe, J. P., Krtolica, A., and Campisi, J. (2005). Stromal-epithelial interactions in aging and cancer: senescent fibroblasts alter epithelial cell differentiation. J Cell Sci *118*, 485-496.

Radisky, D., Hagios, C., and Bissell, M. J. (2001). Tumors are unique organs defined by abnormal signaling and context. Semin Cancer Biol *11*, 87-95.

Radisky, D. C., and Bissell, M. J. (2006). Matrix metalloproteinase-induced genomic instability. Curr Opin Genet Dev *16*, 45-50.

Ries, S., Biederer, C., Woods, D., Shifman, O., Shirasawa, S., Sasazuki, T., McMahon, M., Oren, M., and McCormick, F. (2000). Opposing effects of Ras on p53: transcriptional activation of mdm2 and induction of p19ARF. Cell *103*, 321-330.

Sternlicht, M. D., Lochter, A., Sympson, C. J., Huey, B., Rougier, J. P., Gray, J. W., Pinkel, D., Bissell, M. J., and Werb, Z. (1999). The stromal proteinase MMP3/stromelysin-1 promotes mammary carcinogenesis. Cell *98*, 137-146.

Tsai, K. K., Chuang, E. Y., Little, J. B., and Yuan, Z. M. (2005). Cellular mechanisms for low-dose ionizing radiation-induced perturbation of the breast tissue microenvironment. Cancer Res *65*, 6734-6744.

Wiseman, B. S., and Werb, Z. (2002). Stromal effects on mammary gland development and breast cancer. Science *296*, 1046-1049.

V

Summary and Perspectives

The work in this thesis was undertaken to obtain a better understanding of the parameters that affect P53 regulation with the intention of developing systems to enable analyses to improve therapy based on the stress-response pathway it controls. Though the P53 system is among the best studied in cancer biology, there is much debate on the mechanisms that keep it off, and those that activate it under stress. During the course of my work, as analyses with mouse mutants were done in this and other labs, it became clear that inferences drawn from *in vitro* transfection studies that did not rigorously maintain the stoichiometric relationships between P53 and its negative regulators, Mdm2 and Mdmx, did not give the same results compared with the more biologically faithful studies performed with mouse models. Therefore, my first goal was to develop a system that would enable one to avoid such complications through use of the rigorous inducible system described in Chapter 2. It has also become apparent that propagation of cells on an artificial plastic matrix in two dimensions, the standard approach for mammalian cells, also does not faithfully mirror the complex matrix, tissue, and geometric relations that occur *in vivo*. Given the increasingly complex interactions the P53 system exhibits with other signaling mechanisms that could be affected by such parameters, it became essential to evaluate the impact of tissue architecture and cell-matrix and cell-cell associations on P53 regulation and output. Below, I provide a perspective on these studies which were described in detail in Chapters 3 and 4.

A system to study the influence of change in Hdm2-Hdmx-P53 stoichiometry on P53 activation

It is clear that Hdmx is a major negative inhibitor of P53 transactivation (Francoz et al., 2006; Toledo et al., 2006; Xiong et al., 2006). A good understanding of how Hdm2 regulates Hdmx and how both proteins negatively regulate P53 are valuable for the design of specific therapeutics to reactivate P53 in tumors that overexpress Hdm2 or Hdmx. As the stoichiometry of Hdm2-Hdmx-P53 is tightly regulated and to avoid false conclusions that result from over expression of these components, careful titration of gene expression is necessary. Making mouse models with each mutant gene introduced into its endogenous locus by homologous recombination is the gold standard; however the high cost and length of time required to generate a knock-in mouse prevents the rapid screening and analysis of potentially interesting mutants of Hdm2, Hdmx or P53. An improved Cre-LoxP RMCE system was developed and when used in combination with the Tet-On inducible system generates stable clones with single integration sites and where transgene expression occurs uniformly in a dose-dependent manner.

Since the development of the improved LoxP3/2 system, we have inserted the LoxP-RMCE system into cell lines at random genomic loci and into the endogenous *p53* locus in ES cells and MEF (Toledo, In Press). In this way, any variant/mutant of *p53* gene can be rapidly analyzed in MEFs and eventually in mice should there be interesting phenotypes seen in the MEFs. Given the importance of Mdm2/x in P53 regulation, the LoxP recombination approach can also be applied to the Mdm2/x loci to study variants of Mdm2/x to gain better understanding of their regulation and impact on P53 function. The LoxP sites have also been targeted to the Rosa26 locus for uniform expression of transgenes in mice. Other than gene induction, the

feasibility of DNA polymerase II regulated promoters to drive shRNA expression enables the inducible knockdown of gene expression in cell lines and in the mouse (Dickins et al., 2005; Silva et al., 2005; Stegmeier et al., 2005). Hence, the RMCE system offers enormous applicability for the tightly regulated and reproducible expression of oncogenes and knockdown of tumor suppressor expression in the field of cancer research.

P53 activation in epithelial cells growing in 3D

For tumorigenic progression, a cell must inactivate an activator or overexpress an inhibitor of the P53 pathway. Hence, cancer cell lines are unlikely to yield a true picture of the mechanisms of P53 regulation. Most cancers arise from transformation of epithelial cells. Since epithelial cells are organized into 3D structures *in vivo*, the use of non-tumorigenic epithelial cell cultured *in vitro* as acini to study P53 regulation should more closely approximate the *in vivo* conditions. However, our studies to evaluate the sensitivity of MCF10A towards apoptotic stimuli yield results that differ from a previous study that uses another immortalized but non-tumorigenic mammary epithelial cell line. Since genetic alterations are common during the immortalization process, other than *p14Arf* and *p53* mutation, it is difficult to predict how common or how different the two cell lines are that may explain the differences in their drug responses. Loss of cell polarity is a hallmark of cancer cells. Since MCF10A is an immortalized cell line adopted to grow *in vitro* on tissue culture plate, pathway(s) linking cell architecture and P53 regulation may be attenuated, thus preventing us to see the true differences in P53 regulation in 2D and 3D cells. A number of

immortalized HMEC with wildtype *p53* and p14Arf are available to further verify the MCF10A studies (refer to: http:// www.lbl.gov/ LBL-Programs /mrgs /review. Html). A few primary HMEC with (pre-stasis) or without (post-stasis) p16INK4a are also available (above web site and (Petersen and van Deurs, 1987). However, care has to be taken to verify the lineage (luminal versus basal) and the purity of the preparation. As primary human cells are limited in availability, the mouse offers an easily manipulatable and available system (see next section).

In response to therapeutic agents, a number of processes such as apoptosis, senescence and autophagy are activated to contribute to the final outcome of the therapy (Brown and Attardi, 2005; Kondo et al., 2005). From a therapeutic point of view, the sum of all these processes that negatively regulate cell survival should be reflected by a long-term survival assay such as colony outgrowth. Therefore, assessment of colony outgrowth should more accurately reflect the sensitivity or resistance of cells to a therapeutic agent. We observed a two-fold difference in colony outgrowth in 2D and 3D cells in response to IR, the responses to adriamycin and Nutlin are to be further evaluated. IR does not induce significant apoptosis in MCF10A, we are beginning to evaluate senescence in 2D and 3D cells in response to P53 activation. Recent papers also link P53 activation to the induction of autophagy, a process that involves digestion of intracellular contents by the lysosome (Crighton et al., 2006; Feng et al., 2005). Autophagy is also involved in the lumen clearing process within the acini (Debnath et al., 2002; Mills et al., 2004). It should be interesting to evaluate the role of autophagy in response to P53 activation and further determine if one form of death is preferentially activated over the others in 2D and 3D cells.

Our studies point to the importance of Hdmx regulation in influencing the outcome of P53 activation in 3D cells. Exactly how Hdmx negatively regulates P53 transcription is unknown. Whether it affects P53's promoter choice or if it binds to and regulates a subset of P53 binding sites in the genome or if it affects the binding of other co-activators/ repressors are presently not known. Microarray and ChIP experiments should be helpful to address these questions. It is also unclear how Hdmx is regulated under conditions of P53 activation. Hdmx is phosphorylated by damage-activated kinases and is ubiquitinated by Hdm2 before being targeted for degradation by the proteosome. Mutation of Mdmx at the phosphorylation sites, or at the RING domain to disrupt interaction with Mdm2 should address the importance of Mdmx degradation in P53 activation. As transcription of Hdmx is lower in 3D cells, promoter analyses may reveal transcription factors that respond to changes in cell architecture.

Finally, the subcellular localization of Hdmx poses some interesting questions regarding its regulation and function. In unstressed cells, the majority of Hdmx is found in the cytoplasm while post-translational modifications induced by DNA damage promote Hdmx nuclear retention or entry and subsequent degradation (LeBron et al., 2006). It is puzzling how DNA damage activated kinases such as ATM can phosphorylate Hdmx in the cytosol. Either a downstream kinase such as Chk2 shuttles between the nucleus and cytoplasm to phosphorylate Hdmx in the cytoplasm, or Hdmx can shuttle between the two compartments but only the phosphorylated form is preferentially retained in the nucleus. Cytosolic Hdmx that is brought into the nucleus for degradation also suggests the intriguing possibility that the cytoplasmic pool of Hdmx may perform a function distinct from the nuclear Hdmx to suppress cell

death. The staining pattern of Hdmx colocalizes with cytochrome c and mitoTracker dye (Wade, in preparation), suggesting that Hdmx is localized to the mitochondria and may inhibit the function of pro-apoptotic factor(s) at the mitochondria. Identification of Hdmx binding partner in the mitochondria may reveal potential target for inhibition that will synergize with Hdm2 antagonist (eg Nutlin) to effectively eliminate tumors with wildtype *p53*.

The role of tumor microenvironment on epithelial cell morphogenesis and response to stress *in vitro*

The initiation and progression of a carcinoma is influenced by the tumor microenvironment that includes non-cellular (eg ECM) and cellular components (eg fibroblasts, endothelial and immune cells). Two key experiments elegantly demonstrate that paracrine signals from stromal cells can modulate the oncogenic potential of the adjacent epithelia. Both studies used cell-type specific promoters to disrupt TGF-β signaling in either the fibroblasts or the T cells compartment and lead to an abnormal paracrine signaling loop with eventual carcinoma development in the gastric and colon respectively (Bhowmick et al., 2004; Kim et al., 2006). The role of fibroblasts in the promotion of breast and prostate cancers development is widely studied (Elenbaas and Weinberg, 2001). Consistent with the ability of fibroblasts to promote tumorigenesis, we found that mammary CAF, SF and NF can disrupt the normal morphogenesis of immortalized HMEC in part through paracrine signaling to the epithelial cells. The role of immune cells in breast cancer development is less studied. Inflammation may play a role in breast cancer development as long term

administration of anti-inflammatory agents resulted in 20% reduction in the risk for breast cancer development (Cotterchio et al., 2001). Hence, there are potential interests in the investigation of the roles played by immune cells in breast cancer development.

During the course of the experiments, it also became clear that despite the rapidity and economy of the *in vitro* co-culture system, due to the complexity of tissue microenvironment, further optimization is required to mirror the *in vivo* situation. One approach to study cell-cell crosstalk is transplantation of human fibroblasts and epithelial cells into immune-compromised animals. One advantage is the flexibility to implant any genetically modified cells to decipher pathways and signaling molecules involved in the crosstalk. Additionally, most of the other components of the microenvironment are present unaltered in the mouse. A disadvantage is the lack of the immune system, which plays an important role in the development of cancer. Alternatively, the stromal environment of the cleared fat pad may be activated by chemical or physical means before implantation of the epithelial components (Barcellos-Hoff and Ravani, 2000; Maffini et al., 2004). Another approach is the use of the normal mouse in which the microenvironment is modified by overexpression or gene knockout through the use of cell-type specific promoters (Bhowmick et al., 2004; Kim et al., 2006). For example, the fibroblast-specific protein's (FSP) promoter can be use to evaluate the role of specific genetic alterations in the fibroblast compartment in the course of mouse development and cancer progression (Bhowmick et al., 2004). Many studies point to the important roles played by the microenvironment in cancer

development. The identification of key signaling molecules should yield relevant therapeutic targets for the effective elimination of the cancers.

Approaches to cancer treatment have broadened significantly over the past decade. Conventional therapy typically involves the use of clastogenic agents such as irradiation and DNA damaging drugs. Advances in our understanding of the genetic and biochemical mechanisms by which cancers arise (Hanahan and Weinberg, 2000; Vogelstein and Kinzler, 1993; Vogelstein and Kinzler, 2004) is enabling the development of target-selective agents that exhibit higher specificity for cancer cells. Studies described in the thesis have shown that changes in cell architecture do not impact on P53 activation by DNA damaging agents but affected cell survival in response to a combination of DNA damage and Nutlin treatment. Other molecularly targeted therapies designed to interfere with intracellular signaling (such as Ras, Her2, EGFR, estrogen receptor) are used as adjuvant therapy for breast cancers. The *in vitro* 3D culture system is valuable for testing the responses of oncogene-expressing HMECs to these molecularly based therapies.

References

Barcellos-Hoff, M. H., and Ravani, S. A. (2000). Irradiated mammary gland stroma promotes the expression of tumorigenic potential by unirradiated epithelial cells. Cancer Res *60*, 1254-1260.

Bhowmick, N. A., Chytil, A., Plieth, D., Gorska, A. E., Dumont, N., Shappell, S., Washington, M. K., Neilson, E. G., and Moses, H. L. (2004). TGF-beta signaling in fibroblasts modulates the oncogenic potential of adjacent epithelia. Science *303*, 848-851.
Brown, J. M., and Attardi, L. D. (2005). The role of apoptosis in cancer development and treatment response. Nat Rev Cancer *5*, 231-237.

Cotterchio, M., Kreiger, N., Sloan, M., and Steingart, A. (2001). Nonsteroidal anti-inflammatory drug use and breast cancer risk. Cancer Epidemiol Biomarkers Prev *10*, 1213-1217.
Crighton, D., Wilkinson, S., O'Prey, J., Syed, N.,
Smith, P., Harrison, P. R., Gasco, M., Garrone, O., Crook, T., and Ryan, K. M. (2006). DRAM, a p53-induced modulator of autophagy, is critical for apoptosis. Cell *126*, 121-134.
Debnath, J., Mills, K. R., Collins, N. L., Reginato, M. J., Muthuswamy, S. K., and Brugge, J. S. (2002). The role of apoptosis in creating and maintaining luminal space within normal and oncogene-expressing mammary acini. Cell *111*, 29-40.

Dickins, R. A., Hemann, M. T., Zilfou, J. T., Simpson, D. R., Ibarra, I., Hannon, G. J., and Lowe, S. W. (2005). Probing tumor phenotypes using stable and regulated synthetic microRNA precursors. Nat Genet *37*, 1289-1295.

Elenbaas, B., and Weinberg, R. A. (2001). Heterotypic signaling between epithelial tumor cells and fibroblasts in carcinoma formation. Exp Cell Res *264*, 169-184.

Feng, Z., Zhang, H., Levine, A. J., and Jin, S. (2005). The coordinate regulation of the p53 and mTOR pathways in cells. Proc Natl Acad Sci U S A *102*, 8204-8209.

Francoz, S., Froment, P., Bogaerts, S., De Clercq, S., Maetens, M., Doumont, G., Bellefroid, E., and Marine, J. C. (2006). Mdm4 and Mdm2 cooperate to inhibit p53 activity in proliferating and quiescent cells in vivo. Proc Natl Acad Sci U S A *103*, 3232-3237.

Hanahan, D., and Weinberg, R. A. (2000). The hallmarks of cancer. Cell *100*, 57-70.
Kim, B. G., Li, C., Qiao, W., Mamura, M., Kasperczak, B., Anver, M., Wolfraim, L., Hong, S., Mushinski, E., Potter, M.*, et al*. (2006). Smad4 signalling in T cells is required for suppression of gastrointestinal cancer. Nature *441*, 1015-1019.

Kondo, Y., Kanzawa, T., Sawaya, R., and Kondo, S. (2005). The role of autophagy in cancer development and response to therapy. Nat Rev Cancer *5*, 726-734.

LeBron, C., Chen, L., Gilkes, D. M., and Chen, J. (2006). Regulation of MDMX nuclear import and degradation by Chk2 and 14-3-3. Embo J *25*, 1196-1206.

Maffini, M. V., Soto, A. M., Calabro, J. M., Ucci, A. A., and Sonnenschein, C. (2004). The stroma as a crucial target in rat mammary gland carcinogenesis. J Cell Sci *117*, 1495-1502.

Mills, K. R., Reginato, M., Debnath, J., Queenan, B., and Brugge, J. S. (2004). Tumor necrosis factor-related apoptosis-inducing ligand (TRAIL) is required for induction of autophagy during lumen formation in vitro. Proc Natl Acad Sci U S A *101*, 3438-3443.

Petersen, O. W., and van Deurs, B. (1987). Preservation of defined phenotypic traits in short-term cultured human breast carcinoma derived epithelial cells. Cancer Res *47*, 856-866.

Silva, J. M., Li, M. Z., Chang, K., Ge, W., Golding, M. C., Rickles, R. J., Siolas, D., Hu, G., Paddison, P. J., Schlabach, M. R.*, et al*. (2005). Second-generation shRNA libraries covering the mouse and human genomes. Nat Genet *37*, 1281-1288.

Stegmeier, F., Hu, G., Rickles, R. J., Hannon, G. J., and Elledge, S. J. (2005). A lentiviral microRNA-based system for single-copy polymerase II-regulated RNA interference in mammalian cells. Proc Natl Acad Sci U S A *102*, 13212-13217.

Toledo, F., Krummel, K. A., Lee, C. J., Liu, C. W., Rodewald, L. W., Tang, M., and Wahl, G. M. (2006). A mouse p53 mutant lacking the proline-rich domain rescues Mdm4 deficiency and provides insight into the Mdm2-Mdm4-p53 regulatory network. Cancer Cell *9*, 273-285.

Vogelstein, B., and Kinzler, K. W. (1993). The multistep nature of cancer. Trends Genet *9*, 138-141.

Vogelstein, B., and Kinzler, K. W. (2004). Cancer genes and the pathways they control. Nat Med *10*, 789-799.

Xiong, S., Van Pelt, C. S., Elizondo-Fraire, A. C., Liu, G., and Lozano, G. (2006). Synergistic roles of Mdm2 and Mdm4 for p53 inhibition in central nervous system development. Proc Natl Acad Sci U S A *103*, 3226-3231.